Aza-Michael addition by ball milling

Leonarda Vugrin, Alen Bjelopetrović and Ivan Halasz*

Ruđer Bošković Institute, Bijenička c. 54, 10000 Zagreb, Croatia

E-mail of corresponding author: ivan.halasz@irb.hr

Supplementary information

1. Materials and methods

1.1. Chemicals

All reagents were purchased from commercial sources and used without treatment, unless otherwise indicated. The following chapters describe the details of the syntheses of chalcones used as starting materials.

1.2. Milling equipment

Mechanochemical experiments were performed at the ambient temperature using an IST500 Mixer Mill (InSolido Technologies, Zagreb, Croatia) in transparent poly(methyl-methacrylate) (PMMA) (internal volume 14.0 mL) milling jars operating at a frequency of 30 Hz. Starting materials were added in equimolar ratios (1 mmol) along with two zirconium oxide (ZrO_2) (mass of one milling ball, 1.6 g) or stainless steel (SS) milling balls (mass of one milling ball, 1.4 g), unless otherwise specified. Progress of reaction was followed *in situ* using Raman spectroscopy and *ex situ* by thin-layer chromatography (TLC) using silica plates and dichloromethane or hexane/ethyl-acetate 8/2 as a solvent system. The reactions were conducted for maximum 120 min, after which the crude mixtures were sent for solution ^{1}H NMR (300 MHz and 600 MHz), powder X-ray diffraction (PXRD) and high-resolution mass spectrometry (HR-MS) analysis.

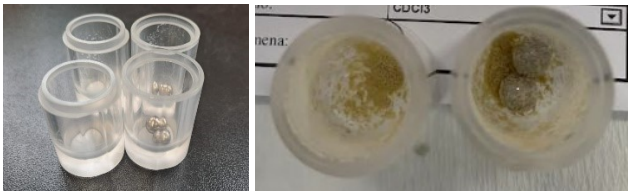

Figure S1. (left) Empty PMMA milling jar with two SS milling balls. (right) PMMA jar with reaction mixture after the milling between chalcone (**1**) (1 mmol) and piperidine (**2a**) (1 equiv.) at 30 Hz milling frequency. The final reaction mixture was in a free-flowing powder form.

Figure S2. Experimental setup for conducting external heating during milling using a heat-gun (Parker side PHLG 2000 E4). The Raman probe was positioned underneath the PMMA milling jar, while the heating device was placed laterally. A thermocouple was put around the external milling jar surface to monitor the temperature. The temperature was followed using both a multimeter and the built-in electronic gauge on the heat gun.

1.3. *In situ* Raman monitoring

Laboratory *in-situ* Raman monitoring was performed using a portable Raman system with a PDLD (now Necsel) BlueBox laser source with the excitation wavelength of 785 nm, equipped with B&W-Tek fiber optic Raman BAC102 probe, and coupled with an OceanOptics Maya2000Pro spectrometer. The Raman probe was positioned about 2 mm under the reaction milling vessel. Time-resolved *in situ* Raman spectra were collected in an automated fashion whereby the substraction of vessel contribution to Raman spectra was done in parallel using an in-house code in MATLAB software.[1]

1.4. ^{1}H NMR spectroscopy

Nuclear magnetic resonance (NMR) spectra were recorded either on NMR Bruker Avance 300 MHz or Bruker Avance 600 MHz spectrometers at 25 °C. Experimental data were processed and analyzed with the program MestReNova. Chemical shifts are given in parts per million (ppm) relative to the residual solvent peak of the non-deuterated solvent, $CDCl_3$ (^{1}H NMR: δ = 7.26 ppm). Coupling constants (*J*) are given in Hertz (Hz).

1.5. PXRD analysis

PXRD patterns were collected on a Panalytical Aeris diffractometer (CuKα radiation and Ni filter where copper X-ray tube was operated at 40 kV and 7.5 mA) in the Bragg-Brentano geometry, using a silicon zero-background sample holder.

The crystal structure of the addition product was solved from and refined against powder diffraction data. The diffraction pattern was indexed with a orthorhombic crystal system, *P*ca2$_1$ space group with the unit cell: a = 10.54231 Å, b = 11.25671 Å, c = 16.17369 Å, β = 90°, V = 1919.360 Å^3). This unit cell volume corresponds well to the formula units comprised from four molecules of addition product (**3a**) in the unit cell and one molecule of **3a** in the asymmetric unit. The crystal structure was solved by global optimization in direct space taking the molecules of starting materials, chalcone (**1**) and piperidine (**2a**) as separate rigid bodies. When an approximate crystal structure model was found, rotations around carbon-nitrogen bond and aromatic phenyl rings were also included in the optimization. All calculations were performed using the program Topas (Bruker-AXS, Karlsruhe, Germany). The cif file for the solved structure was deposited with the Cambridge Crystallographic data center (CSD Refcode: 2343064). These data can be retrieved free of charge from the CCDC upon request. Drawings of the structures were prepared using MERCURY program.

1.6. HR-MS analysis

HR-MS spectra of novel compounds were obtained with Agilent 6550 Series Accurate-Mass-Quadrupole Time-of-Flight (Q-TOF) mass spectrometer. Synthesized materials were not known compounds and were additionally identified by comparison of their spectra data with those of similar samples.

1.7. General reaction scheme

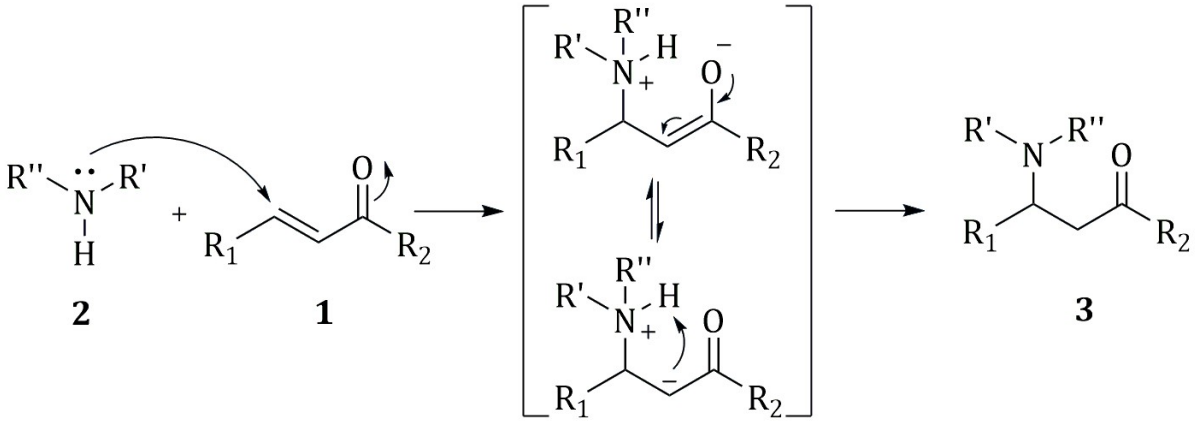

Scheme S1. General reaction mechanism of catalyst-free aza-Michael addition reaction between **1** (Michael acceptor) and nucleophile **2** (Michael donor).[2]

1.8. Solid-state synthesis of chalcones

A mixture of acetophenone (1.0 mmol) and benzaldehyde (1 equiv.) were milled with two milling balls made of zirconium dioxide (mass of one milling ball 1.6 g) at 30 Hz milling frequency at ambient temperature for 120 min. After that, distilled water was added and reaction mixture was recrystallized in EtOH to obtain pure product. The purity and structural identity was confirmed by solution ^{1}H NMR spectroscopy and referenced spectra previously documented in the literature.[3,4]

1.9. Procedure for the amination of chalcones

General procedure for the preparation of **3** (**3a** as an example):
A mixture of **1** (1.0 mmol) and nucleophilic nitrogen source, **2a** (1 equiv.) was milled in transparent PMMA milling jar at 30 Hz for total milling time of 120 min at ambient temperature. In the milling jar, two milling balls made of zirconium dioxide (mass of one milling ball 1.6 g) were added. Alongside the neat-grinding reactions, liquid-assisted grinding (LAG) and external heating were tested with the aim of optimizing the reaction conditions for the addition of piperazine (**2b**) (see Figure S2, Table S2). The milling reaction was monitored in a real time by *in situ* Raman spectroscopy. After that, the crude reaction mixture was further analyzed by PXRD, solution ^{1}H NMR spectroscopy and HR-MS.

Scheme S2. Aza-Michael addition reaction of **1** and secondary aliphatic cyclic amines **2a-c** (1 equiv.) in a ball mill under solvent-free and catalyst-free conditions (*push-push* mechanism).

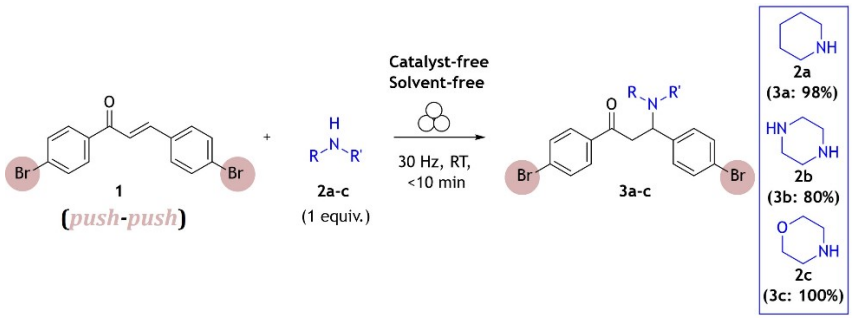

Scheme S3. Aza-Michael addition reaction of **4** and **2a** (1 equiv.) in a ball mill under solvent-free and catalyst-free conditions (example of *push-pull* mechanism).

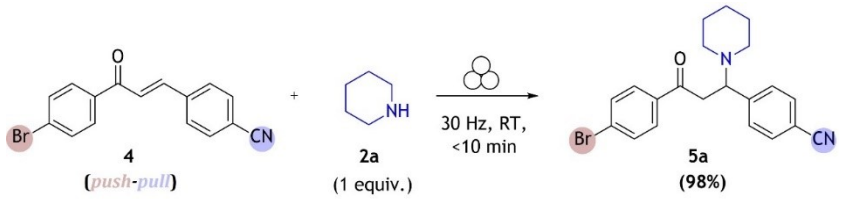

1.10. ^{1}H NMR assignation of the prepared compounds

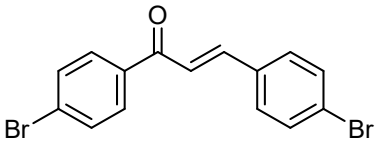

(E)-1,3-bis(4-bromophenyl)prop-2-en-1-one (1):
^{1}H NMR (600 MHz, $CDCl_3$): δ/ ppm = 7.88 (d, J = 8.5 Hz, 2H), 7.75 (d, J = 15.7 Hz, 1H), 7.65 (d, J = 8.5 Hz, 2H), 7.56 (d, J = 8.5 Hz, 2H), 7.50 (d, J = 8.5 Hz, 2H), 7.46 (d, J = 15.7 Hz, 1H).

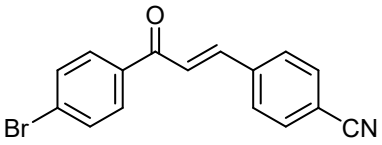

(E)-4-(3-(4-bromophenyl)-3-oxoprop-1-en-1-yl)benzonitrile (4):
^{1}H NMR (600 MHz, $CDCl_3$): δ/ ppm = 7.89 (d, J = 8.4 Hz, 2H), 7.78 (d, J = 15.7 Hz, 1H), 7.72 (s, 4H), 7.67 (d, J = 8.4 Hz, 2H), 7.54 (d, J = 15.7 Hz, 1H).

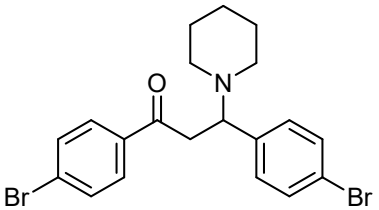

1,3-bis(4-bromophenyl)-3-(piperidin-1-yl)propan-1-one (3a): ^{1}H NMR (600 MHz, $CDCl_3$): δ/ ppm = 7.75 (d, J = 8.3 Hz, 2H), 7.58 (d, J = 8.3 Hz, 2H), 7.41 (d, J = 8.1 Hz, 2H), 7.14 (d, J = 8.1 Hz, 2H), 4.15 (t, J = 6.8 Hz, 1H), 3.52 (dd, J = 16.3, 6.0 Hz, 1H), 3.30 (dd, J = 16.2, 7.7 Hz, 1H), 2.33 (d, J = 61.2 Hz, 4H), 1.49 (d, J = 3.0 Hz, 4H), 1.34 (d, J = 5.5 Hz, 2H).
HRMS, m/z: [M]+ calc. for $C_{20}H_{21}Br_2NO$, 451.19; found, 452.00.

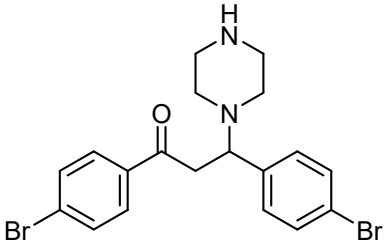

1,3-bis(4-bromophenyl)-3-(4l2-piperazin-1-yl)propan-1-one (3b): ^{1}H NMR (600 MHz, $CDCl_3$): *δ*/ ppm = 7.69 (d, *J* = 8.5 Hz, 2H), 7.56 (d, *J* = 8.4 Hz, 2H), 7.39 (d, *J* = 8.3 Hz, 2H), 7.10 (d, *J* = 7.0 Hz, 2H), 4.06 (t, *J* = 6.4 Hz, 1H), 3.44 (dd, *J* = 16.3, 6.2 Hz, 1H), 3.22 (dd, *J* = 16.3, 8.1 Hz, 1H), 2.79 (m, 2H), 2.36 (m, 6H). HRMS, m/z: [M]+ calc. for $C_{19}H_{20}Br_2N_2O$, 452.18; found, 453.00.

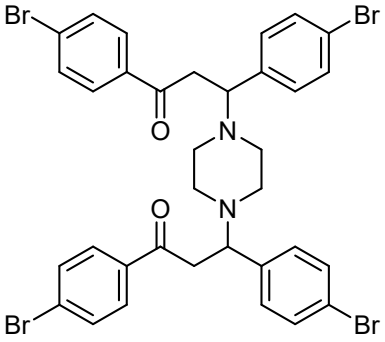

3,3'-(piperazine-1,4-diyl)bis(1,3-bis(4-bromophenyl)propan-1-one) (3b'): ^{1}H NMR (600 MHz, $CDCl_3$): *δ*/ ppm = 7.74 (d, *J* = 8.53 Hz, 2H), 7.65 (d, *J* = 8.4 Hz, 2H), 7.58 (d, *J* = 8.54 Hz, 2H), 7.42 (d, *J* = 8.3 Hz, 2H), 7.15 (d, *J* = 8.3 Hz, 2H), 7.10 (t, *J* = 7.0 Hz, 120H), 4.12 (t, *J* = 6.8 Hz, 1H), 3.52 (dd, *J* = 16.3, 6.1 Hz, 1H), 3.28 (dd, *J* = 16.2, 7.6 Hz, 1H), 2.84 (s, 8H).
HRMS, m/z: [M]+ calc. for $C_{34}H_{30}Br_4N_2O_2$, 818.24; found, 818.91.

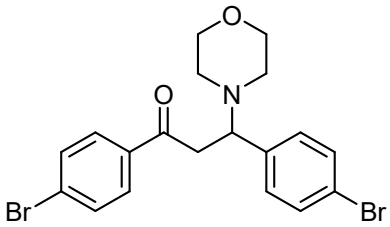

1,3-bis(4-bromophenyl)-3-morpholinopropan-1-one (3c): ^{1}H NMR (600 MHz, $CDCl_3$): *δ*/ ppm = 7.73 (d, *J* = 8.5 Hz, 2H), 7.58 (d, *J* = 8.5 Hz, 2H), 7.42 (d, *J* = 8.4 Hz, 2H), 7.17 (d, *J* = 8.4 Hz, 1H), 4.09 (t, *J* = 6.7 Hz, 1H), 3.68 (m, 4H), 2.40 (m, 4H).
HRMS, m/z: [M]+ calc. for $C_{19}H_{19}Br_2NO_2$, 453.17; found, 453.98.

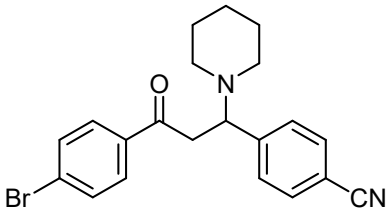

4-(3-(4-bromophenyl)-3-oxo-1-(piperidin-1-yl)propyl)benzonitrile (5a): ^{1}H NMR (600 MHz, $CDCl_3$): *δ*/ ppm = 7.76 (d, *J* = 7.9 Hz, 2H), 7.58 (t, *J* = 10.1 Hz, 4H), 7.39 (d, *J* = 7.3 Hz, 2H), 4.24 (s, 1H), 3.55 (dd, *J* = 16.4, 4.7 Hz, 1H), 3.31 (dd, *J* = 16.4, 7.6 Hz, 1H), 2.34 (d, *J* = 39.2 Hz, 4H), 1.51 (s, 4H), 1.35 (s, 2H). HRMS, m/z: [M]+ calc. for $C_{21}H_{21}BrN_2O$, 396.08; found, 397.09.

Table S1. Outcome of reaction between **1** and **2a-c** determined by solution ^{1}H NMR spectroscopy.

Entry	Chalcone	Amine (amount)	NMR yield (%)[a]
1	**1** (Br-Br)	**2a** (1 equiv.)	98
2	**1** (Br-Br)	**2a** (0.5 equiv.)	58
3	**1** (Br-Br)	**2a** (1 equiv.)	70[b]
5	**1** (Br-Br)	**2b** (1 equiv.)	71 (single-product)
6	**1** (Br-Br)	**2b** (1 equiv.)	80[g] (single-product)
7	**1** (Br-Br)	**2c**	87

		(1 equiv.)	
8	**4** (Br-CN)	**2a** (1 equiv.)	78

[a]Reaction setup: IST500 vibratory ball mill, 30 Hz, **1** or **4** (1 mmol), 14.0 mL PMMA jar, two ZrO_2 milling balls (1.6 g), 2 h, air, r.t. ^{1}H NMR yield calculated by integral signal ratio of starting chalcone (**1**: δ = 7.88 ppm, 2H; **4**: δ = 7.89 ppm, 2H) and product (aromatic region). [b] Materials were put in the cell in the vapour of the **2a** during one week. [g] Liquid-assisted grinding (LAG) (20 µL $CHCl_3$) with external heating at 50 °C.

Table S2. Outcome of optimization of reaction between **1** and **2b**.

Entry	Chalcone	Amine (amount)	NMR yield of **3b**(%)[a]
1	**1**	**2b** (1 equiv.)	71
2	**1**	**2b** (0.5 equiv.)	26
3	**1**	**2b** (1 equiv.)	59[b]
4	**1**	**2b** (1 equiv.)	65[c]
5	**1**	**2b** (1 equiv.)	32[d]
6	**1**	**2b** (1 equiv.)	32[e]
7	Mixture from **entry 2**	-	72[e]
8	Mixture from **entry 3**	-	**84**[e]
9	**1** (Br-Br)	**2b** (2 equiv.)	**49**

[a]Reaction setup: IST500 vibratory ball mill, 30 Hz, **1** (1 mmol), 14.0 mL PMMA jar, two ZrO_2 milling balls (1.6 g), 2 h, air, r.t. ^{1}H NMR yield calculated by integral ratio of starting chalcone and product. [b]4 h duration of milling. [c] Overnight milling. [d]Reaction conducted in 5 mL $CHCl_3$, 4 h duration of stirring in solution. [e]LAG (20 µL $CHCl_3$), 4 h of milling.

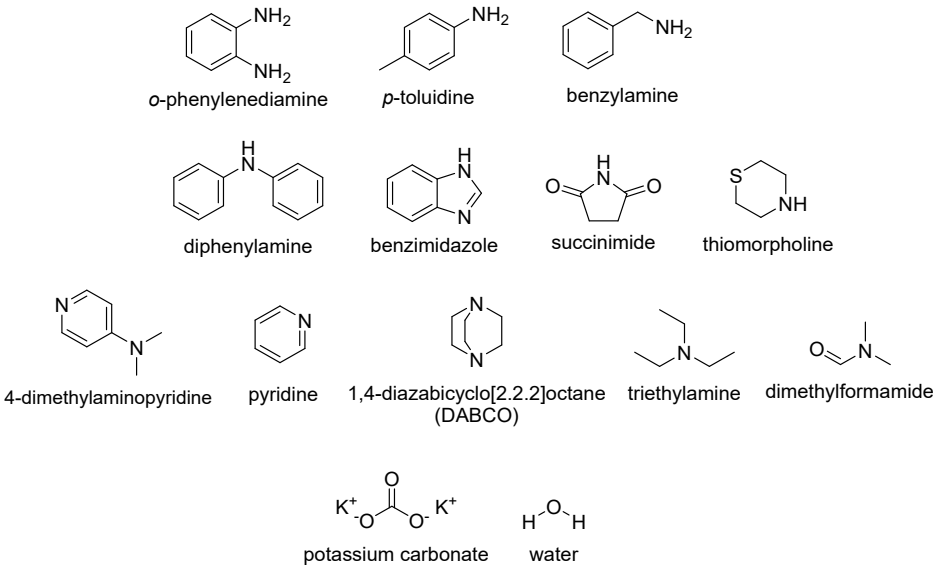

Scheme S4. List of used nitrogen nucleophiles as Michael donors in aza-Michael addition reaction which did not promote reaction to the desired products using standard mechanochemical protocol.

2. PXRD data

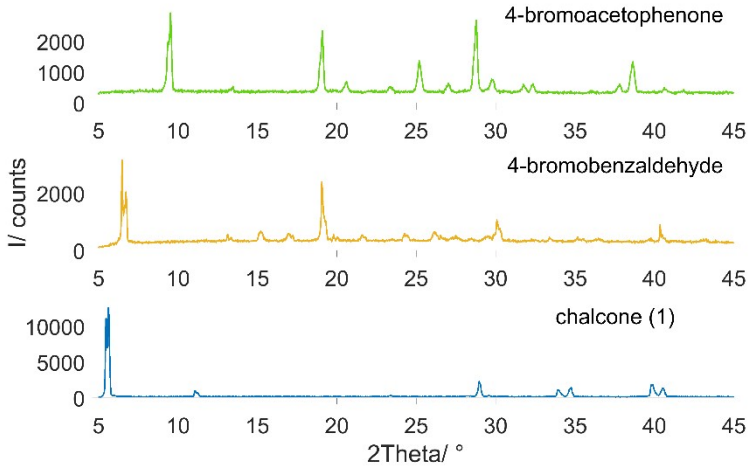

Figure S3. Comparison of powder X-ray diffraction patterns: (from top to bottom) 4-bromoacetophenone, 4-bromobenzaldehyde and **1** (Br-Br chalcone).

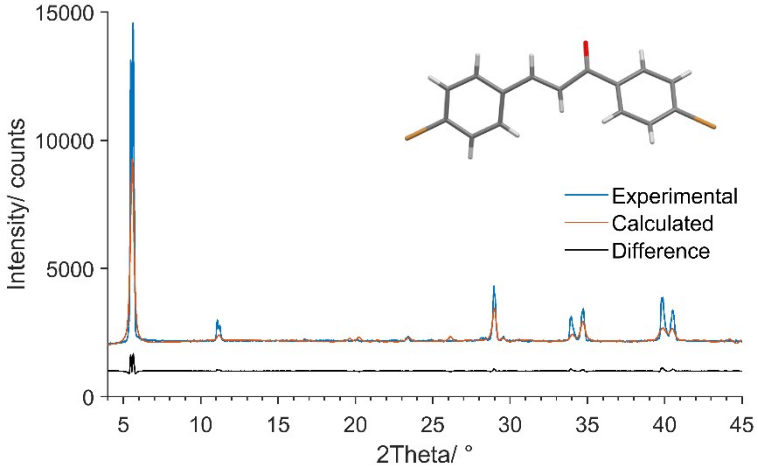

Figure S4. X-ray diffraction pattern of **1** (Br-Br chalcone). The diffraction pattern corresponds to the diffractogram of desired product (CSD refcode for calculated diffractogram: LEHROG).[5]

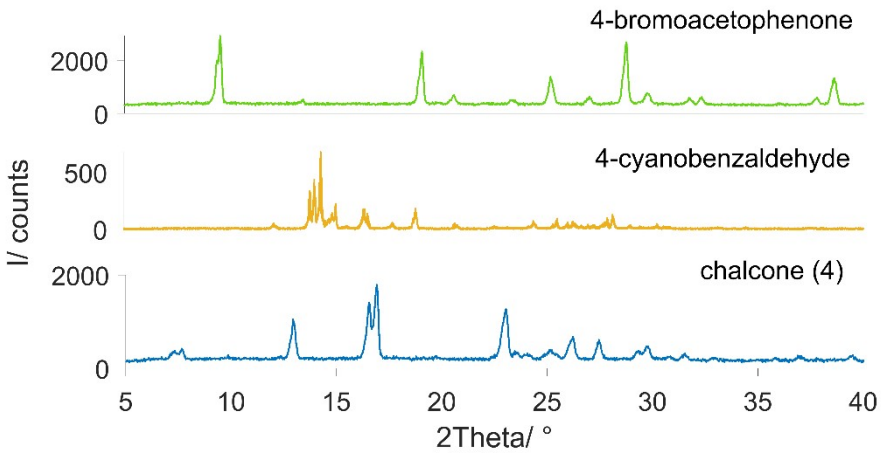

Figure S5. Comparison of powder X-ray diffraction patterns: (from top to bottom) 4-bromoacetophenone, 3-cyanobenzaldehyde and **4** (Br-CN chalcone).

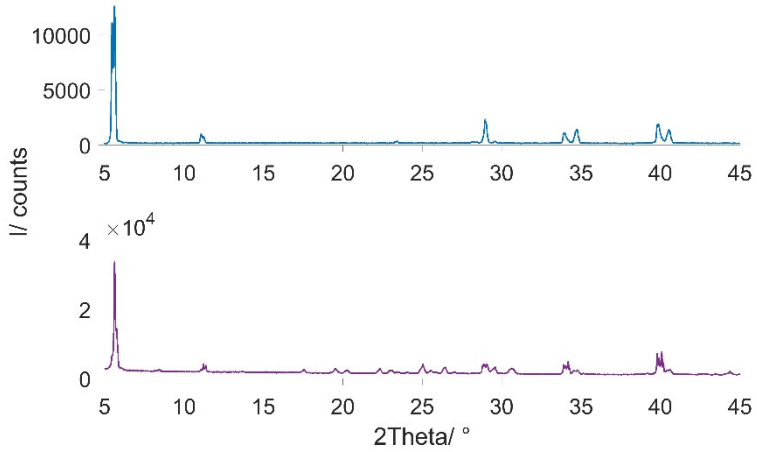

Figure S6. Comparison of powder X-ray diffraction patterns: (from top to bottom) **1** and crude reaction mixture collected after milling of **1** for 120 min at 30 Hz milling frequency (control experiment).

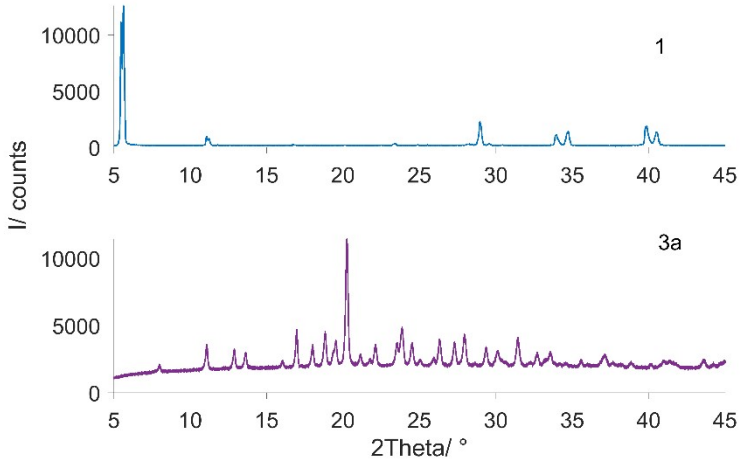

Figure S7. Comparison of powder X-ray diffraction patterns of reactant **1** and crude reaction mixture collected after milling **1** and **2a** that corresponds to the pure product **3a**.

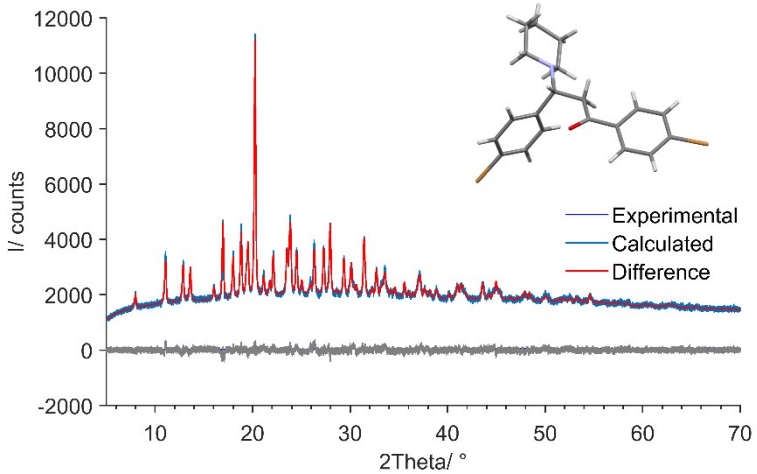

Figure S8. X-ray diffraction pattern of **3a**. The powder diffraction pattern corresponds to the diffractogram of desired product (CSD refcode for solved pattern: 2343064).

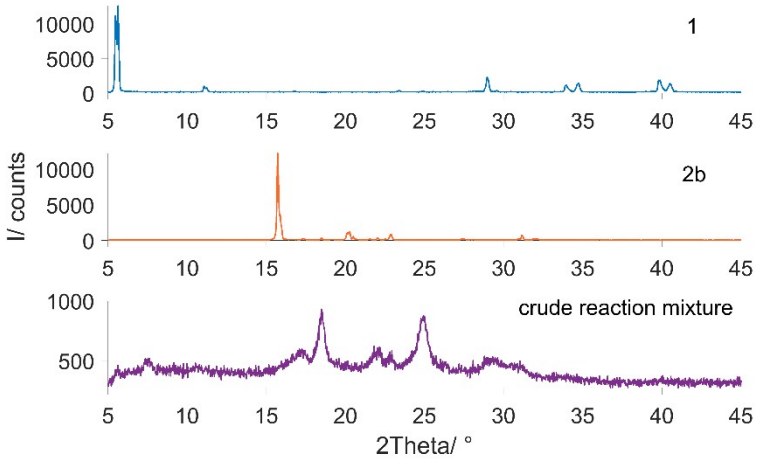

Figure S9. Comparison of powder X-ray diffraction patterns of reactants **1** and **2b** with crude reaction mixture collected immediately after milling of starting materials in equimolar ratio for 120 min at 30 Hz milling frequency. The resulting diffraction pattern is amorphous and according to the ^{1}H NMR spectra data corresponds to a 71% conversion towards single addition product **3b**).

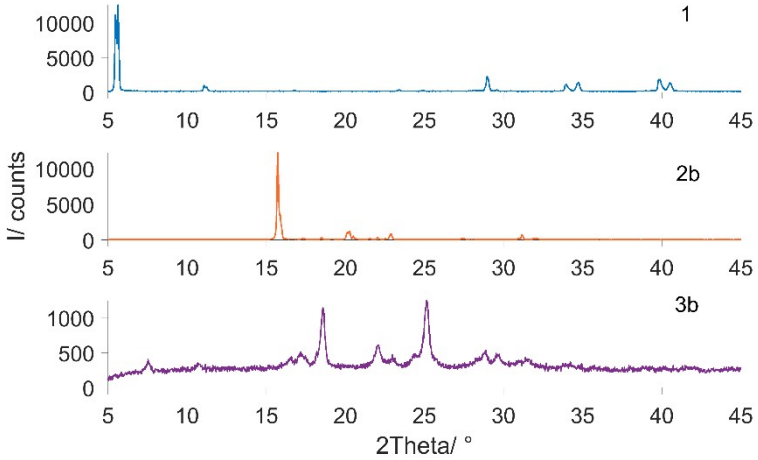

Figure S10. Comparison of powder X-ray diffraction patterns of reactants **1** and **2b** with crude reaction mixture collected immediately after liquid-assisted grinding (V($CHCl_3$) = 20 µL) of starting materials in equimolar ratio for 120 min at 30 Hz milling frequency, with external heating at 50°C. The resulting diffraction pattern is amorphous and according to the ^{1}H NMR spectra data corresponds to a 80% conversion towards single addition product **3b**).

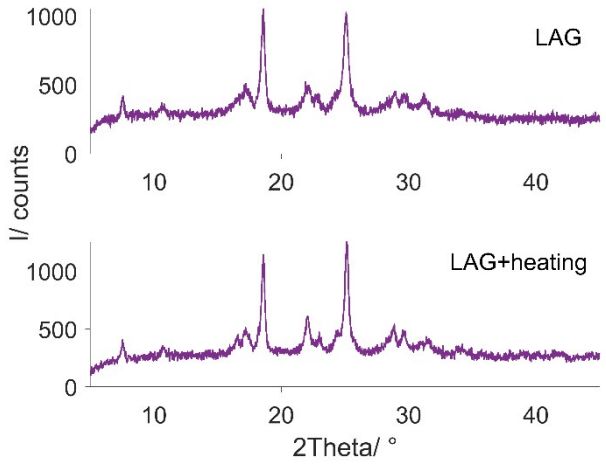

Figure S11. Comparison of powder X-ray diffraction patterns of crude powder reaction mixtures prepared by (top) liquid-assisted grinding V($CHCl_3$) = 20 µL and (bottom) liquid-assisted grinding V($CHCl_3$) = 20 µL and heating at 50 °C of reactants **1** and **2b** in equimolar ratio for 120 min at 30 Hz milling frequency. The resulting diffraction pattern is less amorphous when heating is performed. ^{1}H NMR conversion is higher in the case when heating is applied (80% to single addition product, **3b**).

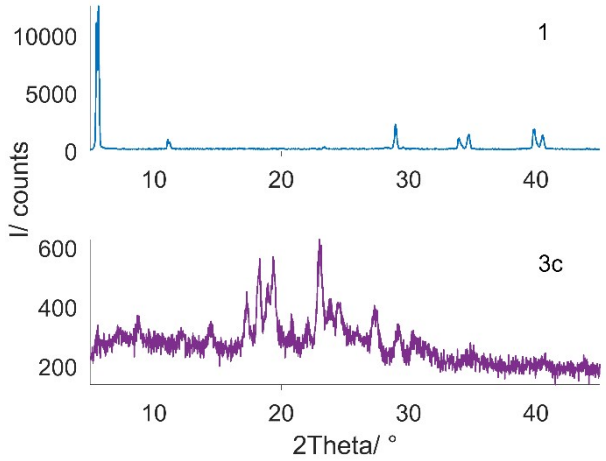

Figure S12. Comparison of powder X-ray diffraction patterns of reactant **1** and crude reaction mixture collected immediately after milling of **1** and **2c** in equimolar ratio for 120 min at 30 Hz milling frequency. The resulting diffraction pattern is amorphous and according to the ^{1}H NMR spectra data corresponds to a product **3c**.

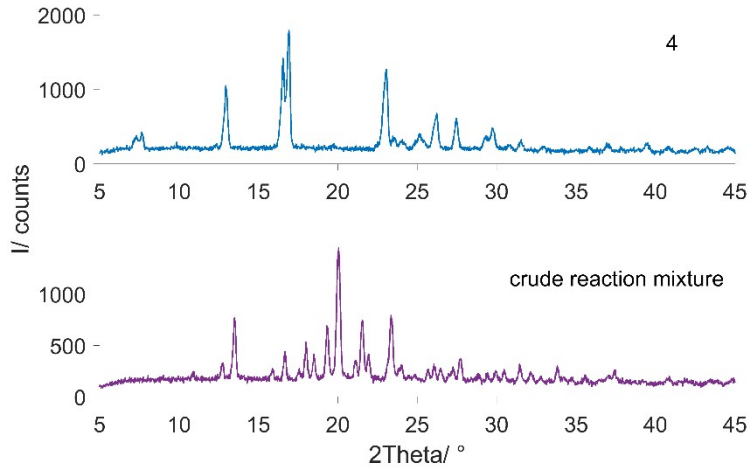

Figure S13. Comparison of powder X-ray diffraction patterns of reactant **4** and collected crude reaction mixture immediately after milling of starting materials, **4** and **2a** in equimolar ratio for 120 min at 30 Hz milling frequency.

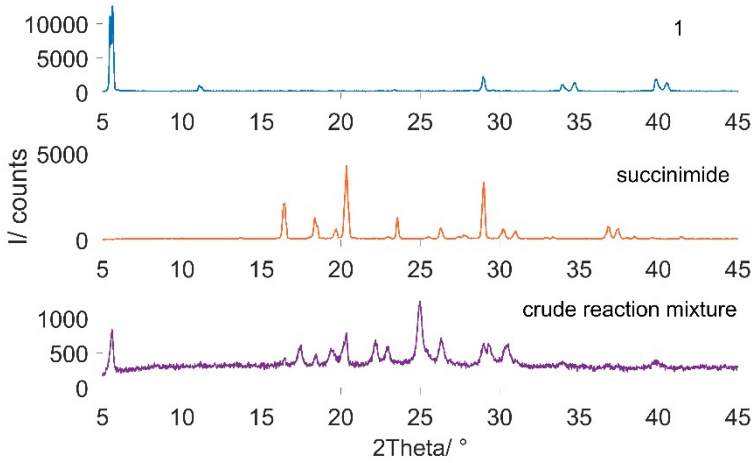

Figure S14. Comparison of powder X-ray diffraction patterns of reactants **1** and succinimide with collected crude reaction mixture immediately after milling of starting materials in equimolar ratio for 120 min at 30 Hz milling frequency. The diffraction pattern corresponds to a mixture of starting materials, with no observation of a new phase (in accordance to the ^{1}H NMR spectra).

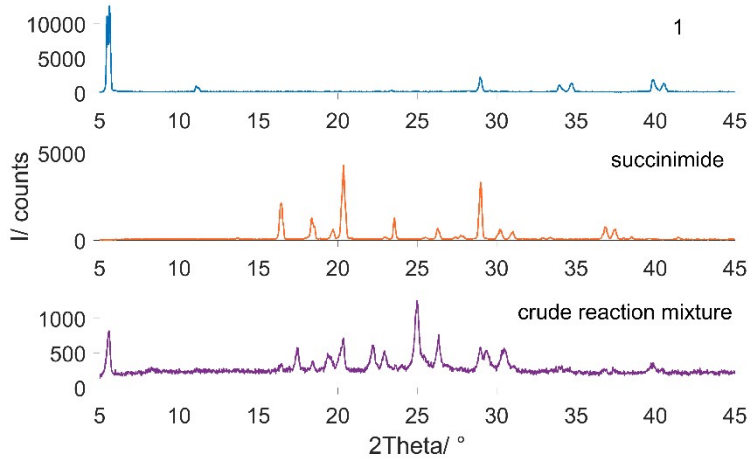

Figure S15. Comparison of powder X-ray diffraction patterns of reactants **1** and succinimide with collected crude reaction mixture immediately after overnight milling of starting materials in equimolar ratio at 30 Hz milling frequency. The diffraction pattern corresponds to a mixture of starting materials, with no observation of a new phase (in accordance to the ^{1}H NMR spectra).

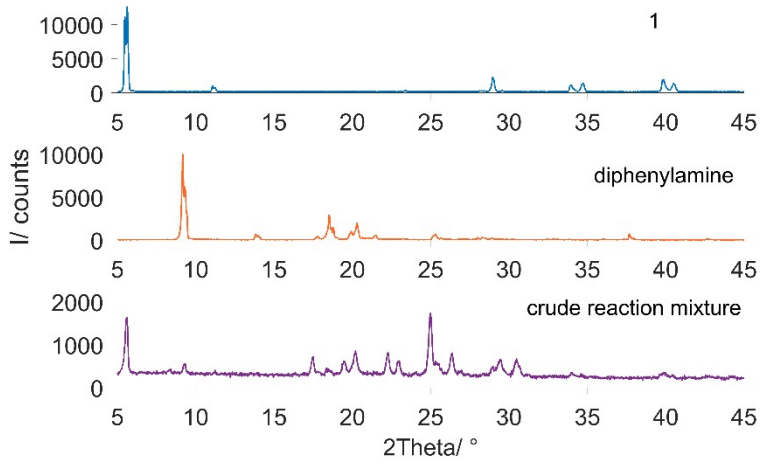

Figure S16. Comparison of powder X-ray diffraction patterns of reactants **1** and diphenylamine with collected crude reaction mixture immediately after milling of starting materials in equimolar ratio for 120 min at 30 Hz milling frequency. The diffraction pattern corresponds to a mixture of starting materials, with no observation of a new phase (in accordance to the ^{1}H NMR spectra). The same is observed after overnight grinding under the same conditions.

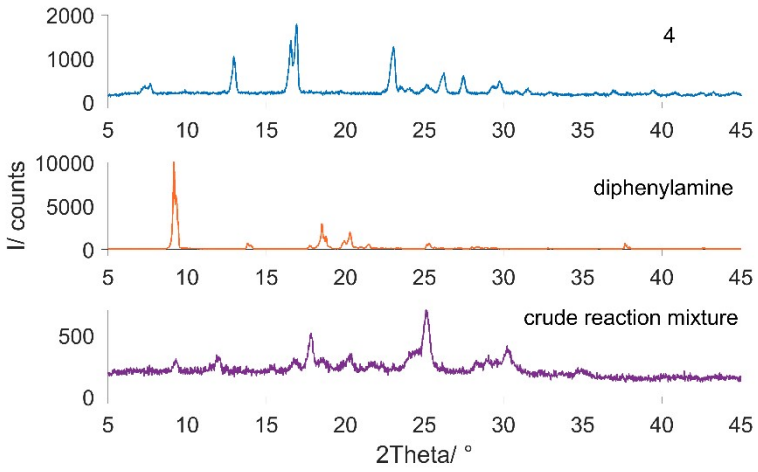

Figure S17. Comparison of powder X-ray diffraction patterns of reactants **4** and diphenylamine with collected crude reaction mixture immediately after milling of starting materials in equimolar ratio for 120 min at 30 Hz milling frequency. The diffraction pattern corresponds to a mixture of starting materials, with no observation of a new phase (in accordance to the ^{1}H NMR spectra).

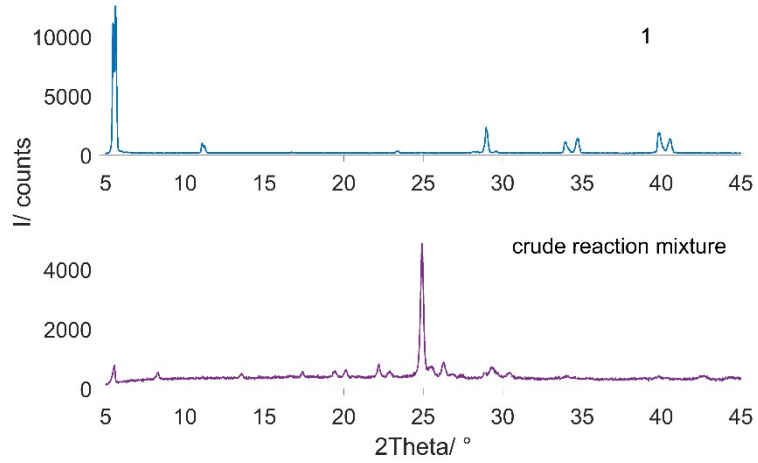

Figure S18. Comparison of powder X-ray diffraction patterns of reactants **1** and collected crude reaction mixture immediately after overnight milling of starting materials **1** and benzylamine in equimolar ratio at 30 Hz milling frequency. The diffraction pattern corresponds to a mixture of starting materials, with no observation of a new phase (in accordance to the ^{1}H NMR spectra).

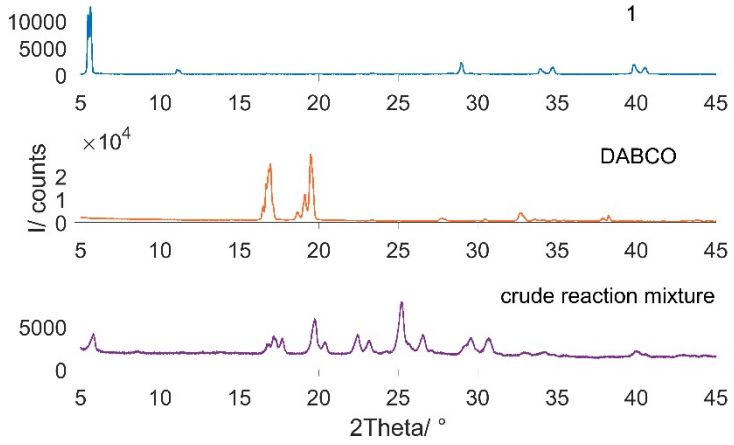

Figure S19. Comparison of powder X-ray diffraction patterns of reactants **1** and DABCO with collected crude reaction mixture immediately after milling of starting materials in equimolar ratio for 120 min at 30 Hz milling frequency. The diffraction pattern corresponds to a mixture of starting materials, with no observation of a new phase (in accordance to the ^{1}H NMR spectra).

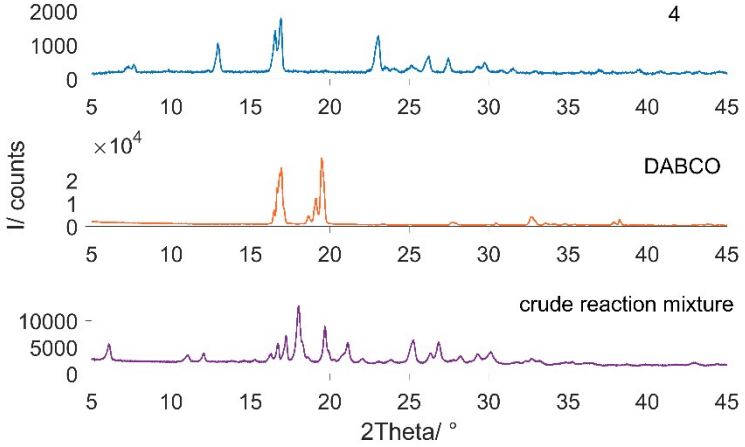

Figure S20. Comparison of powder X-ray diffraction patterns of reactants, **4** and DABCO (1 equiv.) with collected crude reaction mixture immediately after milling for 120 min at 30 Hz milling frequency. The diffraction pattern corresponds to a mixture of starting materials, with no observation of a new phase (in accordance to the ^{1}H NMR spectra).

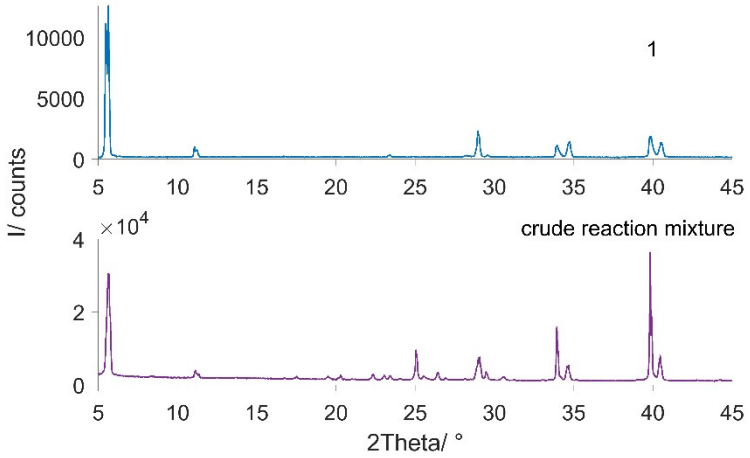

Figure S21. Comparison of powder X-ray diffraction patterns of reactant **1** and collected crude reaction mixture immediately after milling of starting materials **1** and triethylamine in equimolar ratio for 120 min at 30 Hz milling frequency. The diffraction pattern corresponds to a mixture of starting materials, with no observation of a new phase (in accordance to the ^{1}H NMR spectra).

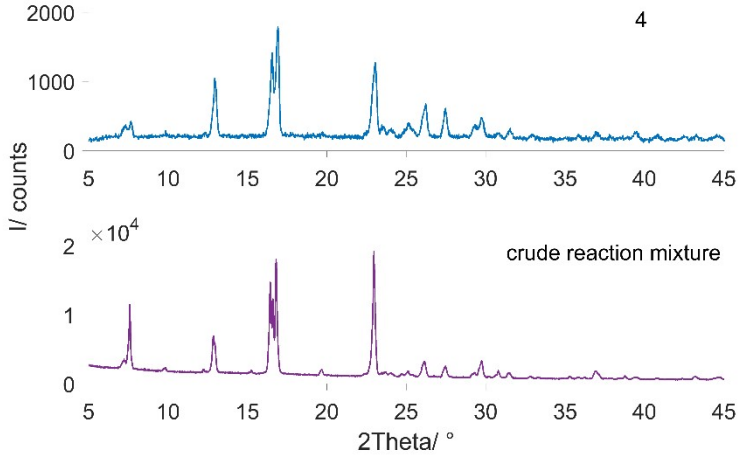

Figure S22. Comparison of powder X-ray diffraction patterns of reactant **4** and collected crude reaction mixture immediately after milling of starting materials, **4** and triethylamine for 120 min at 30 Hz milling frequency. The diffraction pattern corresponds to a mixture of starting materials, with no observation of a new phase (in accordance to the ^{1}H NMR spectra).

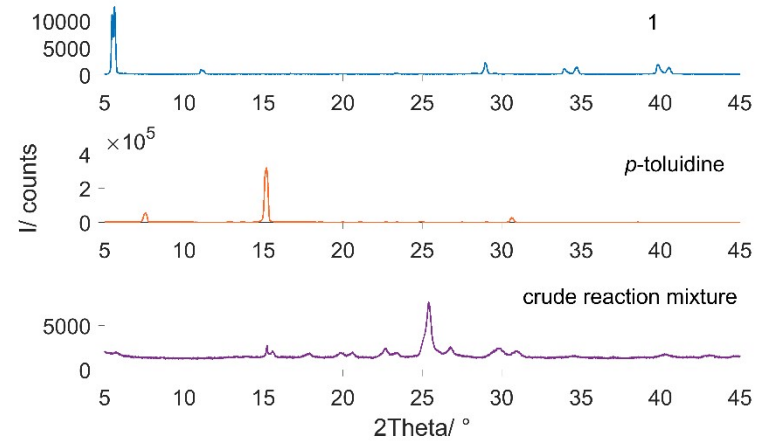

Figure S23. Comparison of powder X-ray diffraction patterns of reactants **1** and *p*-toluidine with collected crude reaction mixture immediately after milling of starting materials in equimolar ratio for 120 min at 30 Hz milling frequency. The diffraction pattern corresponds to a mixture of starting materials, with no observation of a new phase (in accordance to the ^{1}H NMR spectra).

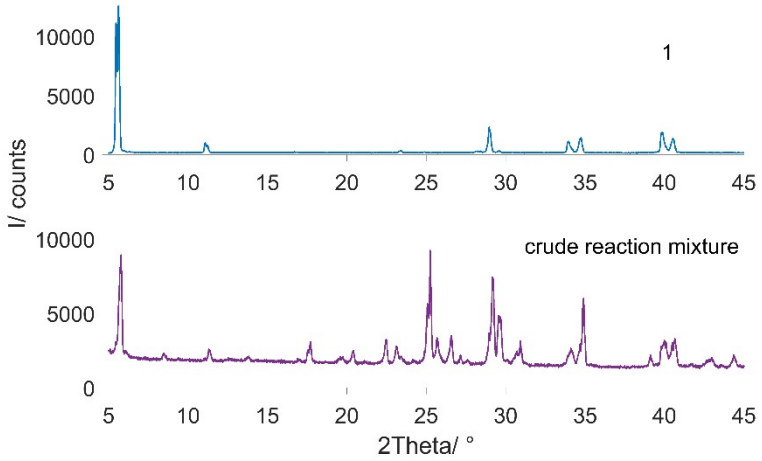

Figure S24. Comparison of powder X-ray diffraction patterns of reactant **1** and collected crude reaction mixture immediately after milling of starting materials, **1** and dimethylformamide in equimolar ratio for 120 min at 30 Hz milling frequency. The diffraction pattern corresponds to a mixture of starting materials, with no observation of a new phase (in accordance to the ^{1}H NMR spectra).

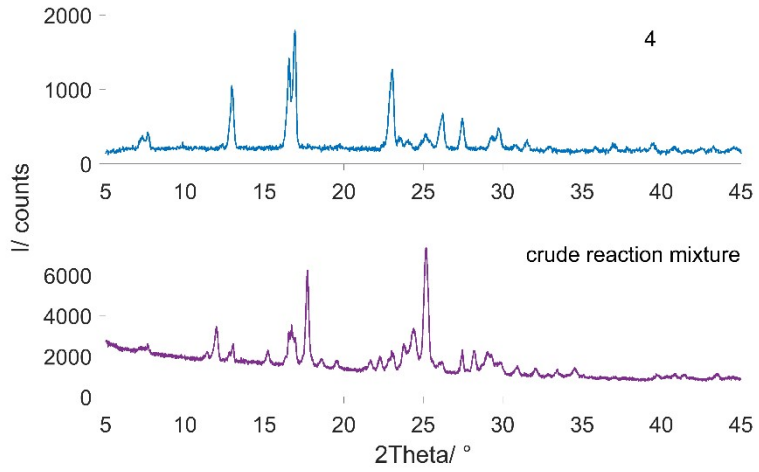

Figure S25. Comparison of powder X-ray diffraction patterns of reactant **4** and collected crude reaction mixture immediately after milling of starting materials, **4** and dimethylformamide in equimolar ratio for 120 min at 30 Hz milling frequency. The diffraction pattern corresponds to a mixture of starting materials, with no observation of a new phase (in accordance to the ^{1}H NMR spectra).

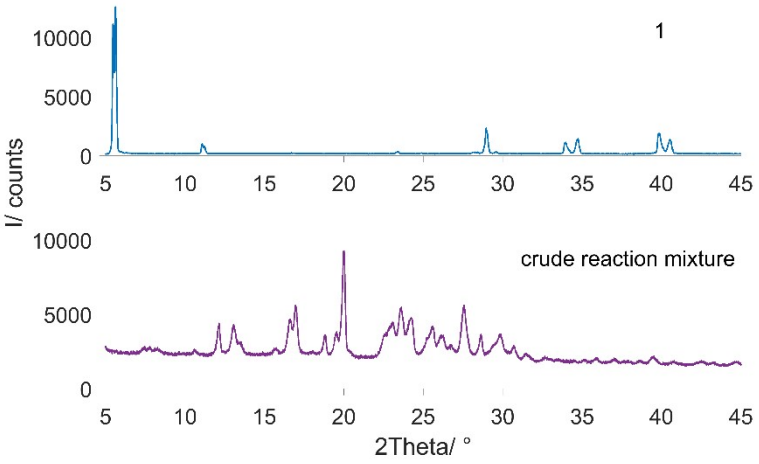

Figure S26. Comparison of powder X-ray diffraction patterns of reactant **1** and collected crude reaction mixture immediately after milling of starting materials, **1** and 4-dimethylaminopyridine in equimolar ratio for 120 min at 30 Hz milling frequency. The diffraction pattern corresponds to a mixture of starting materials, with no observation of a new phase (in accordance to the ^{1}H NMR spectra).

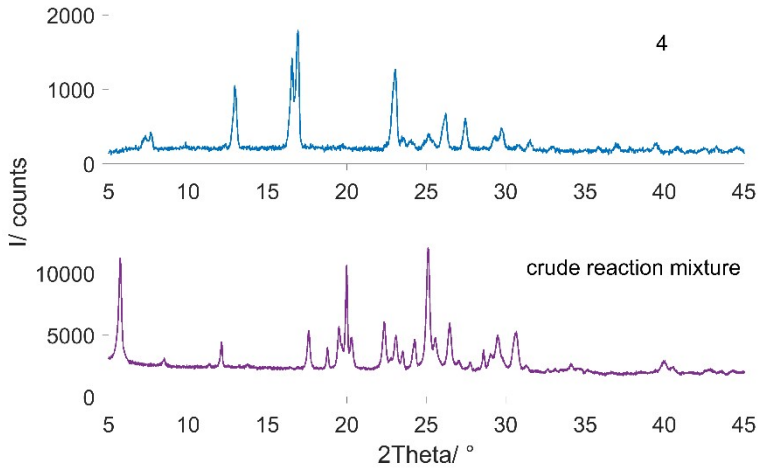

Figure S27. Comparison of powder X-ray diffraction patterns of reactant **4** and collected crude reaction mixture immediately after milling of starting materials, **4** and 4-dimethylaminopyridine in equimolar ratio for 120 min at 30 Hz milling frequency. The diffraction pattern corresponds to a mixture of starting materials, with no observation of a new phase (in accordance to the ^{1}H NMR spectra).

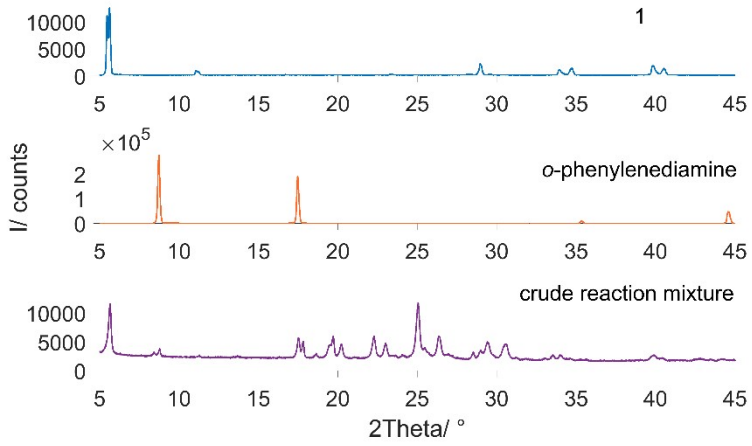

Figure S28. Comparison of powder X-ray diffraction patterns of reactant **1** and collected crude reaction mixture immediately after milling of starting materials, **1** and *o*-phenylenediamine in equimolar ratio for 120 min at 30 Hz milling frequency. The diffraction pattern corresponds to a mixture of starting materials, with no observation of a new phase (in accordance to the ^{1}H NMR spectra).

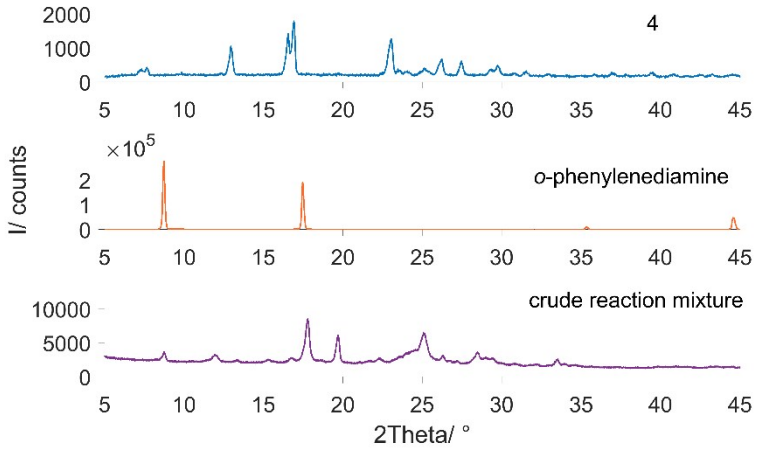

Figure S29. Comparison of powder X-ray diffraction patterns of reactant **4** and collected crude reaction mixture immediately after milling of starting materials, **4** and o-phenylenediamine in equimolar ratio for 120 min at 30 Hz milling frequency. The diffraction pattern corresponds to a mixture of starting materials, with no observation of a new phase (in accordance to the ^{1}H NMR spectra).

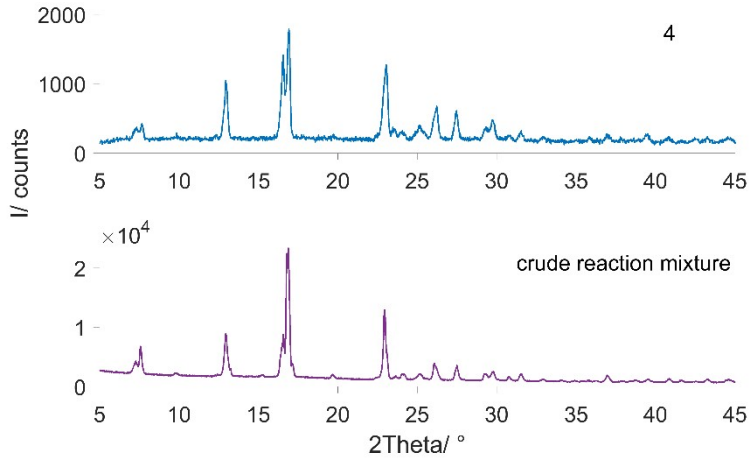

Figure S30. Comparison of powder X-ray diffraction patterns of reactant **4** and collected crude reaction mixture immediately after milling of starting materials, **4** and pyridine for 120 min at 30 Hz milling frequency. The diffraction pattern corresponds to a mixture of starting materials, with no observation of a new phase (in accordance to the ^{1}H NMR spectra).

3. HR-MS data

Compound 3a:

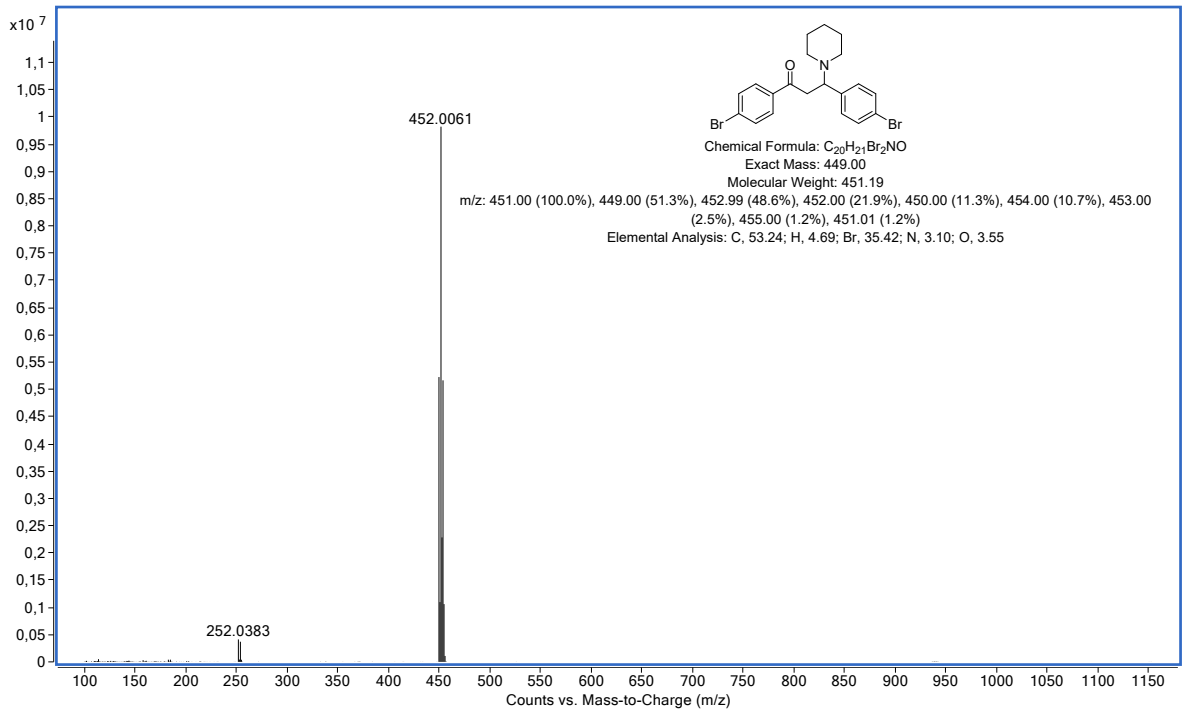

Figure S31. HR-MS spectra of **3a** recorded in positive ion mode that shows the molecular ion peak (retention time at 6.216 min) at 452.0061 m/z corresponding to the protonated molecular ion.

Compound 3b:

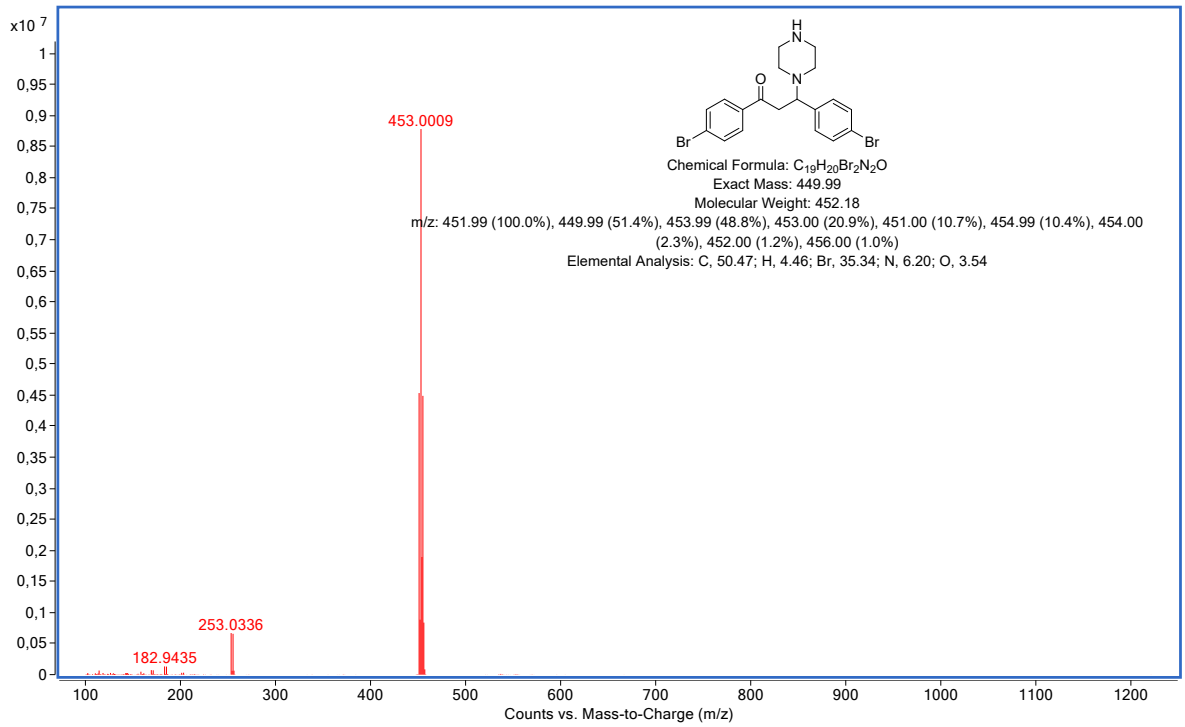

Figure S32. HR-MS spectra of a reaction mixture of single(**3b**) and double (**3b'**) addition product. (top) The most intense peak (retention time at 6.019 min) at 453.0009 m/z indicates the molecular ion peak of **3b**.

Compound 3b':

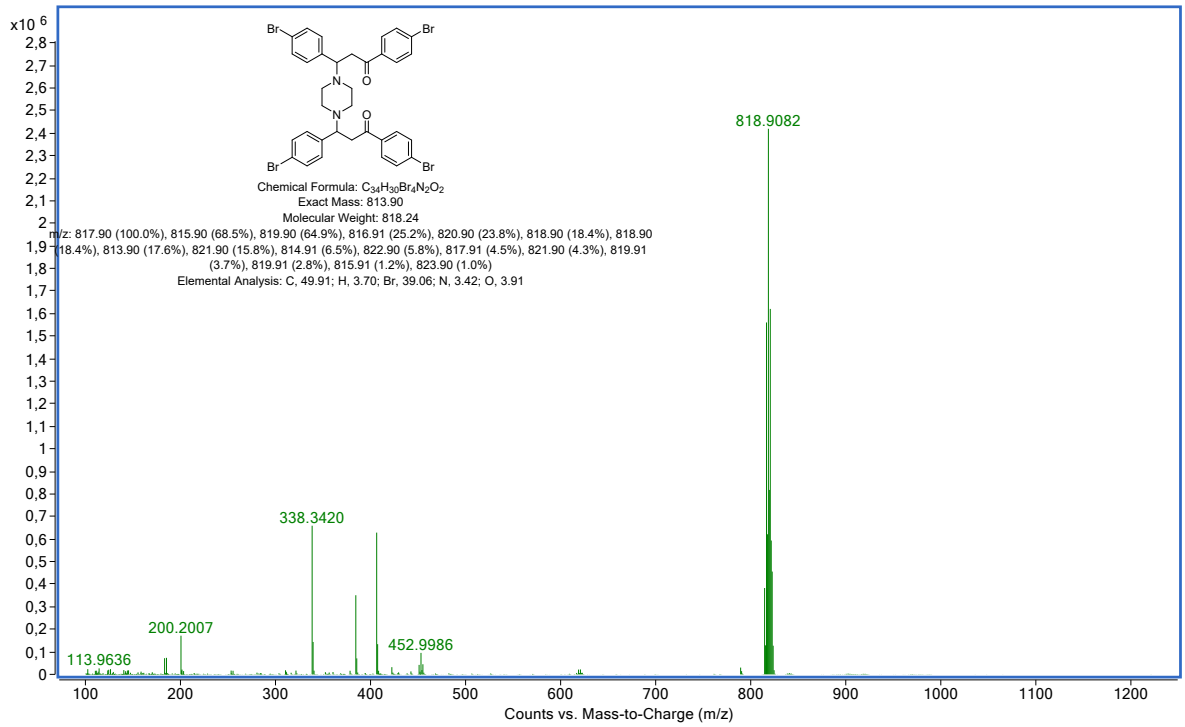

Figure S33. HR-MS spectra of **3b'** (retention time at 8.352 min).

Compound 3c:

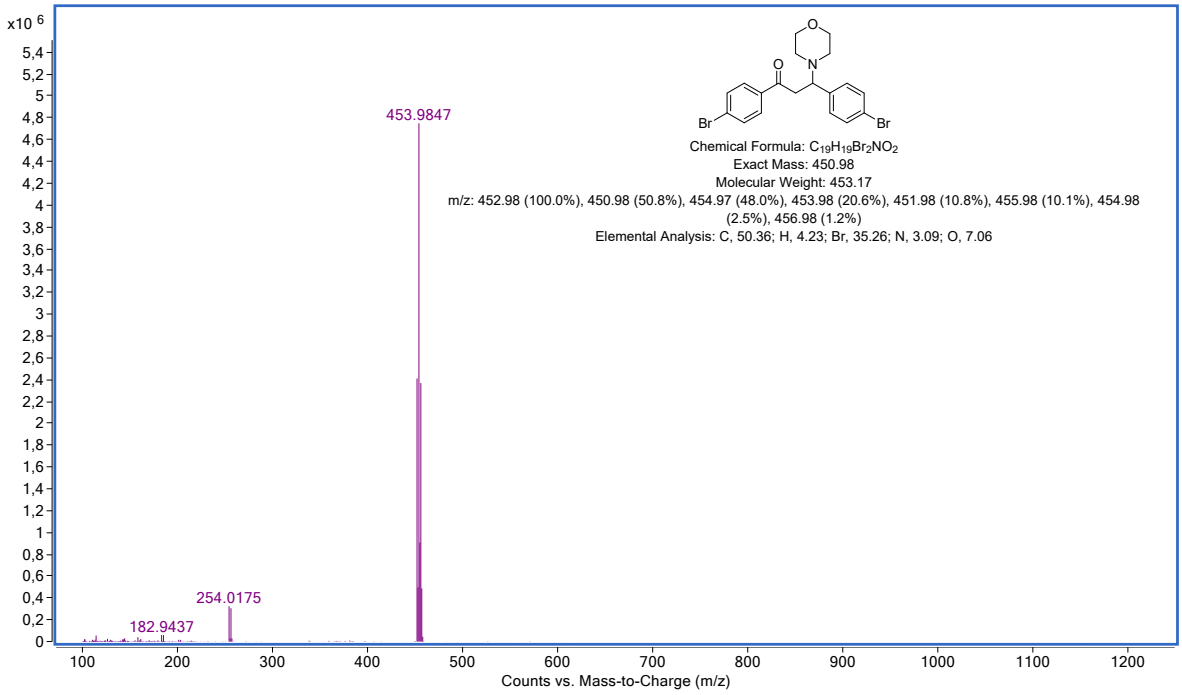

Figure S34. HR-MS spectra of **3c** recorded in a positive ion mode that shows the molecular ion peak (retention time at 6.258 min) at 453.9847 m/z corresponding to the protonated molecular ion.

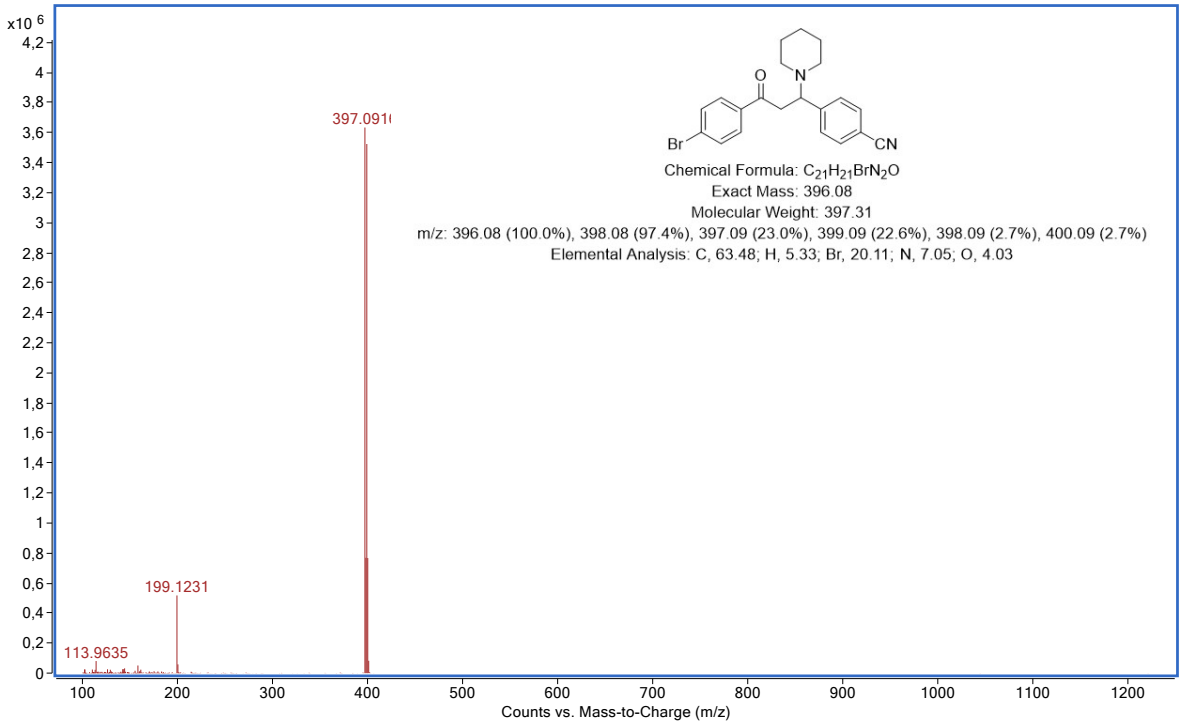

Figure S35. HR-MS spectra of a product **5** formed after milling **4** (Br-CN chalcone) and **2a**. The spectra is recorded in a positive ion mode and shows the molecular ion peak (retention time at 5.568 min) at 397.0916 m/z corresponding to the protonated molecular ion.

^{1}H NMR spectra

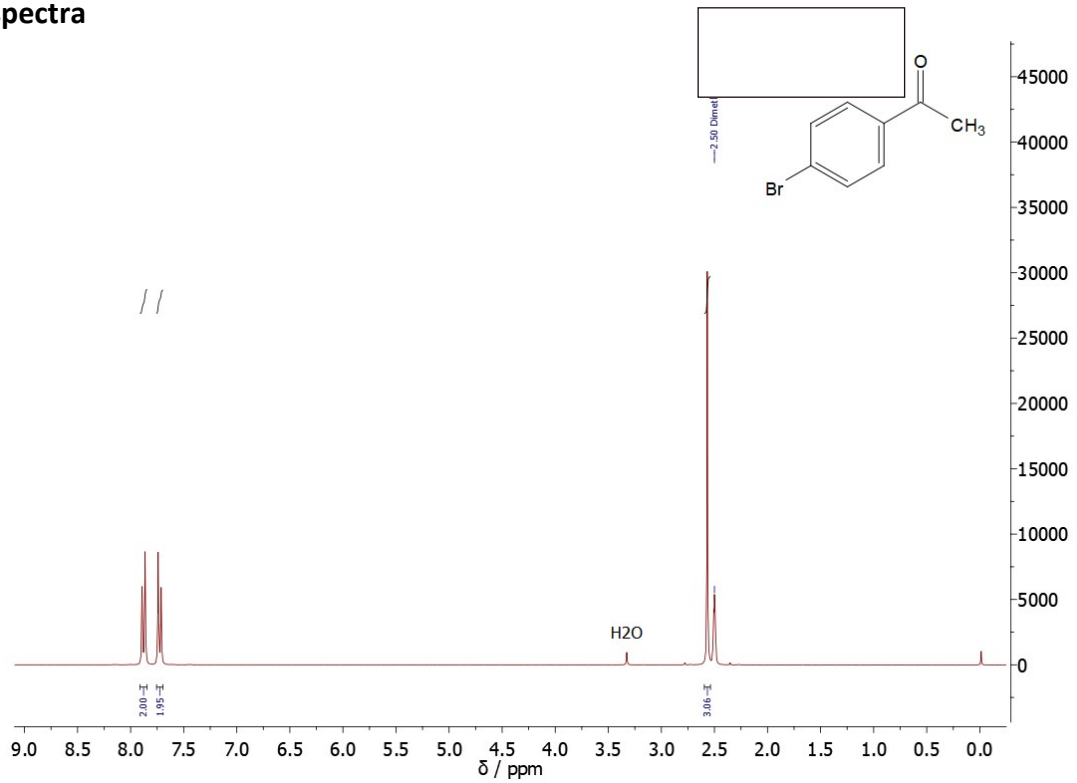

Figure S36. ^{1}H NMR spectrum (DMSO, 300 MHz) of starting material, 4-bromoacetophenone for the preparation of chalcone **1**.

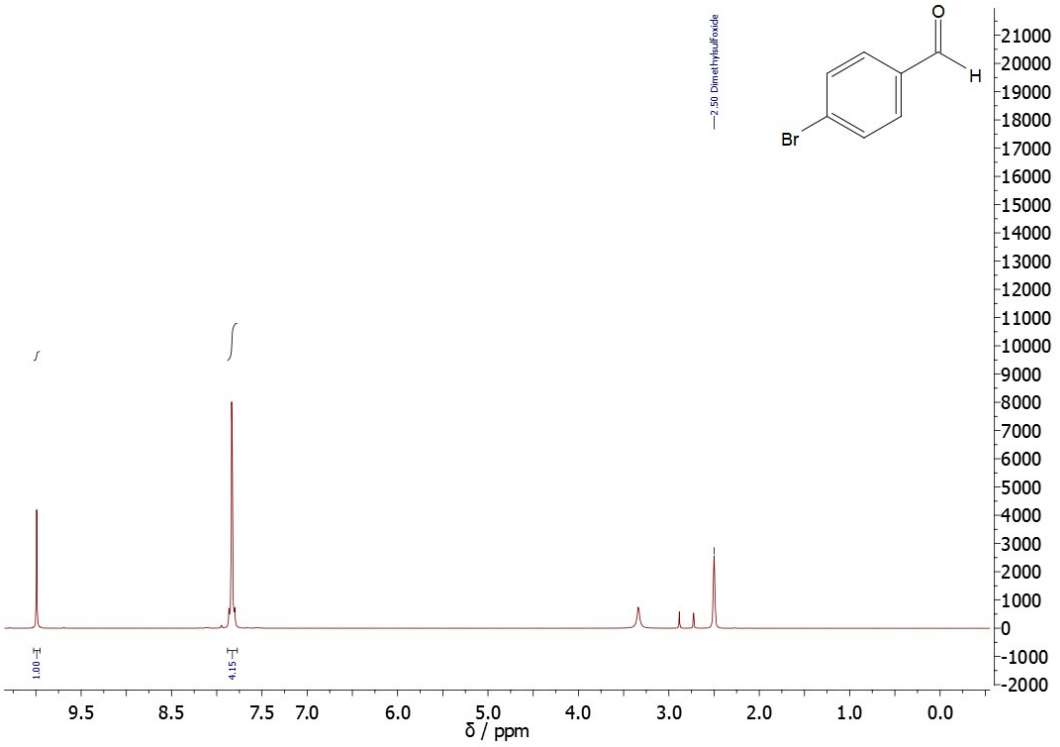

Figure S37. ^{1}H NMR spectrum (DMSO, 300 MHz) of starting material, 4-bromobenzaldehyde for the preparation of chalcone **1**.

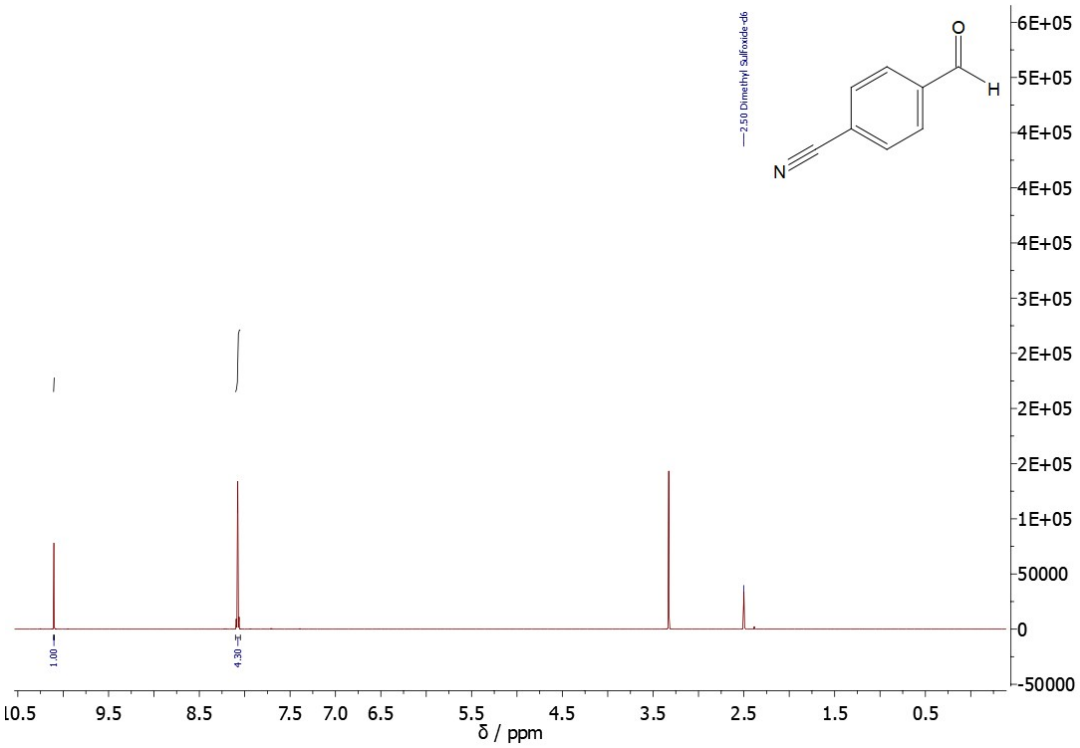

Figure S38. ^{1}H NMR spectrum (DMSO, 600 MHz) of starting material, 4-formylbenzonitrile for the preparation of chalcone **4**.

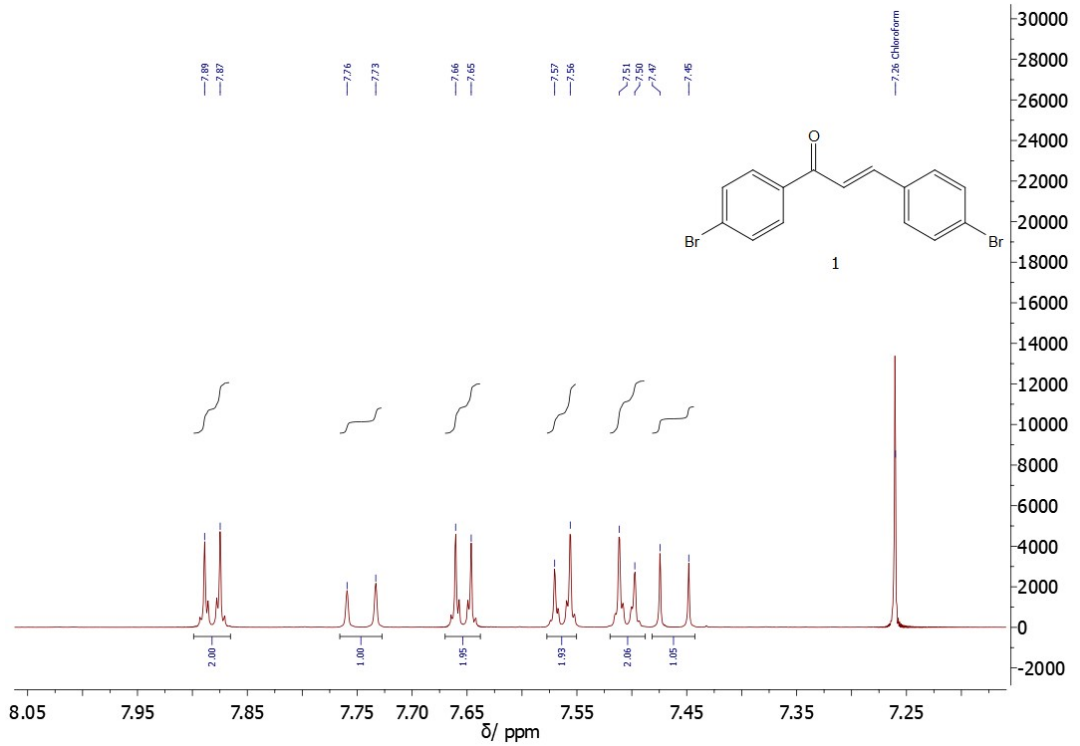

Figure S39. ^{1}H NMR spectrum ($CDCl_3$, 600 MHz) of pure **1** (Br-Br chalcone).

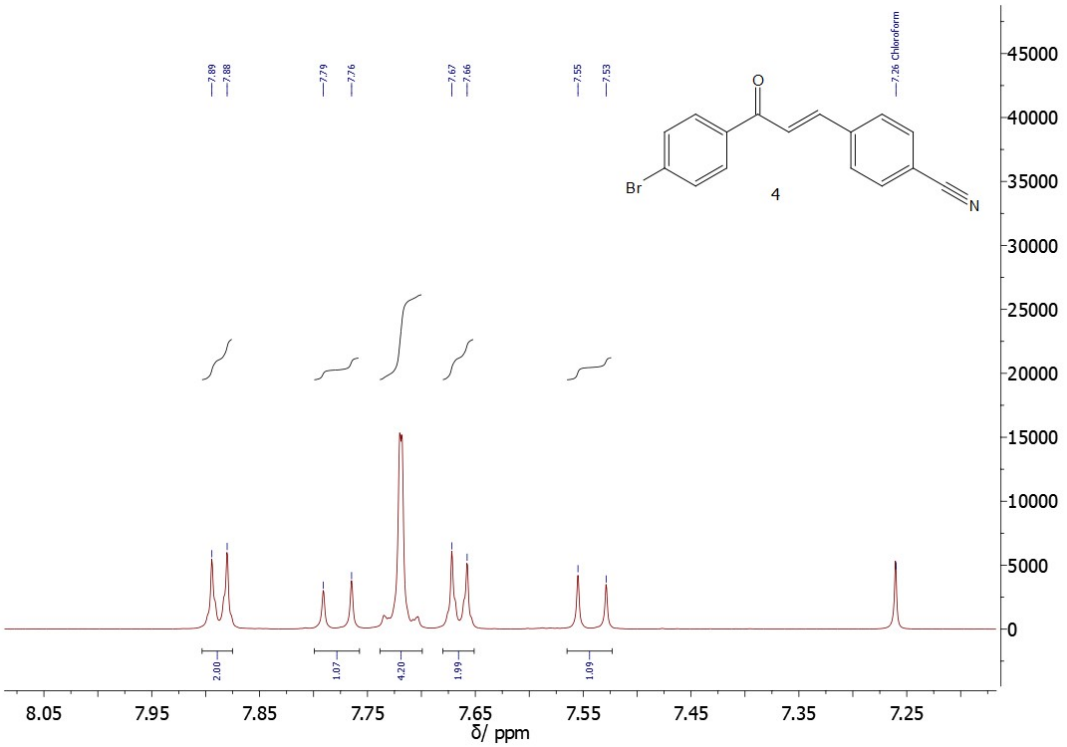

Figure S40. ^{1}H NMR spectrum ($CDCl_3$, 600 MHz) of pure **4** (Br-CN chalcone).

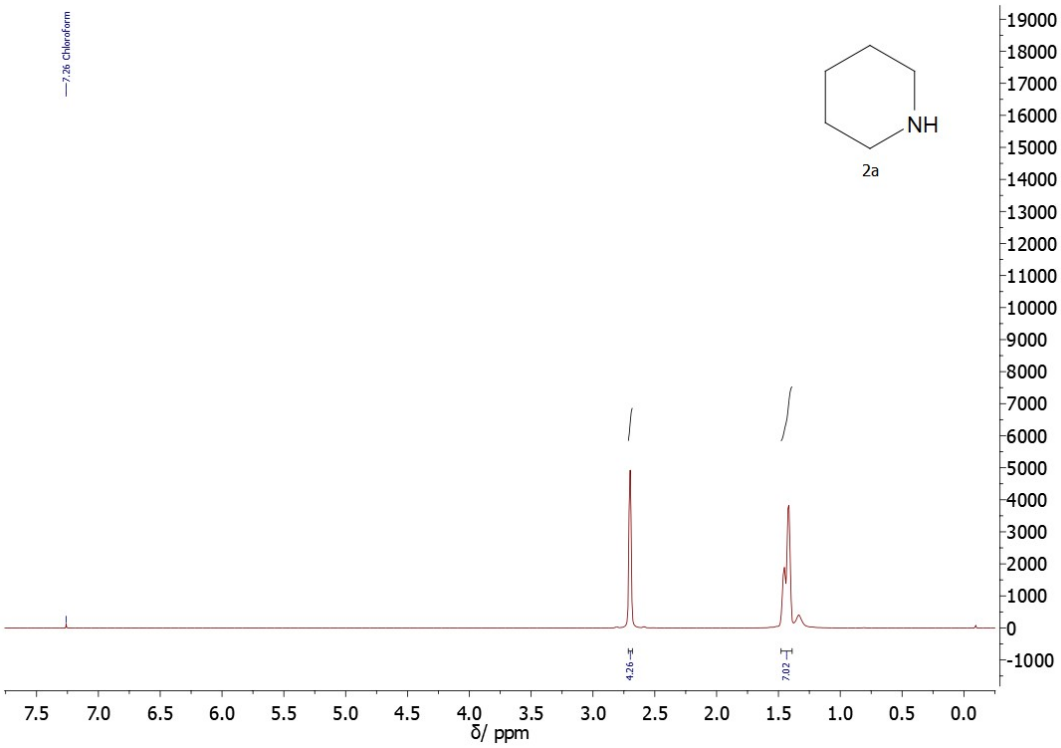

Figure S41. ^{1}H NMR spectrum ($CDCl_3$, 600 MHz) of **2a**.

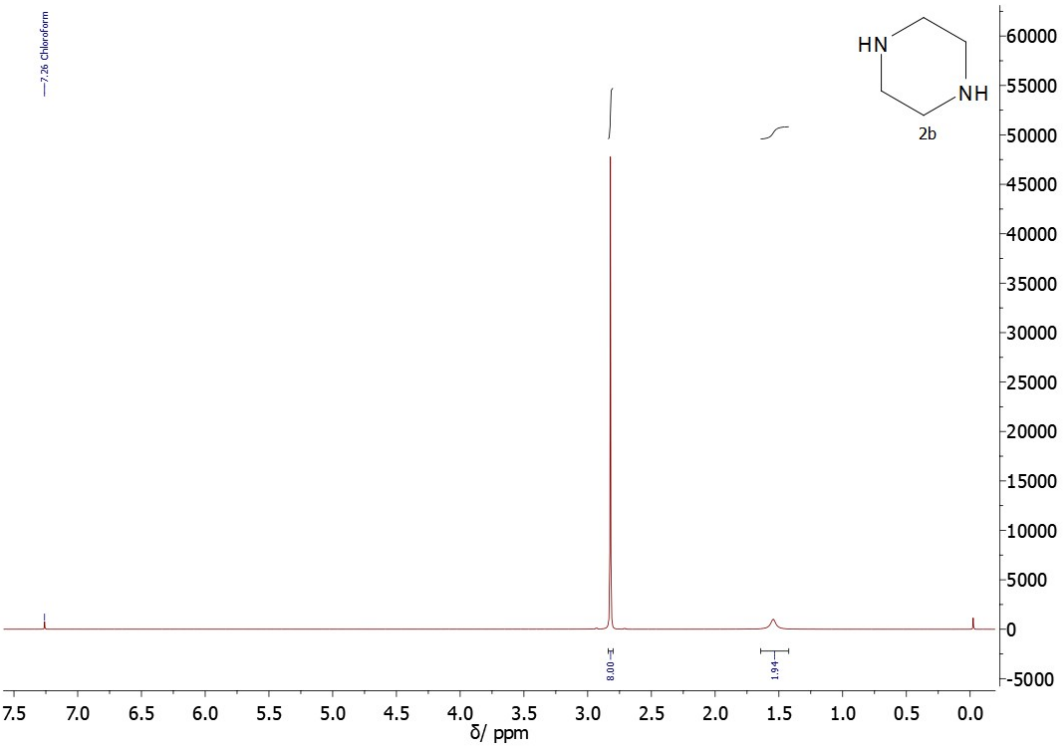

Figure S42. ^{1}H NMR spectrum ($CDCl_3$, 600 MHz) of **2b**.

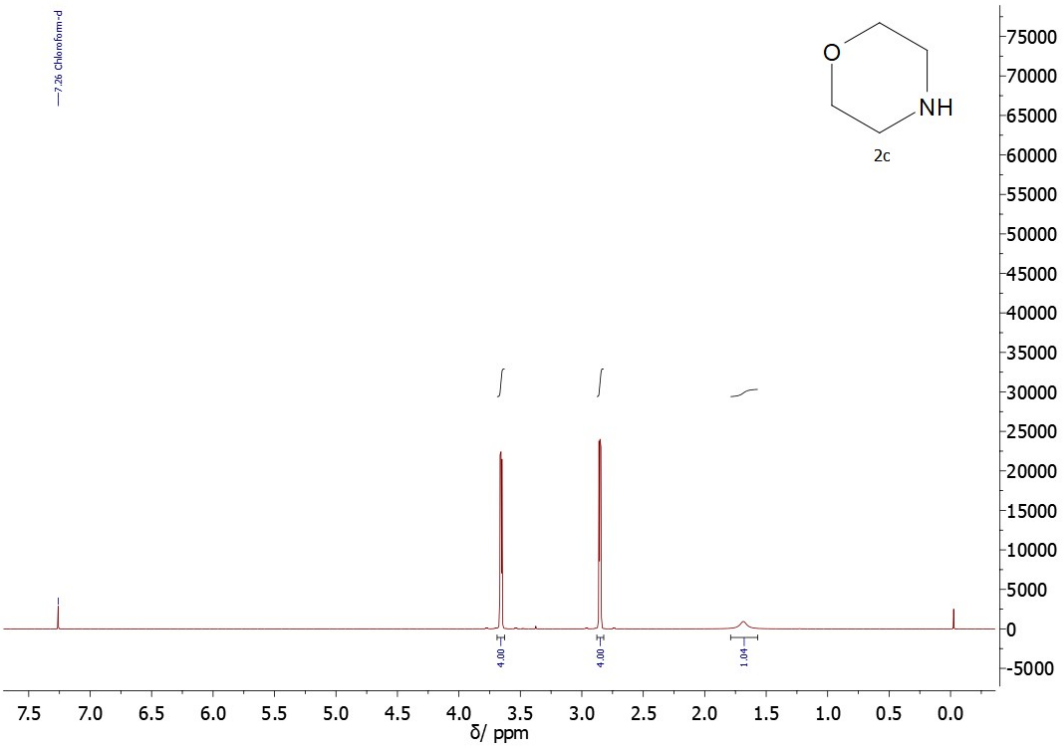

Figure S43. ^{1}H NMR spectrum ($CDCl_3$, 600 MHz) of **2c**.

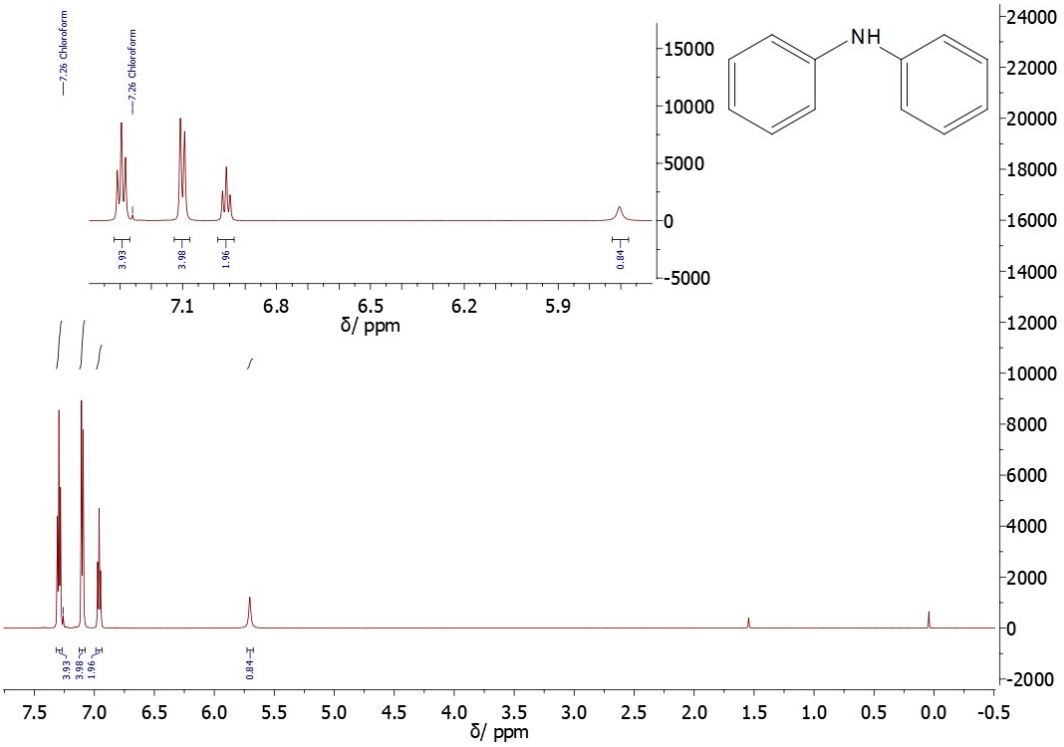

Figure S44. ^{1}H NMR spectrum ($CDCl_3$, 600 MHz) of 1,2-diphenylamine.

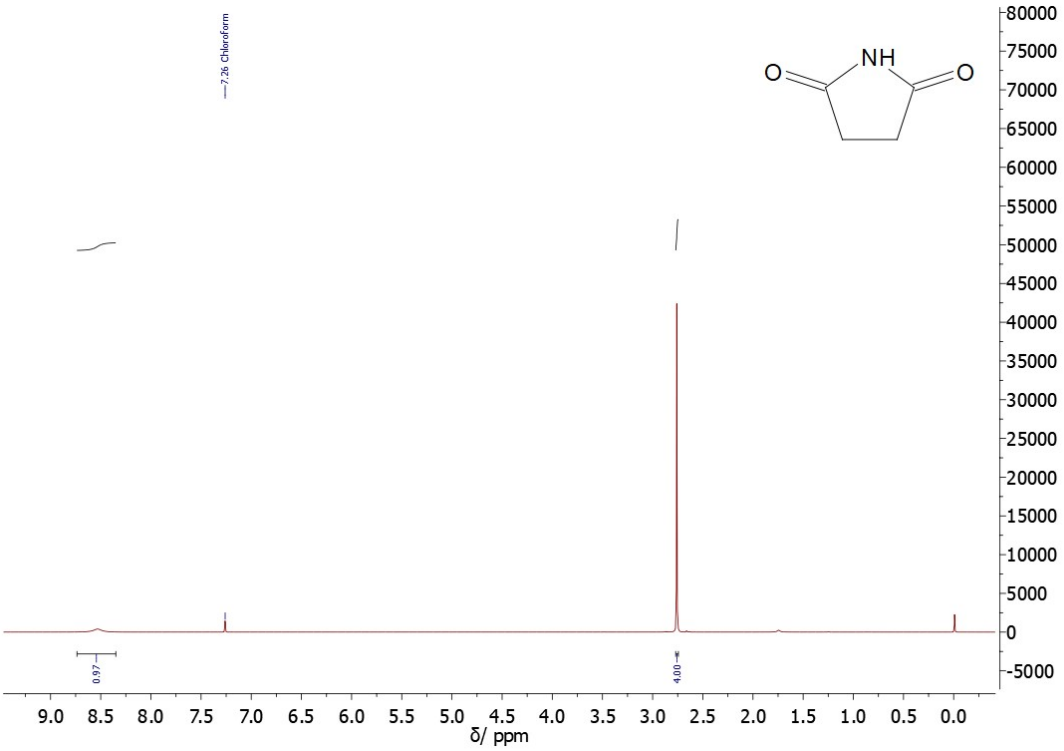

Figure S45. ^{1}H NMR spectrum ($CDCl_3$, 600 MHz) of succinimide.

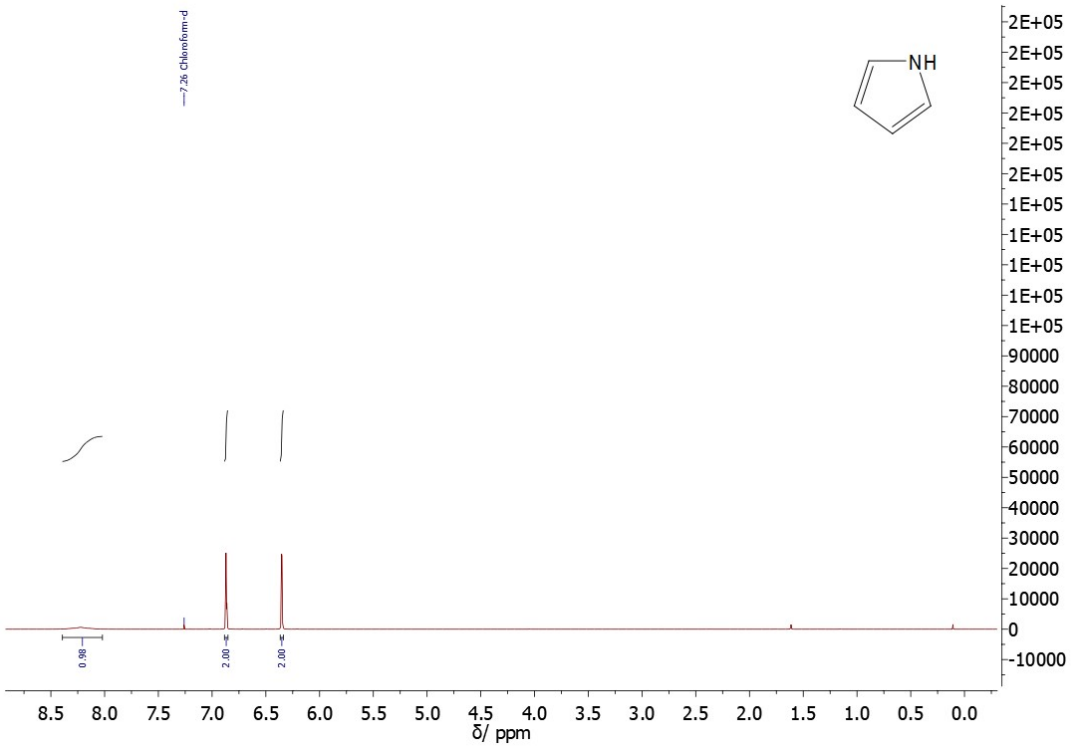

Figure S46. ^{1}H NMR spectrum ($CDCl_3$, 600 MHz) of pyrrole.

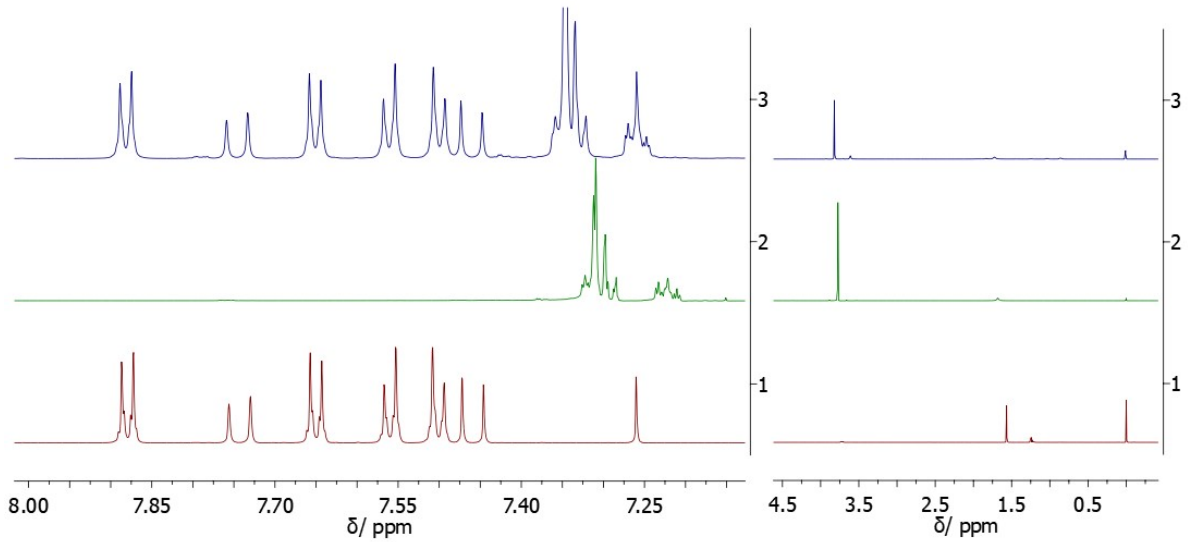

Figure S47. Comparison of ^{1}H NMR spectra ($CDCl_3$, 600 MHz) of (left) aromatic and (right) aliphatic region of reaction mixture (blue line) after milling of compound **1** (red line) and benzylamine (green line) for 120 min in a vibratory ball mill. The same result was obtained after overnight milling.

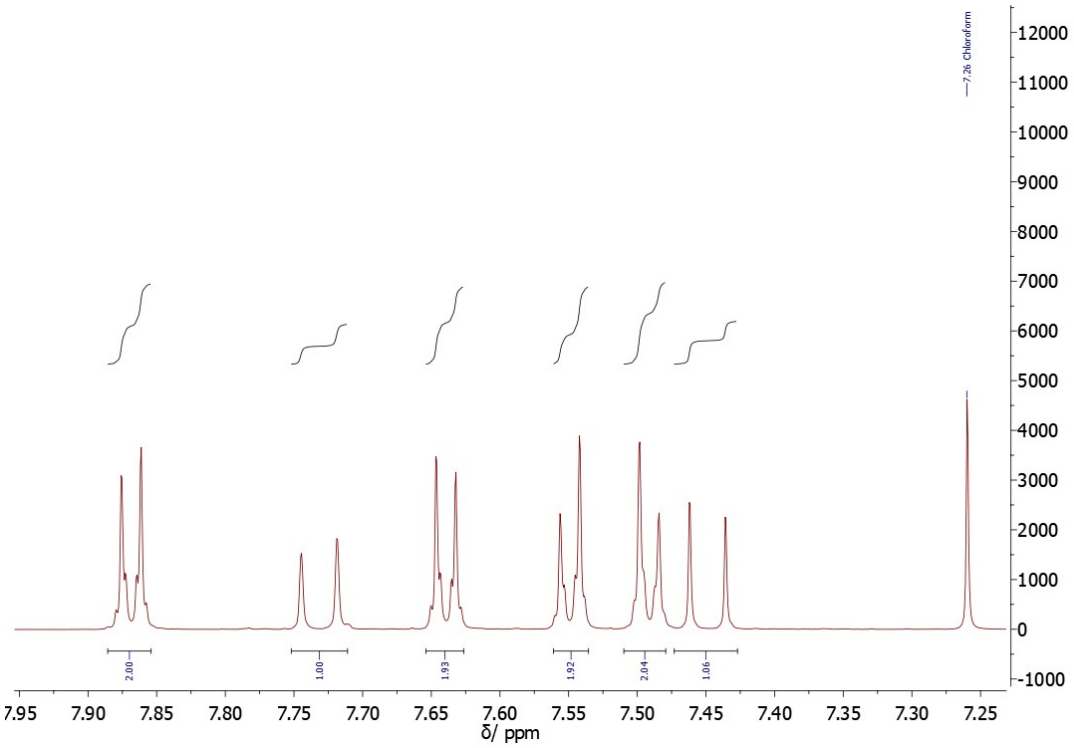

Figure S48. ^{1}H NMR spectrum ($CDCl_3$, 600 MHz) of reaction mixture after milling of compound **1** and DABCO for 120 min in a vibratory ball mill. No product formation was observed.

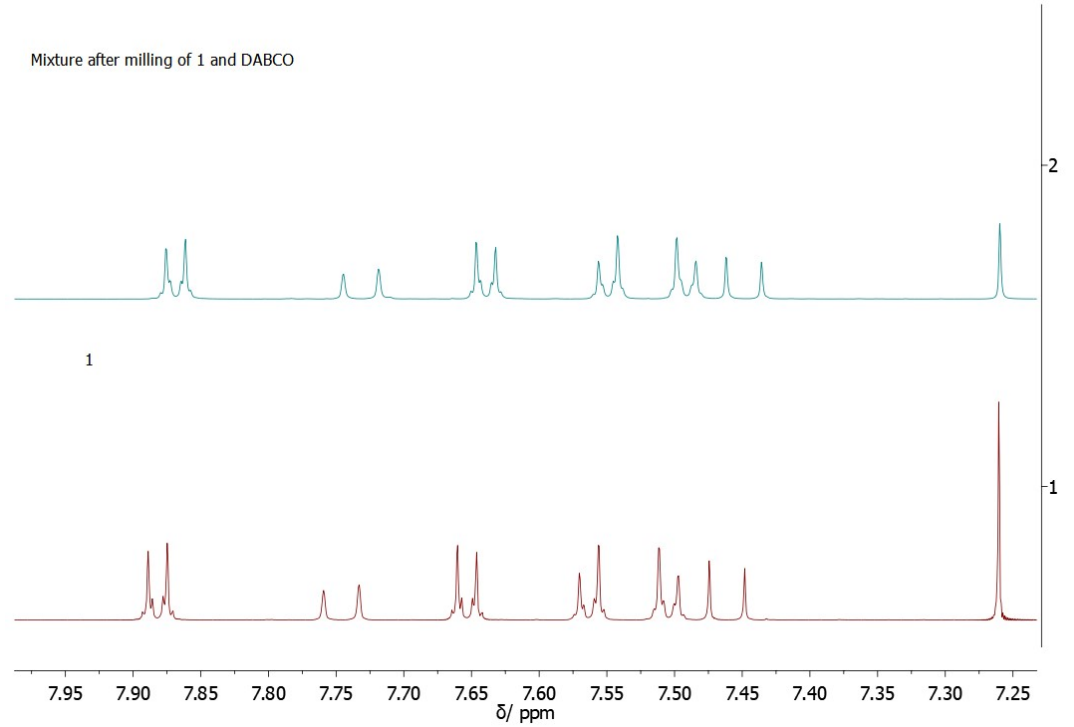

Figure S49. Comparison of ^{1}H NMR spectra ($CDCl_3$, 600 MHz) of: (top) reaction mixture after milling of compound **1** and DABCO for 120 min in a vibratory ball mill, (bottom) chalcone **1**.

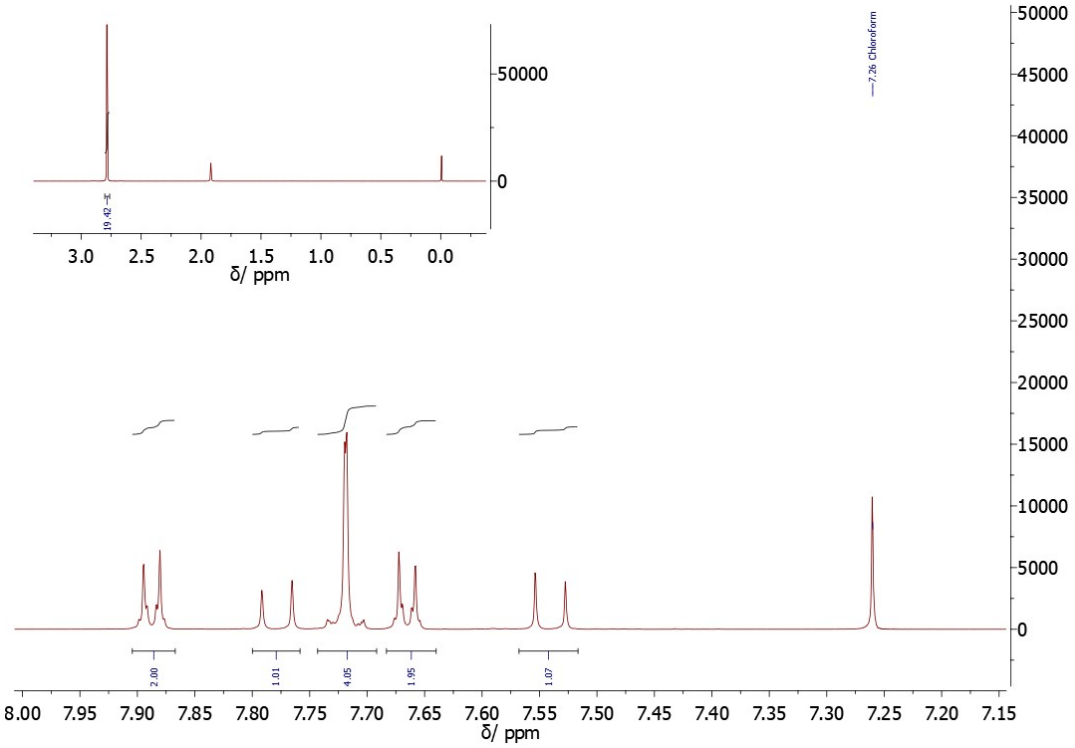

Figure S50. ^{1}H NMR spectra ($CDCl_3$, 600 MHz) of reaction mixture collected after milling of compound **4** and DABCO for 120 min in a vibratory ball mill.

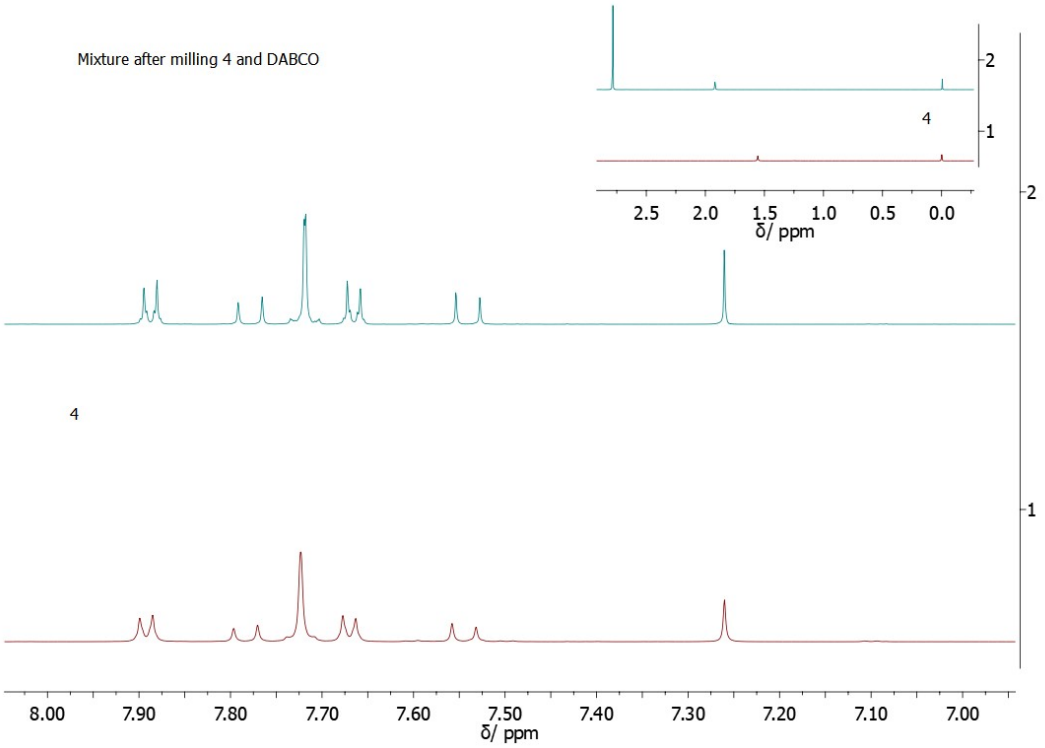

Figure S51. Comparison of ^{1}H NMR spectra ($CDCl_3$, 600 MHz) of: (top) reaction mixture after milling of compound **4** and DABCO for 120 min in a vibratory ball mill, (bottom) chalcone **1**.

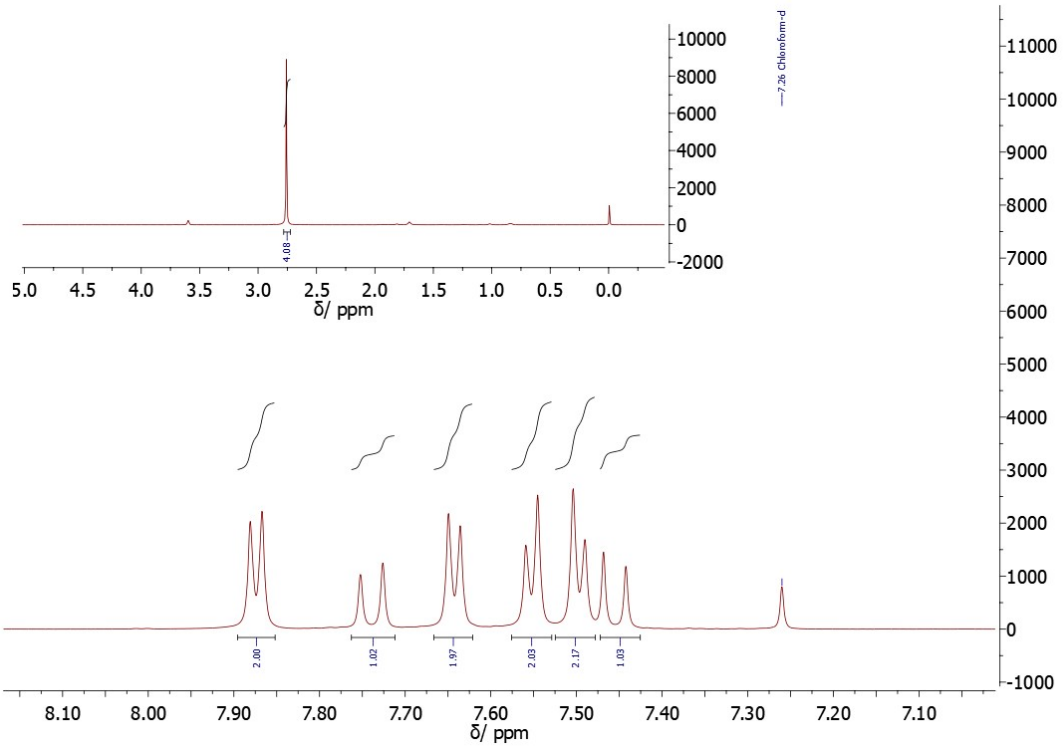

Figure S52. ^{1}H NMR spectrum ($CDCl_3$, 600 MHz) of reaction mixture after milling of compound **1** and succinimide for 120 min in a vibratory ball mill. No product formation was observed. The same result is obtained after overnight milling.

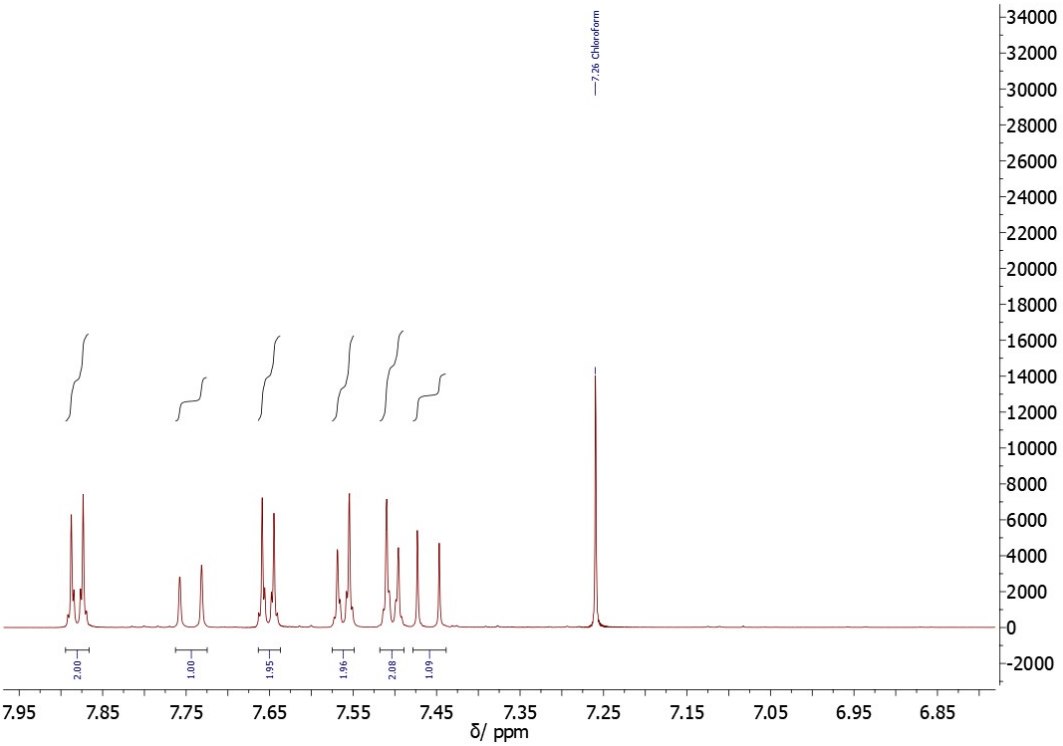

Figure S53. ^{1}H NMR spectrum ($CDCl_3$, 600 MHz) of reaction mixture after milling of compound **1** and thiomorpholine (1.4 equiv.) for 120 min in a vibratory ball mill. New phase was observed and potentially corresponds to the desired product (conversion 29.26%). The full identification was not complemented.

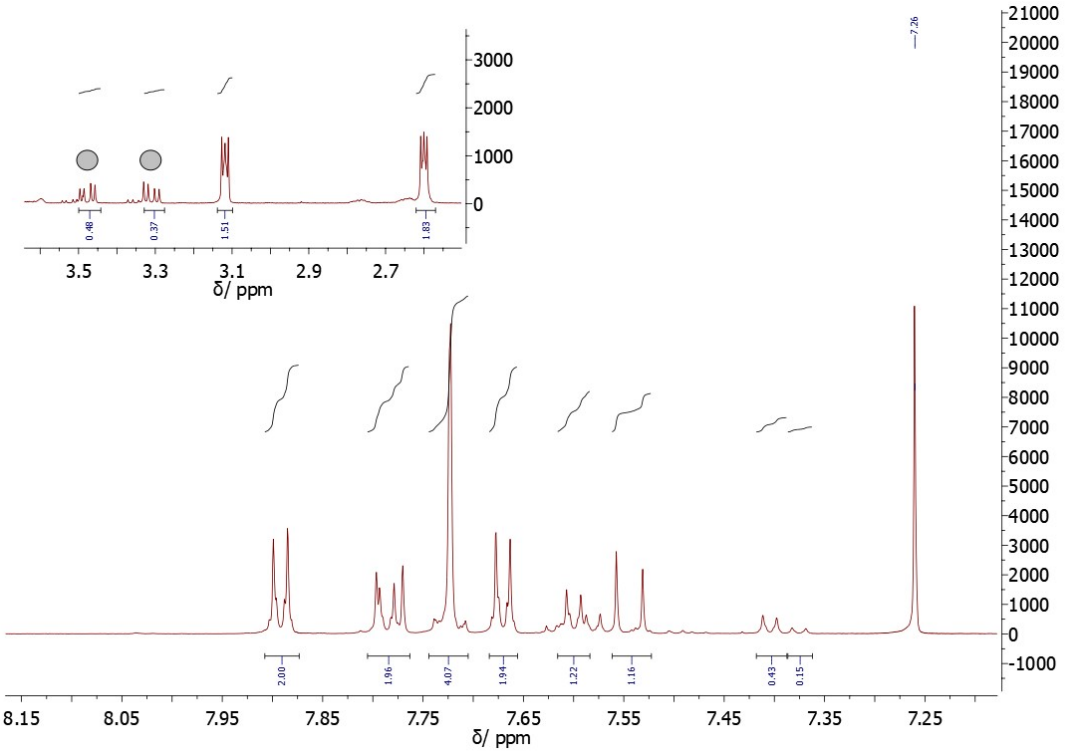

Figure S54. ^{1}H NMR spectrum ($CDCl_3$, 600 MHz) of reaction mixture after milling of compound **4** and thiomorpholine (1.4 equiv.) for 120 min in a vibratory ball mill. New phase (indicated by gray circles) was observed, potentially corresponding to the desired product (conversion 29.26%). The full identification was not completed.

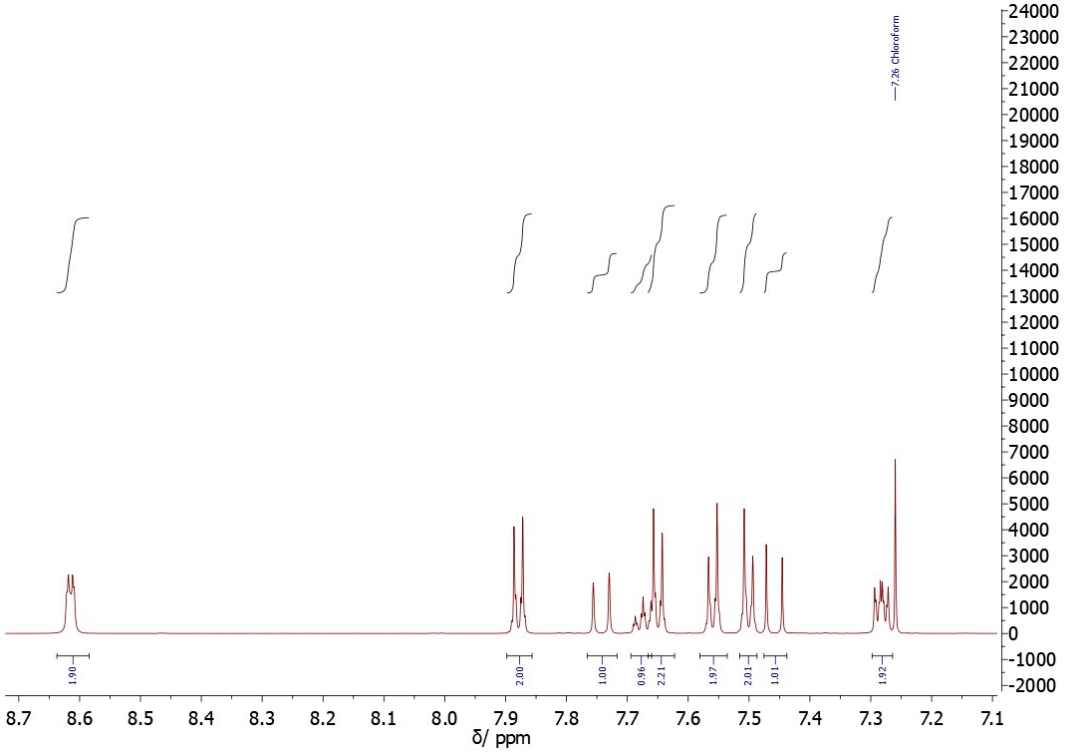

Figure S55. ^{1}H NMR spectrum ($CDCl_3$, 600 MHz) of reaction mixture after milling of compound **1** and pyridine (1.4 equiv.) for 120 min in a vibratory ball mill. No product formation was observed.

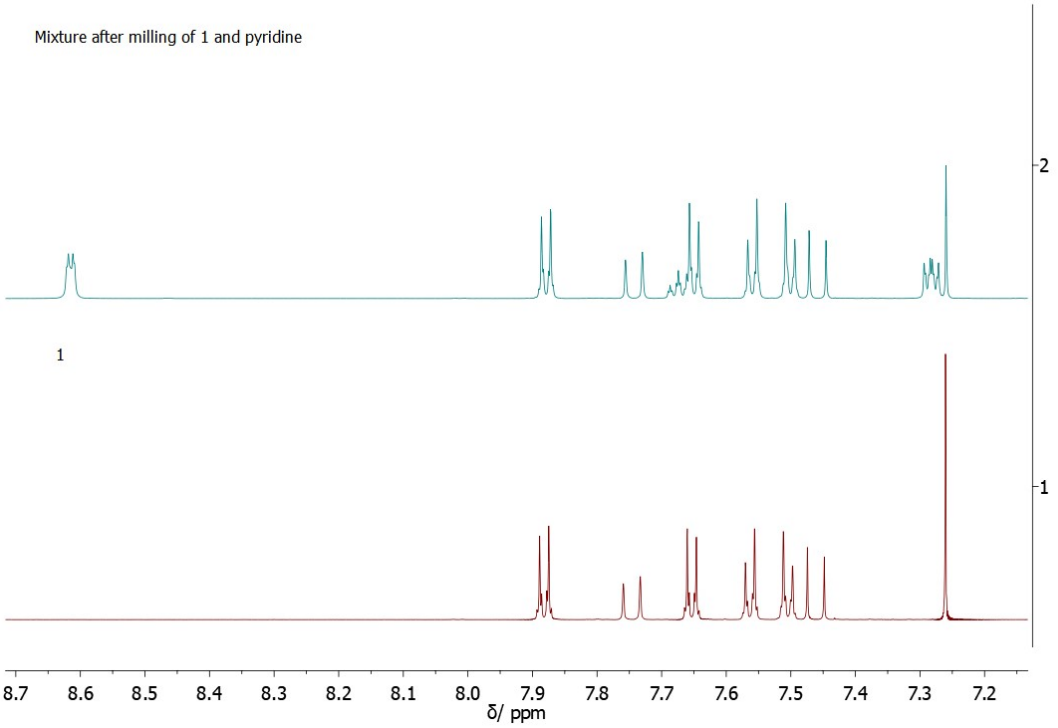

Figure S56. Comparison of ^{1}H NMR spectra ($CDCl_3$, 600 MHz) of: (top) reaction mixture after milling of compound **1** and pyridine (1.4 equiv.) for 120 min in a vibratory ball mill, (bottom) starting material, **1**.

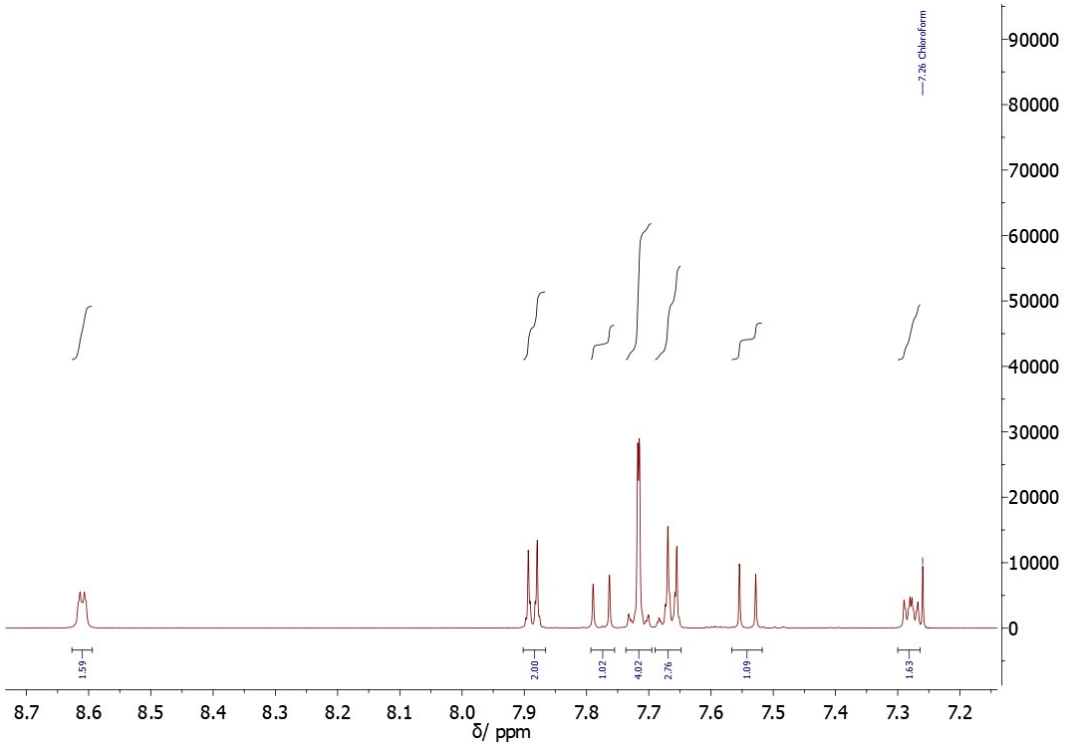

Figure S57. ^{1}H NMR spectrum ($CDCl_3$, 600 MHz) of reaction mixture after milling of compound **4** and pyridine (1.4 equiv.) for 120 min in a vibratory ball mill. No product formation was observed.

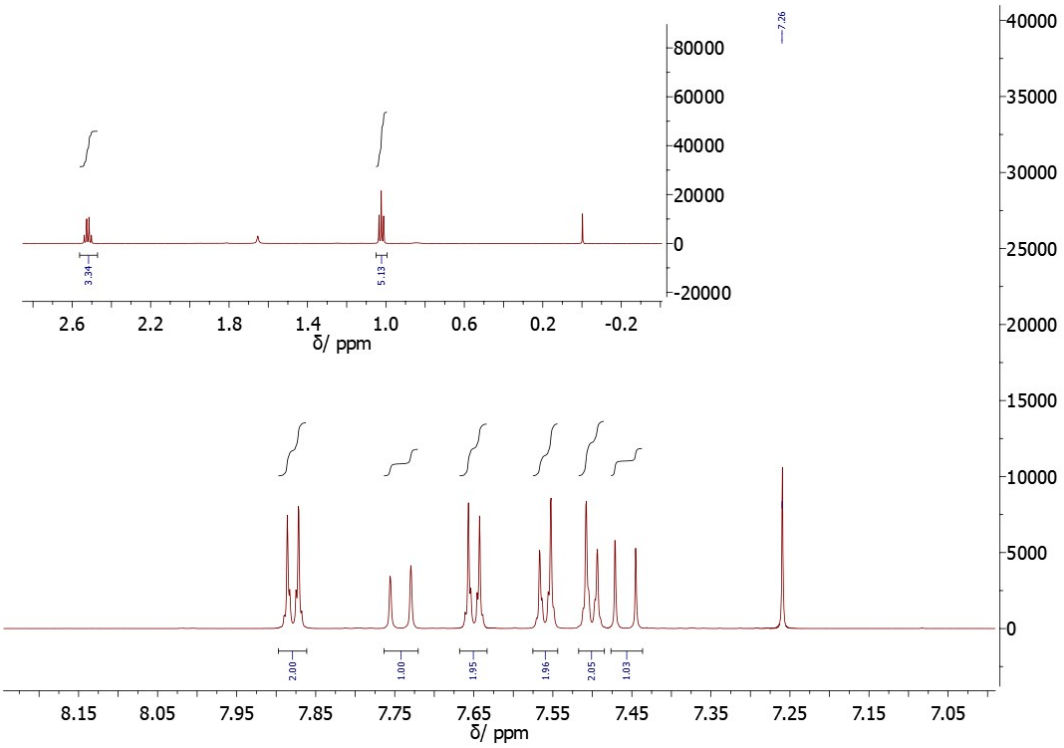

Figure S58. ^{1}H NMR spectrum ($CDCl_3$, 600 MHz) of reaction mixture after milling of compound **1** and triethylamine (1.4 equiv.) for 120 min in a vibratory ball mill. No product formation was observed.

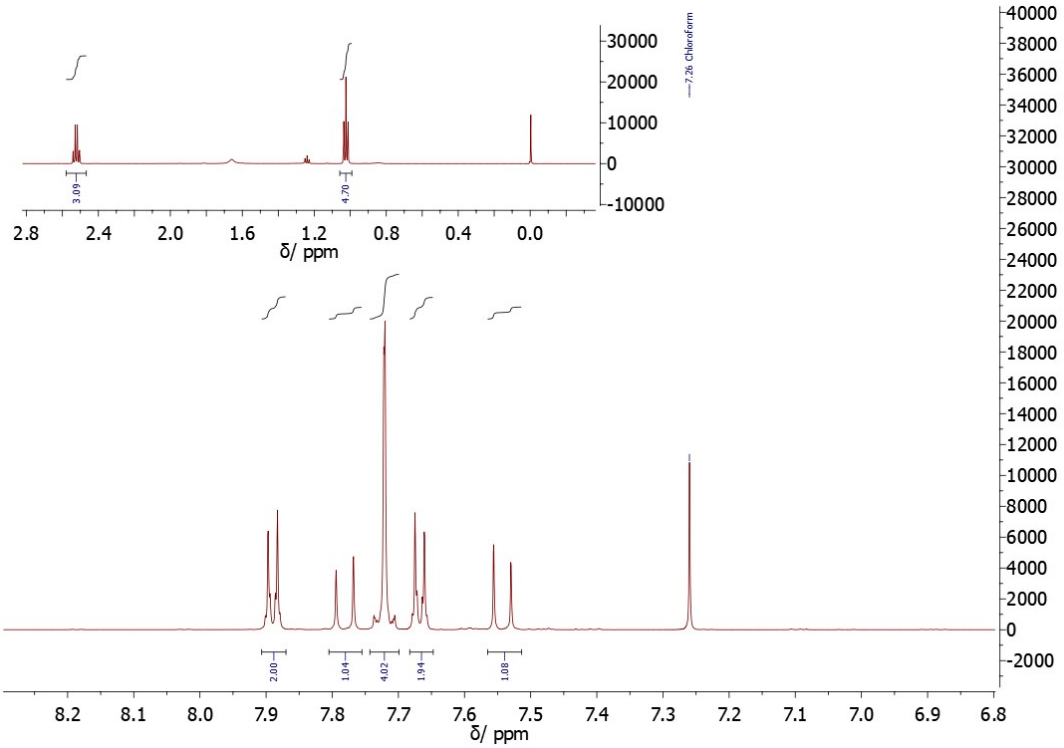

Figure S59. ^{1}H NMR spectrum ($CDCl_3$, 600 MHz) of reaction mixture after milling of compound **4** and triethylamine (1.4 equiv.) for 120 min in a vibratory ball mill. No product formation was observed.

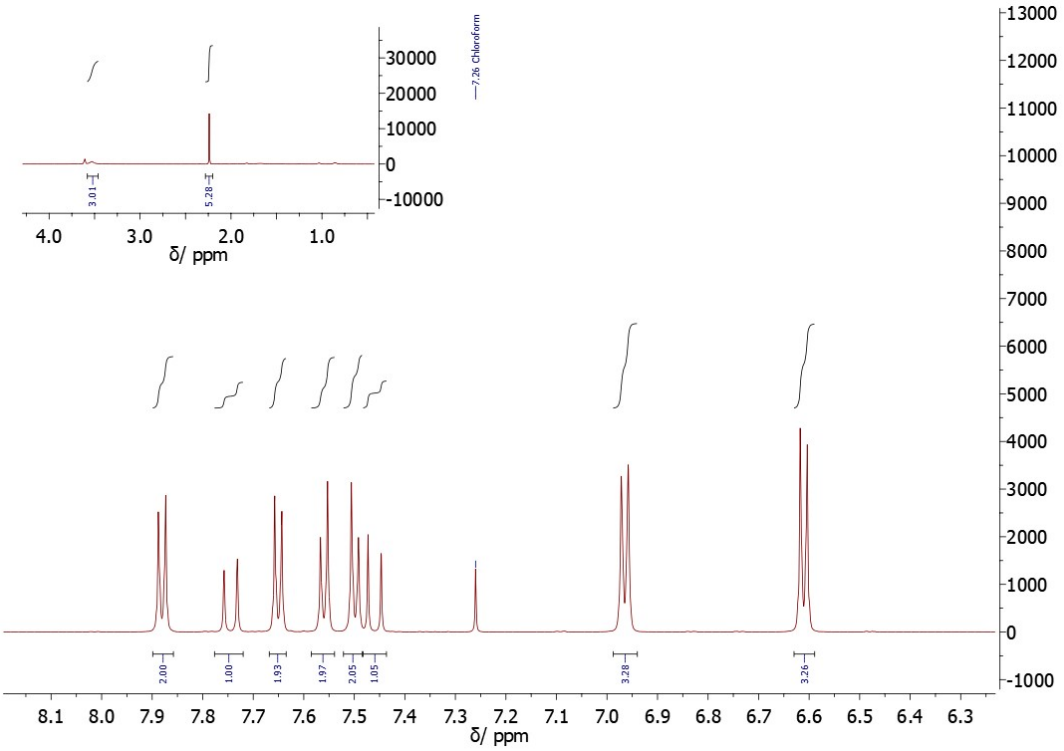

Figure S60. ^{1}H NMR spectrum ($CDCl_3$, 600 MHz) of reaction mixture after milling of compound **1** and *p*-toluidine (1.4 equiv.) for 120 min in a vibratory ball mill. No product formation was observed.

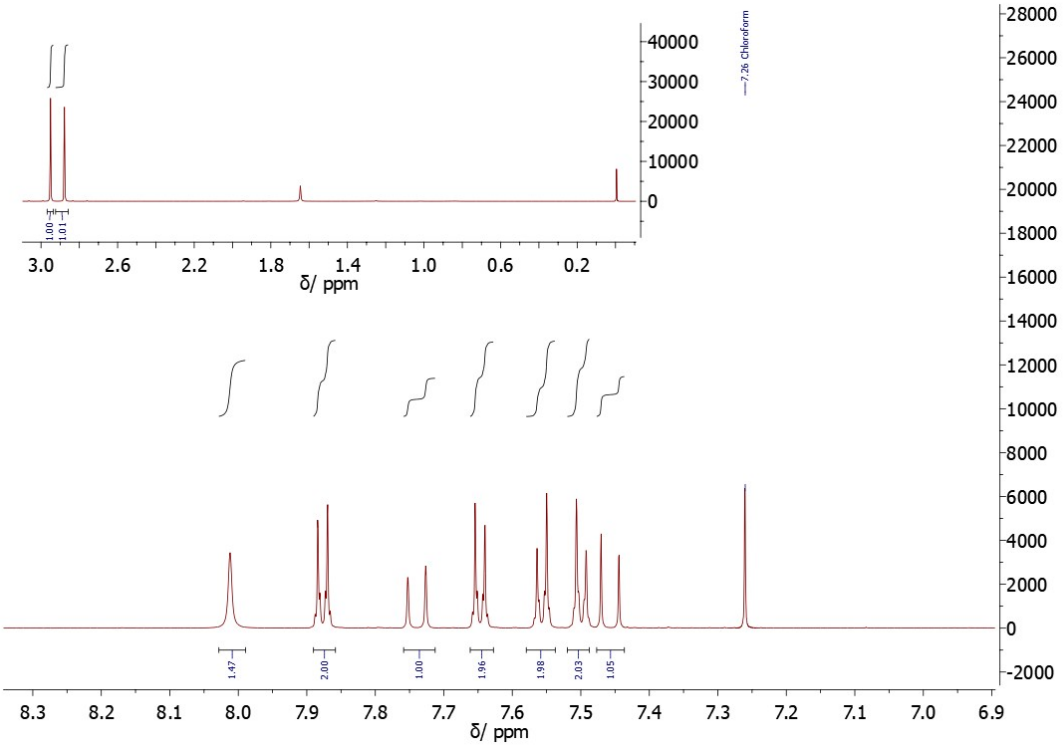

Figure S61. ^{1}H NMR spectrum ($CDCl_3$, 600 MHz) of reaction mixture after milling of compound **1** and dimethylformamide (1.4 equiv.) for 120 min in a vibratory ball mill. No product formation was observed.

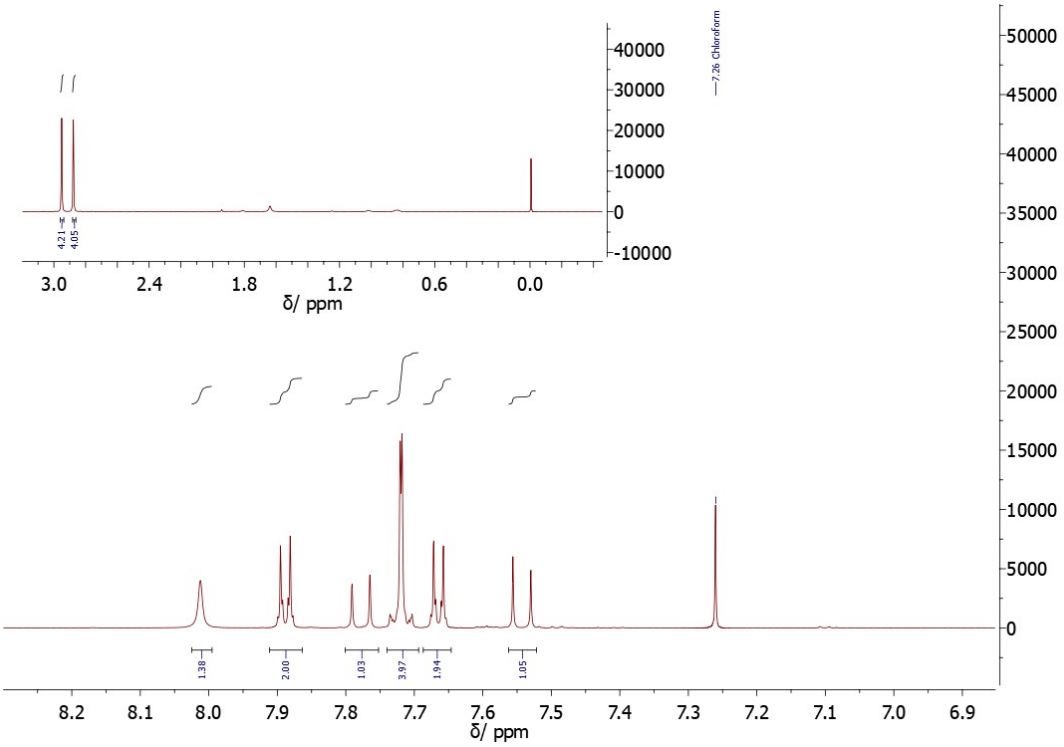

Figure S62. ^{1}H NMR spectrum ($CDCl_3$, 600 MHz) of reaction mixture after milling of compound **4** and dimethylformamide (1.4 equiv.) for 120 min in a vibratory ball mill. No product formation was observed.

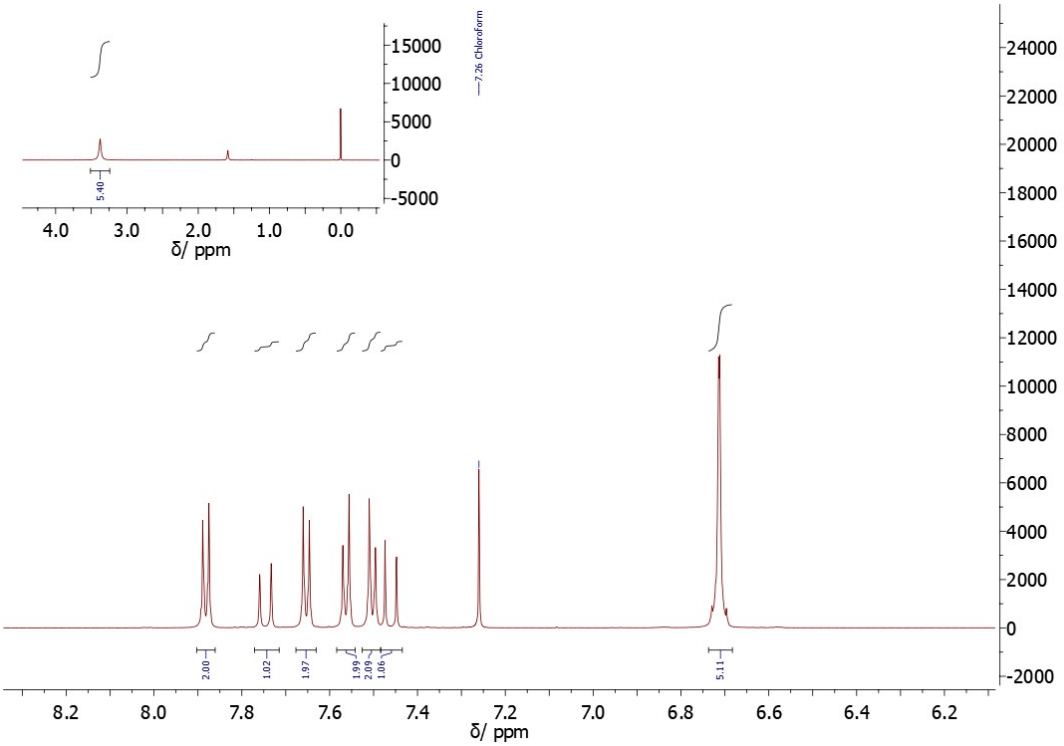

Figure S63. ^{1}H NMR spectrum ($CDCl_3$, 600 MHz) of reaction mixture after milling of compound **1** and *o*-phenylenediamine (1.4 equiv.) for 120 min in a vibratory ball mill. No product formation was observed.

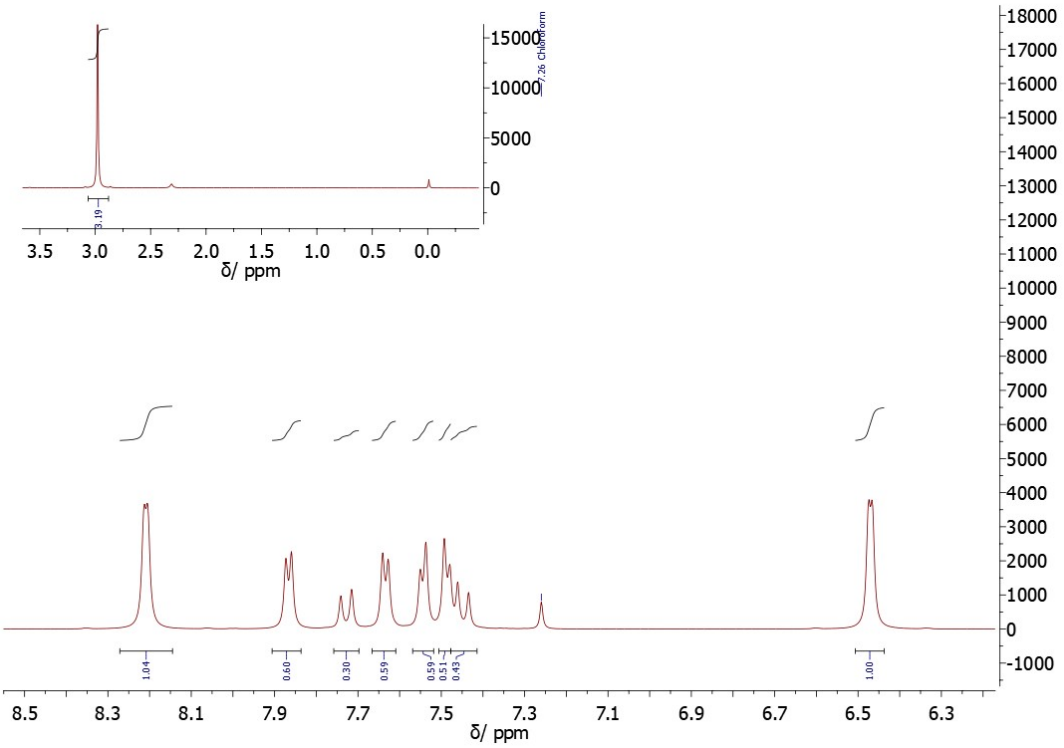

Figure S64. ^{1}H NMR spectrum ($CDCl_3$, 600 MHz) of reaction mixture after milling of compound **1** and 4-dimethylaminopyridine (1.4 equiv.) for 120 min in a vibratory ball mill. No product formation was observed.

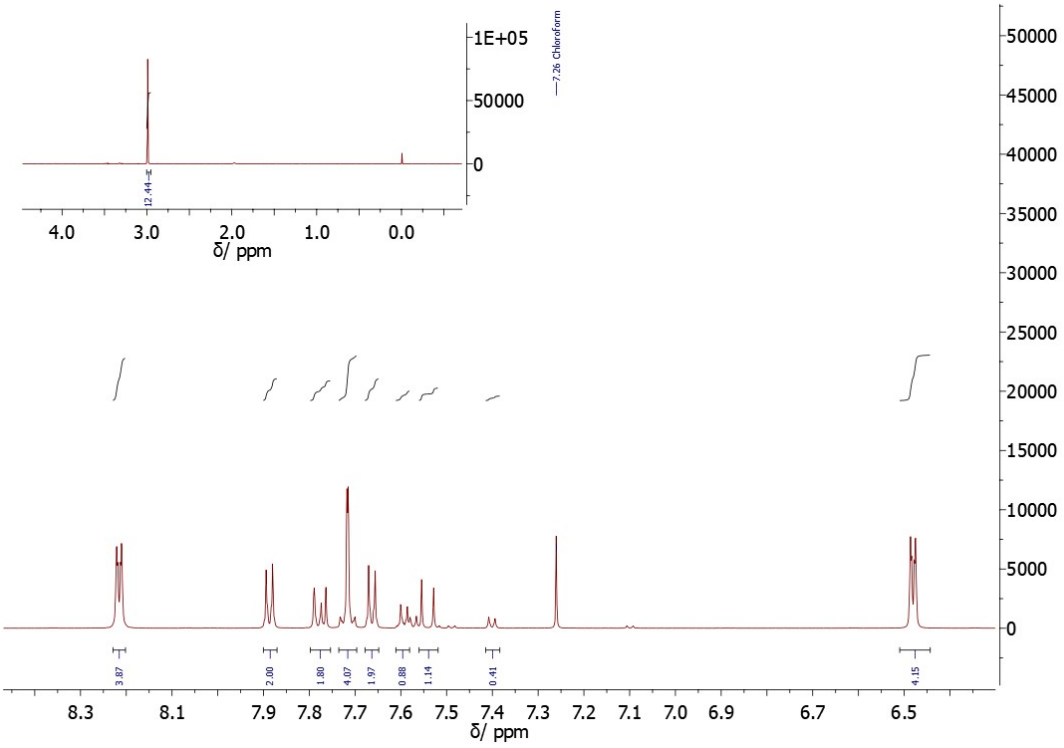

Figure S65. ^{1}H NMR spectrum ($CDCl_3$, 600 MHz) of reaction mixture after milling of compound **4** and 4-dimethylaminopyridine (1.4 equiv.) for 120 min in a vibratory ball mill. No product formation was observed.

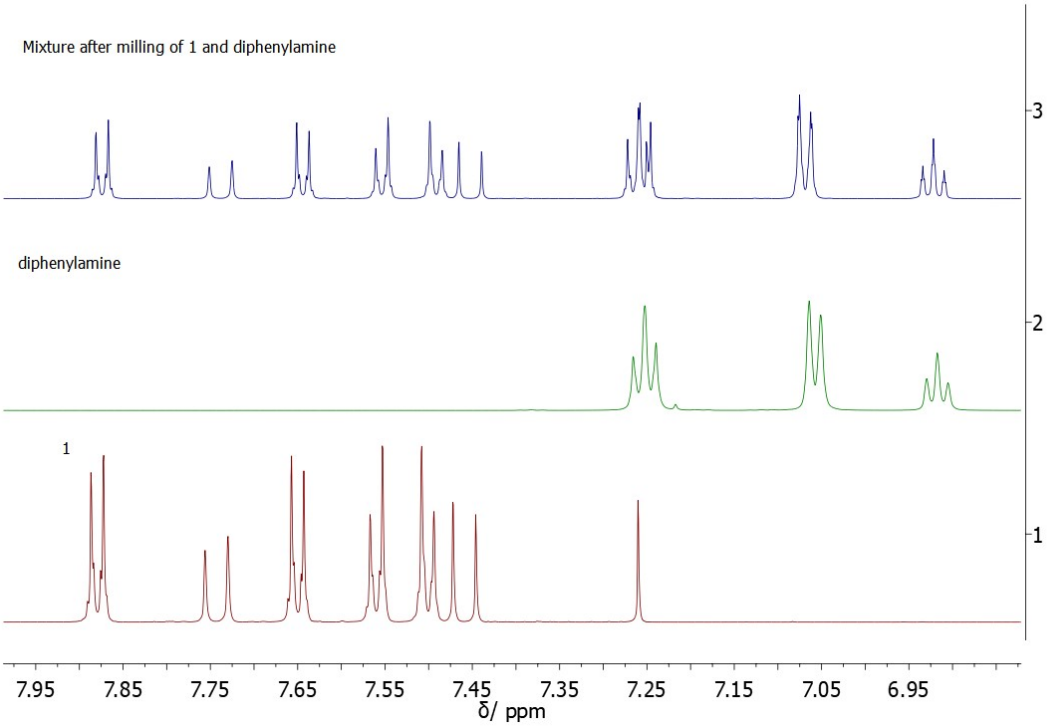

Figure S66. Comparison of ^{1}H NMR spectra ($CDCl_3$, 600 MHz) of: (top) reaction mixture after milling of (middle) compound diphenylamine (1 equiv.) and (bottom) **1** for 120 min in a vibratory ball mill. The same result is obtained after overnight milling.

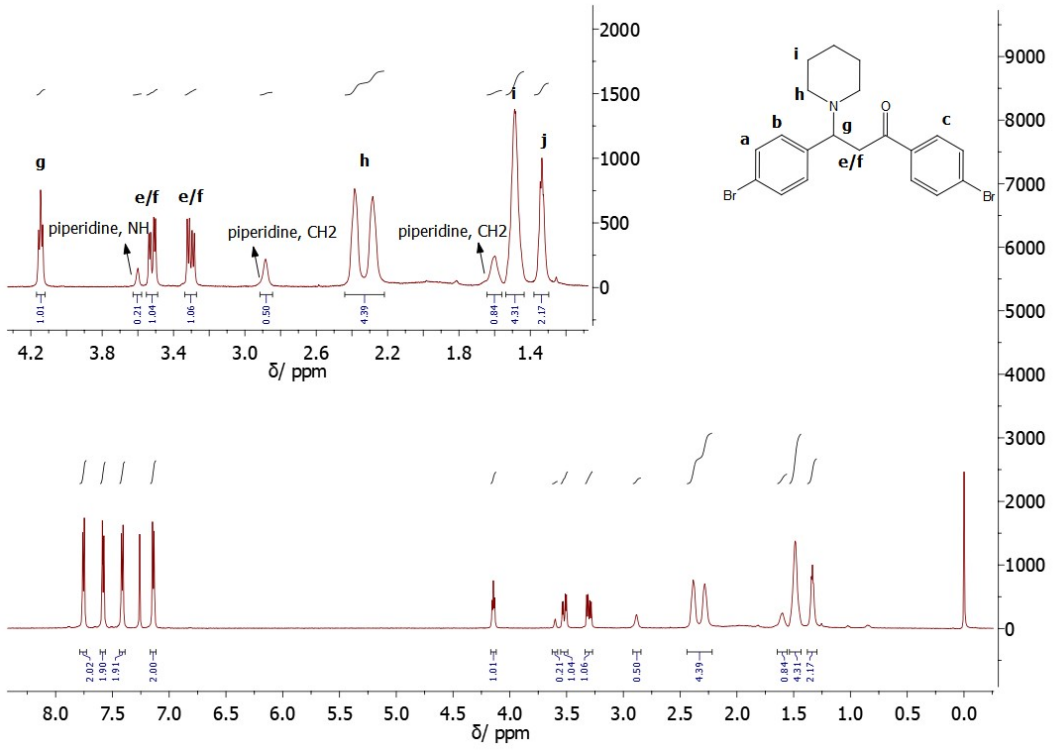

Figure S67. ^{1}H NMR spectrum ($CDCl_3$, 600 MHz) of **3a**, formed by milling **1** and **2a** (1.4 equiv.) (with highlighted and annotated protons).

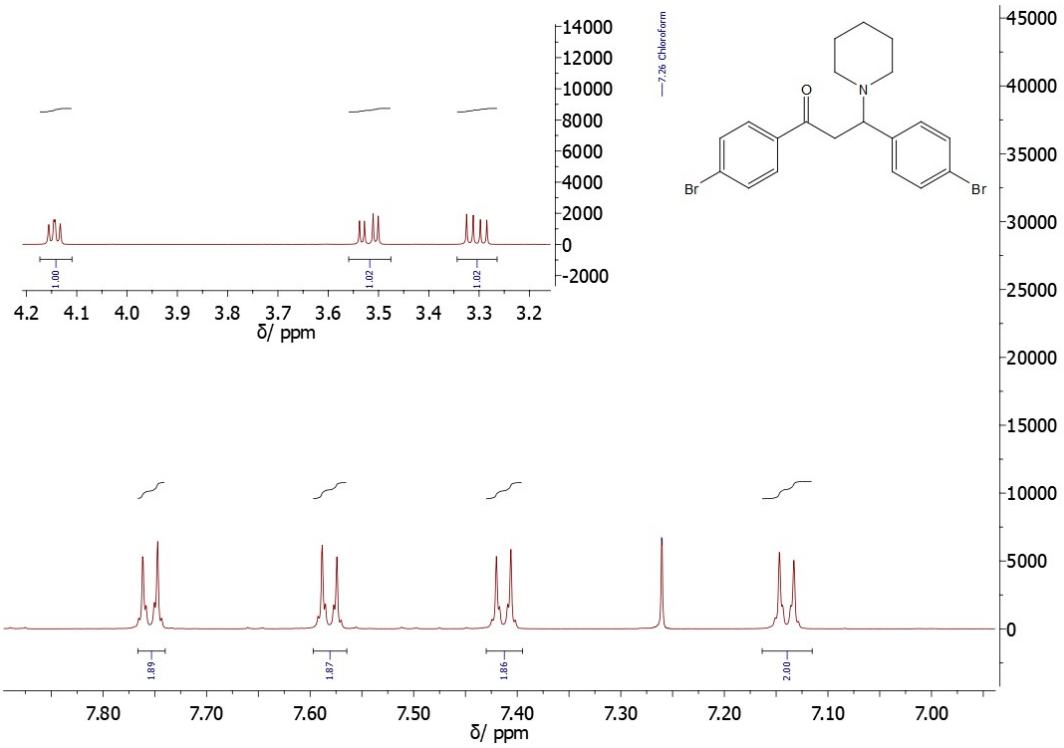

Figure S68. ^{1}H NMR spectrum ($CDCl_3$, 600 MHz) of **3a**, formed by milling **1** and **2a** (1 equiv.) for 120 min (sample sent immediately after the reaction for NMR measurements).

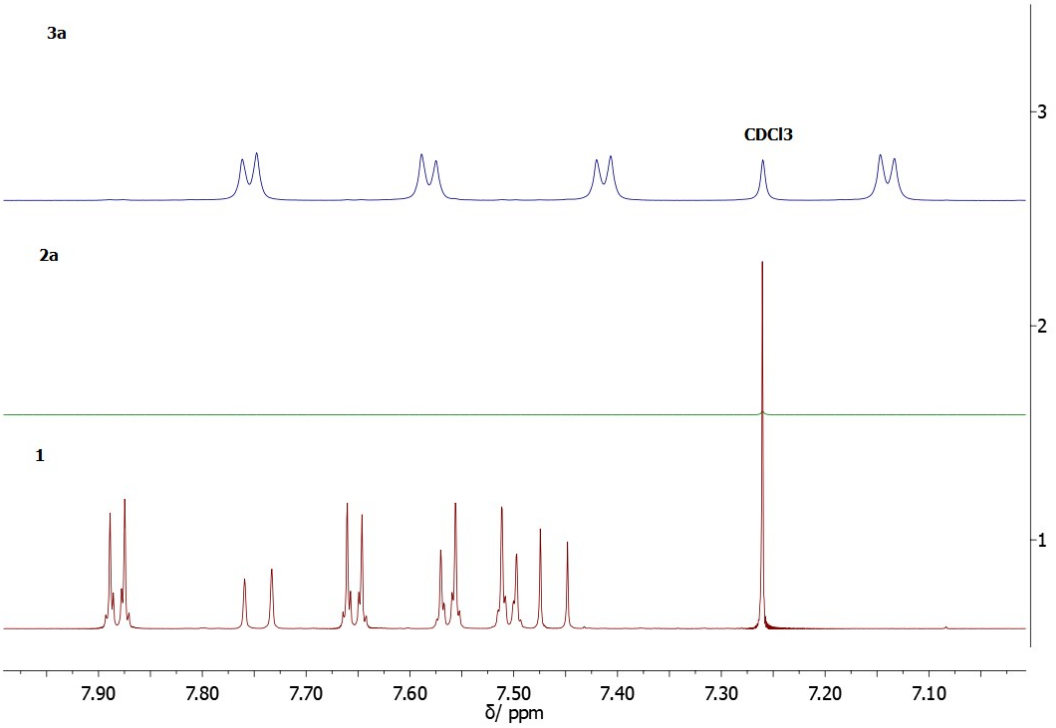

Figure S69. Comparison of ^{1}H NMR spectra ($CDCl_3$, 600 MHz) aromatic region of **3a**, and starting materials, **1** and **2a**.

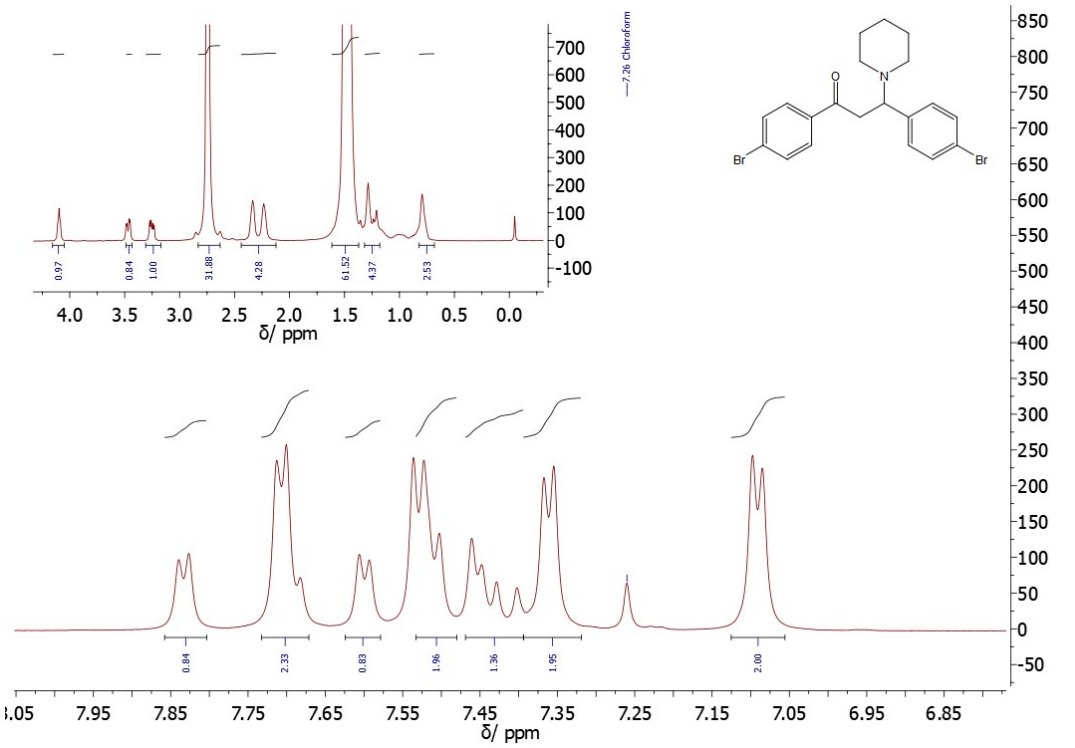

Figure S70. ^{1}H NMR spectrum ($CDCl_3$, 600 MHz) of **3a**, formed within one week of ageing of **1** in the vapor of **2a**.

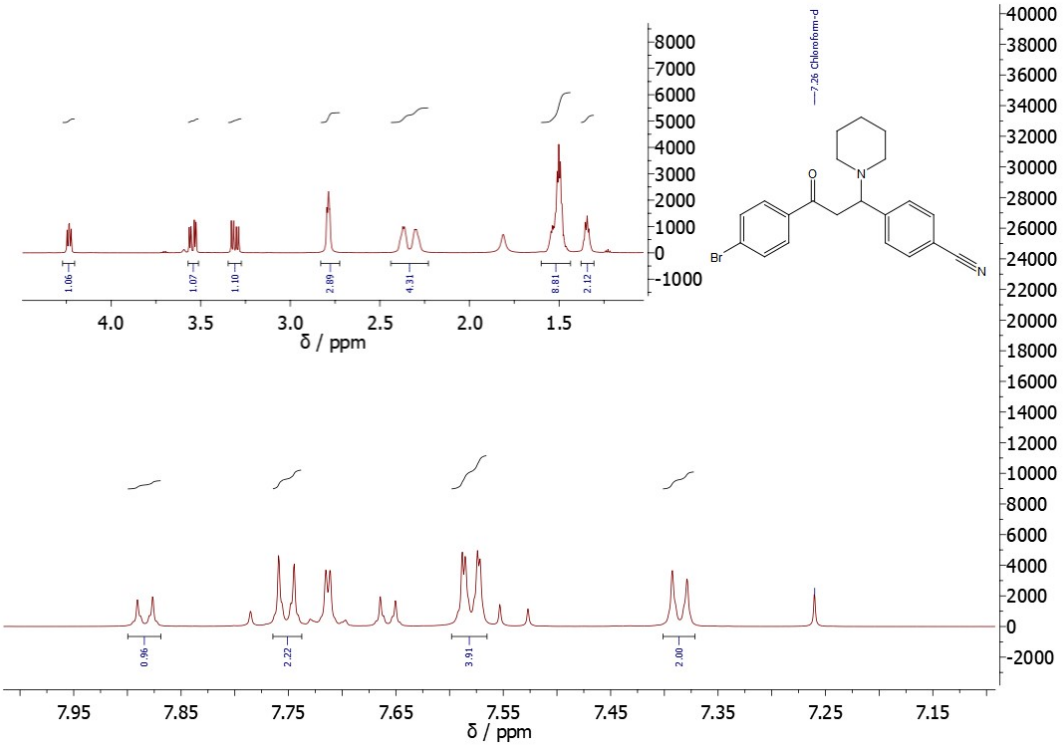

Figure S71. ^{1}H NMR spectrum ($CDCl_3$, 600 MHz) of a mixture collected after milling of **4** and **2a** which indicate a 68% conversion to compound **5**.

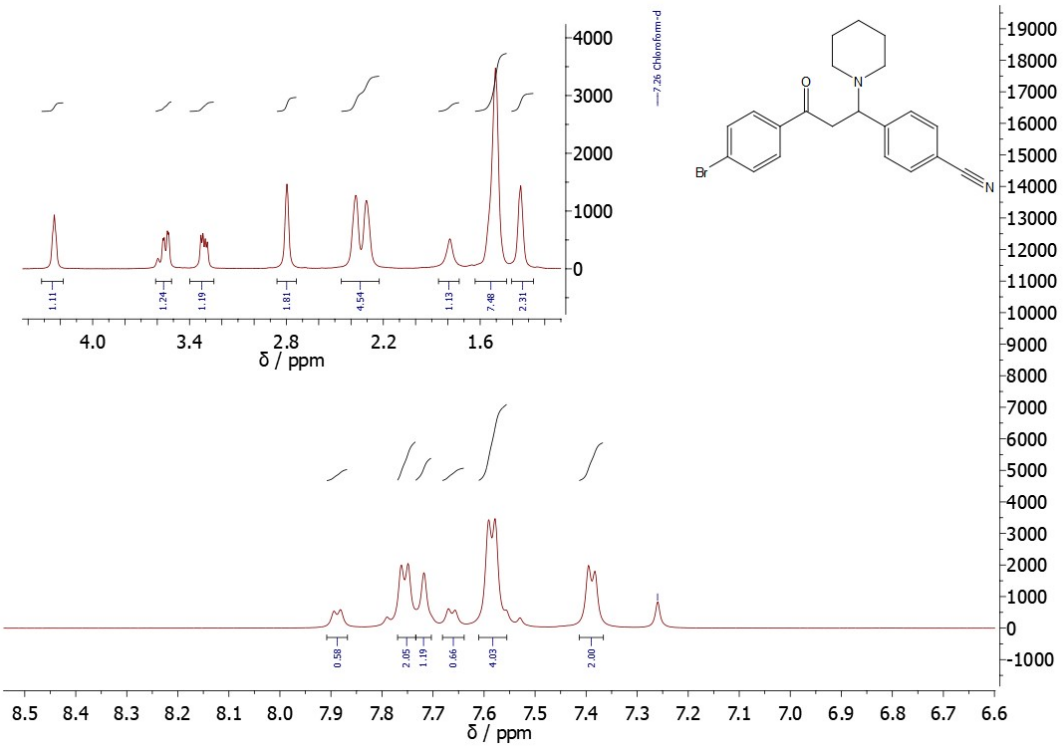

Figure S72. ^{1}H NMR spectrum ($CDCl_3$, 600 MHz) of a compound **5**.

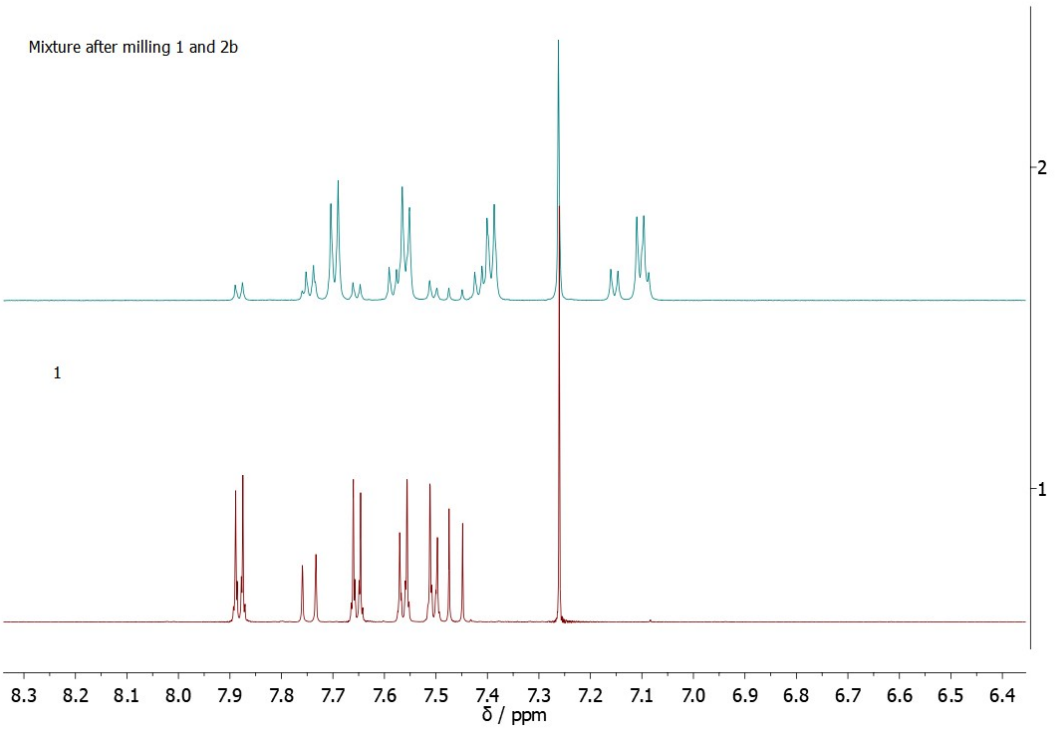

Figure S73. Comparison of ^{1}H NMR spectra ($CDCl_3$, 600 MHz) aromatic region of (top) mixture collected after milling of **1** and **2b** (1 equiv.) for 120 min and (bottom) starting materials, **1**.

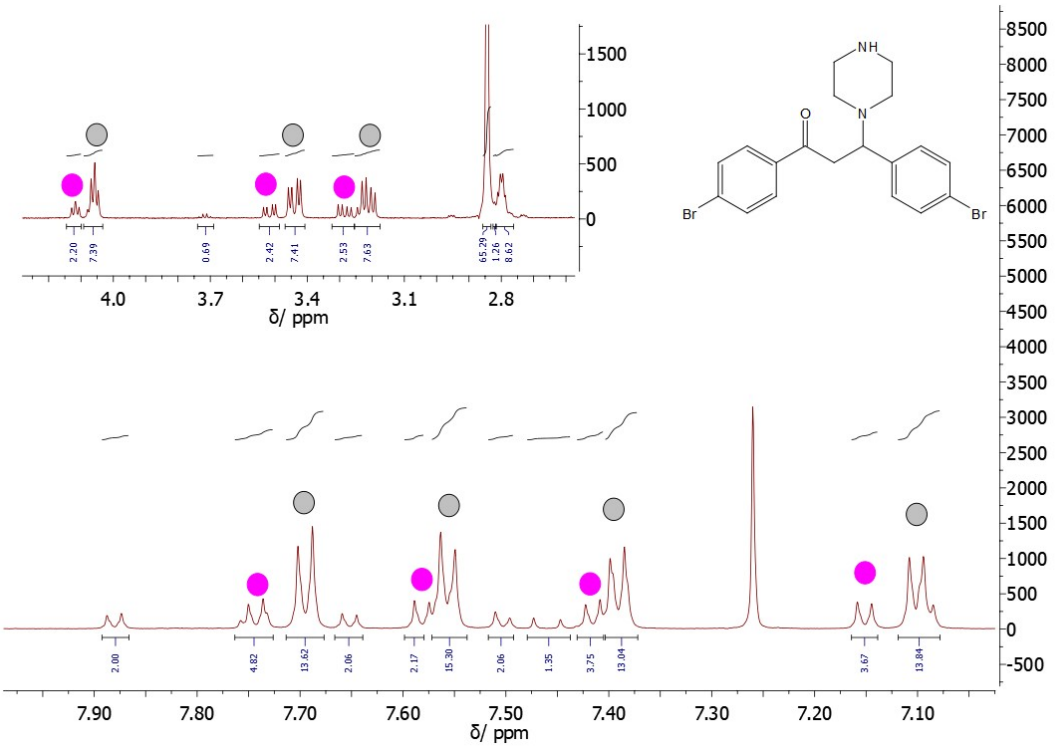

Figure S74. ^{1}H NMR spectrum ($CDCl_3$, 600 MHz) of a mixture of single (**3b**) and double (**3b'**) addition product after milling **1** and **2b** for 120 min (Table S1, Entry 5). Peaks corresponding to compound **3b** are highlighted with gray circles, while for **3b'** with magenta colored circles. The NMR conversion to **3b** is 71%.

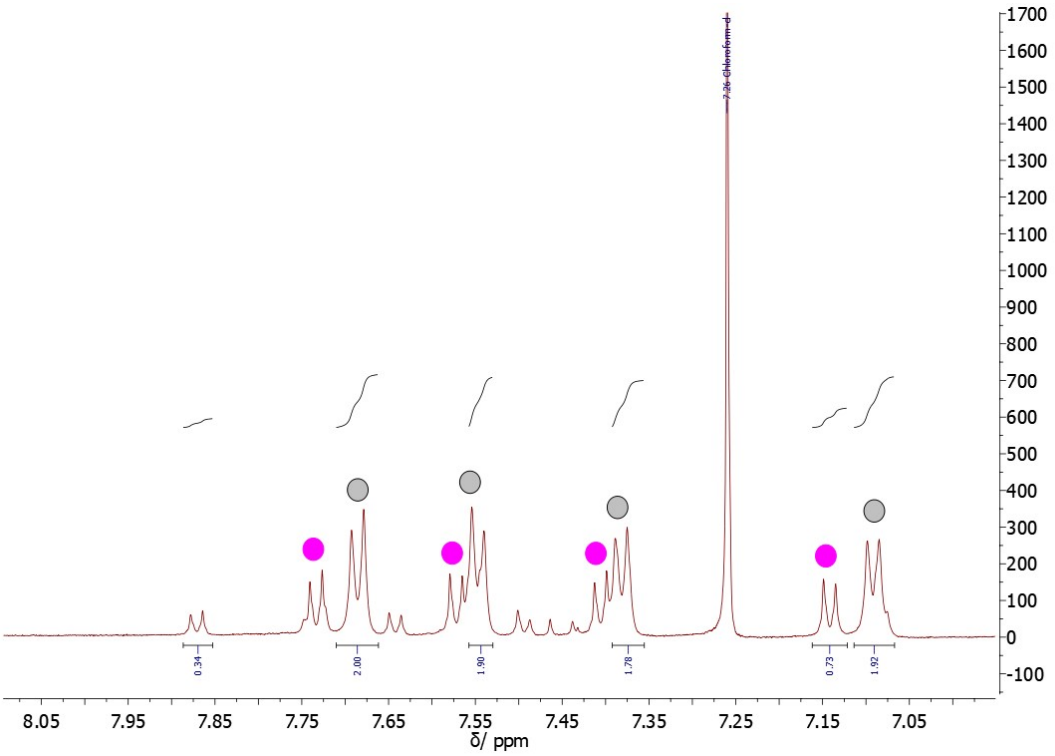

Figure S75. ^{1}H NMR spectrum ($CDCl_3$, 600 MHz) of a mixture of single (**3b**) and double (**3b'**) addition product after overnight milling **1** and **2b**. Peaks corresponding to compound **3b** are highlighted with gray circles, while for **3b'** with magenta colored circles.

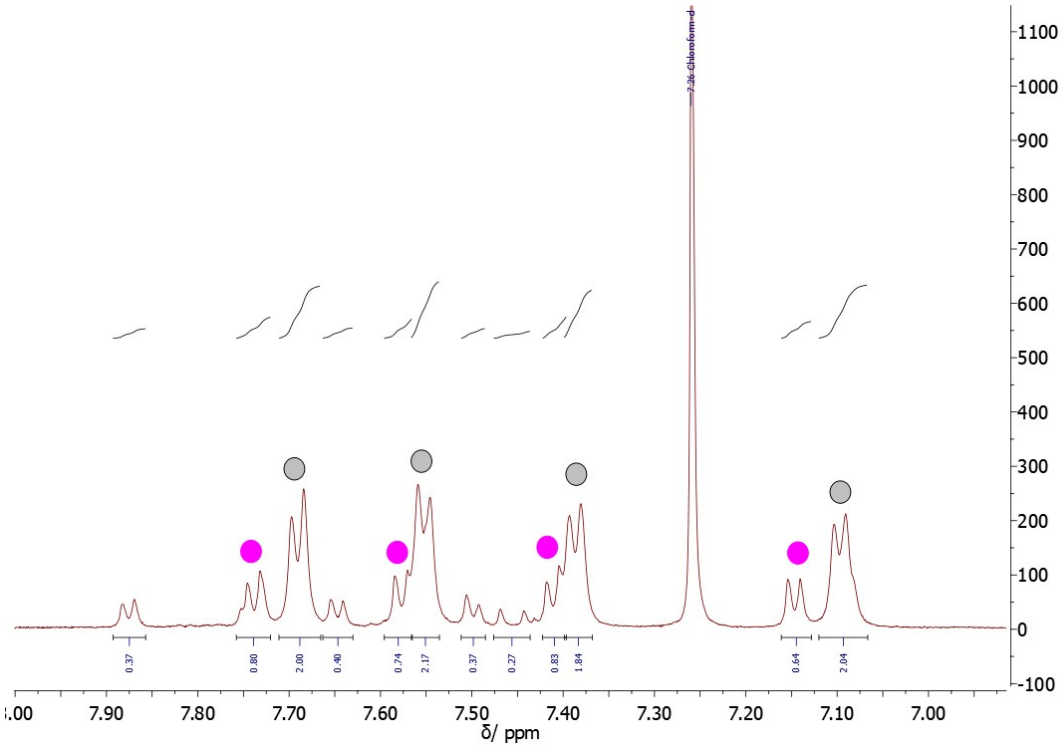

Figure S76. ^{1}H NMR spectrum ($CDCl_3$, 600 MHz) of a mixture of single (**3b**) and double (**3b'**) addition product after liquid-assisted grinding ($V(CHCl_3)$ = 20 µL) **1** and **2b** for 120 min. Peaks corresponding to compound **3b** are highlighted with gray circles, while for **3b'** with magenta colored circles.

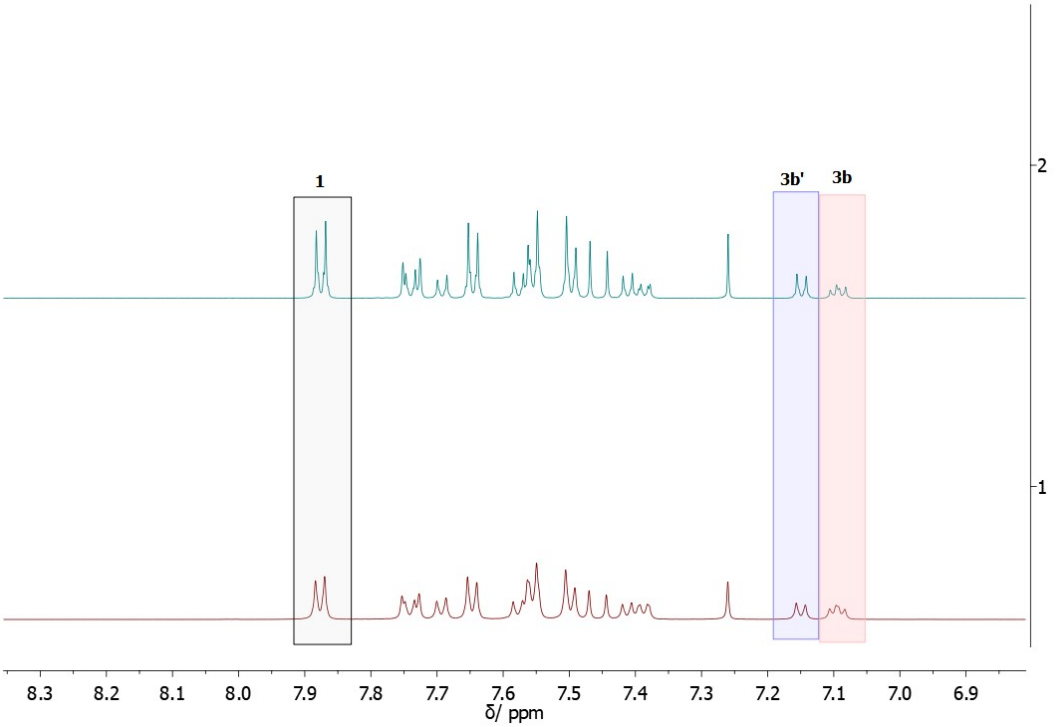

Figure S77. Comparison of ^{1}H NMR spectra ($CDCl_3$, 600 MHz) of a mixture of single (**3b**) and double (**3b'**) addition products after milling **1** and **2b** (0.5 equiv.) for 120 min. (top) Sample recorded after 24 h of standing in NMR tube in the solvent, (bottom) sample recorded immediately.

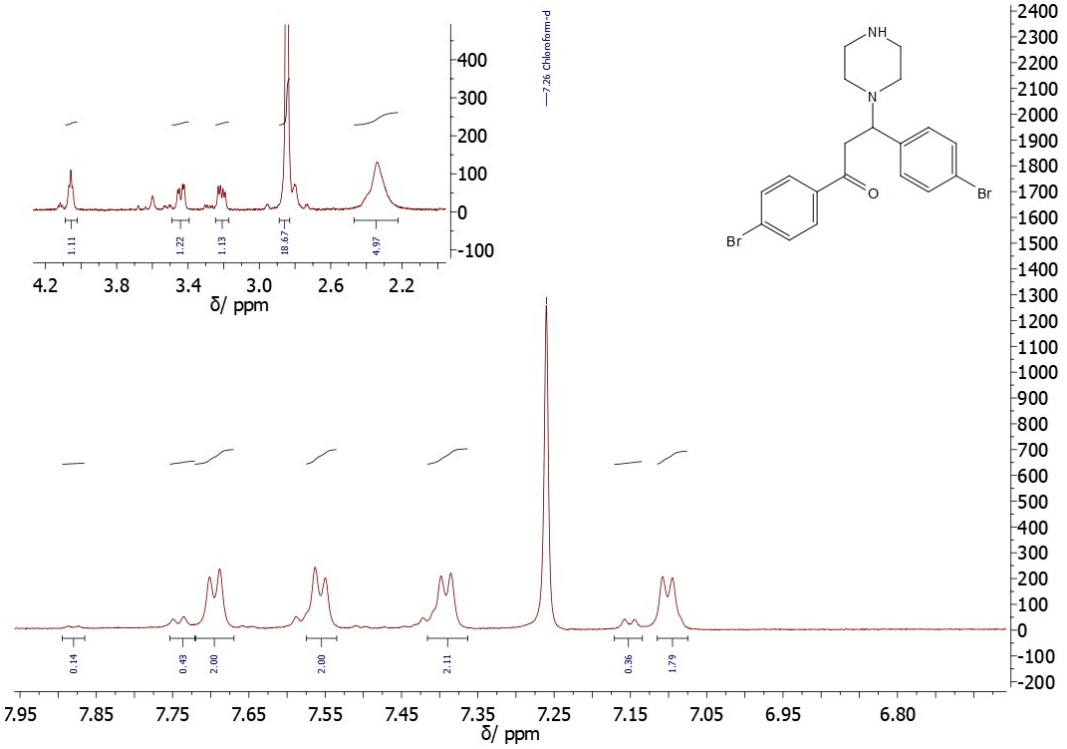

Figure S78. ^{1}H NMR spectrum ($CDCl_3$, 600 MHz) of a **3b** formed dominantly after heating followed by liquid-assisted grinding (V($CHCl_3$) = 20 µL) of **1** and **2b** for 120 min.

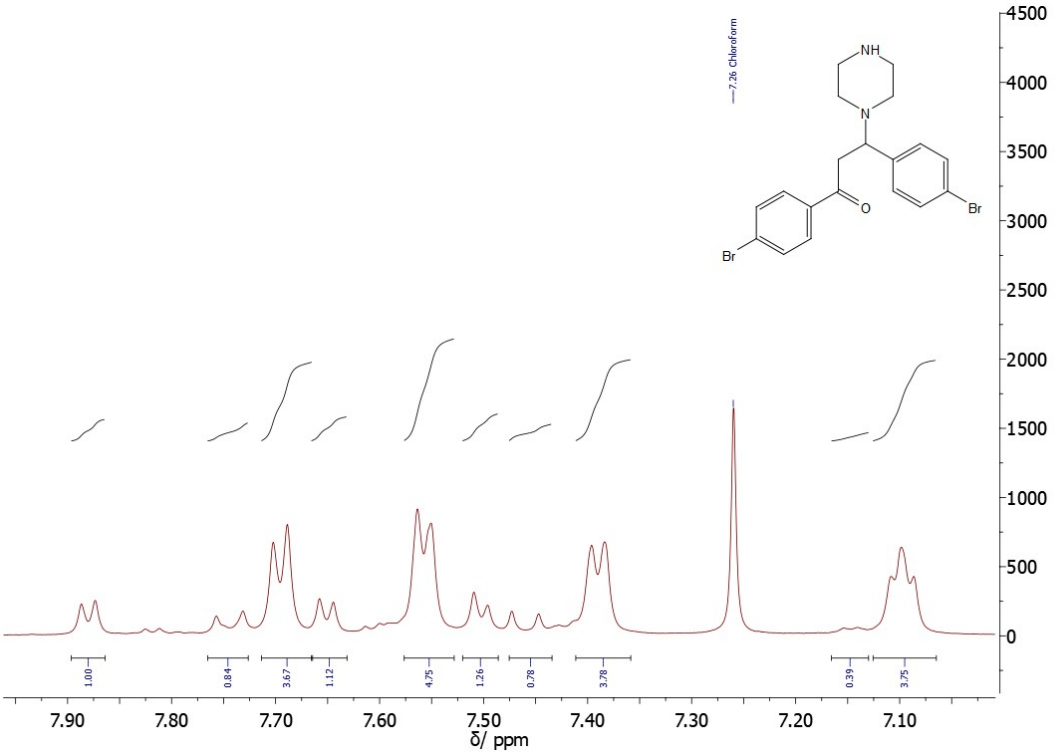

Figure S79. ^{1}H NMR spectrum ($CDCl_3$, 600 MHz) of a **3b** formed after liquid-assisted grinding (V($CHCL_3$ =20 µL) of previously formed crude reaction mixture where the conversion to **3b** was 26% for 120 min. The yield of **3b** increased up to 72%.

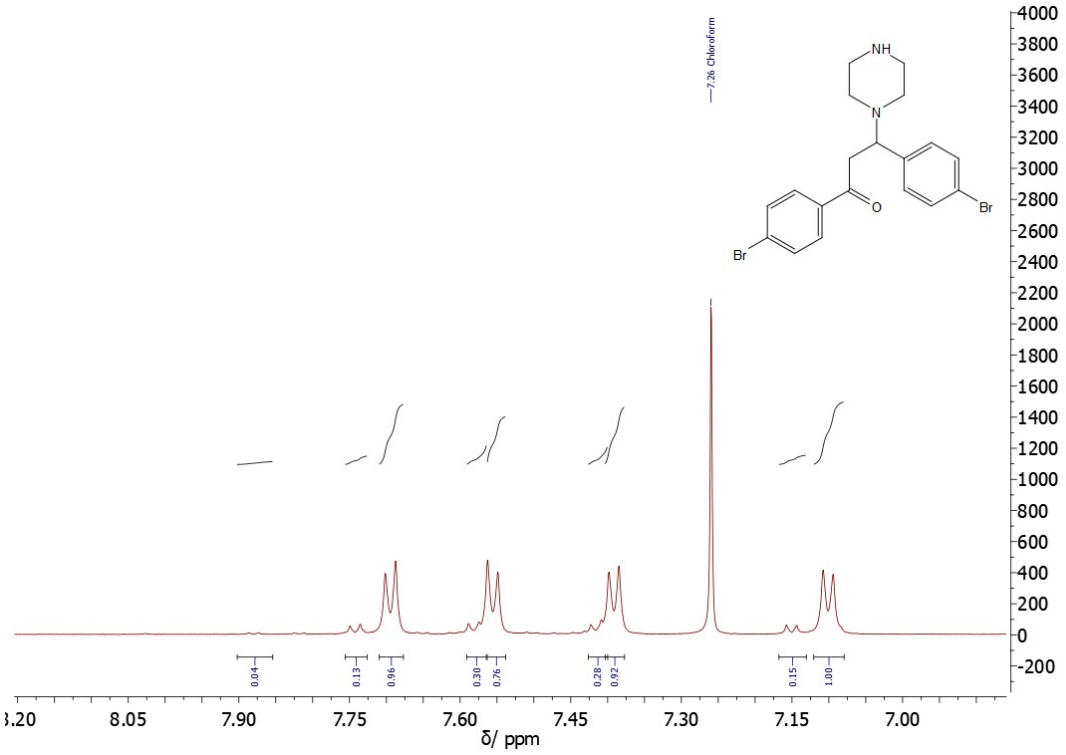

Figure S80. ^{1}H NMR spectrum ($CDCl_3$, 600 MHz) of a **3b** formed after liquid-assisted grinding (V($CHCL_3$ =20 µL) of previously formed crude reaction mixture where the conversion to **3b** was 59% for 120 min. The yield of **3b** increased up to 86%.

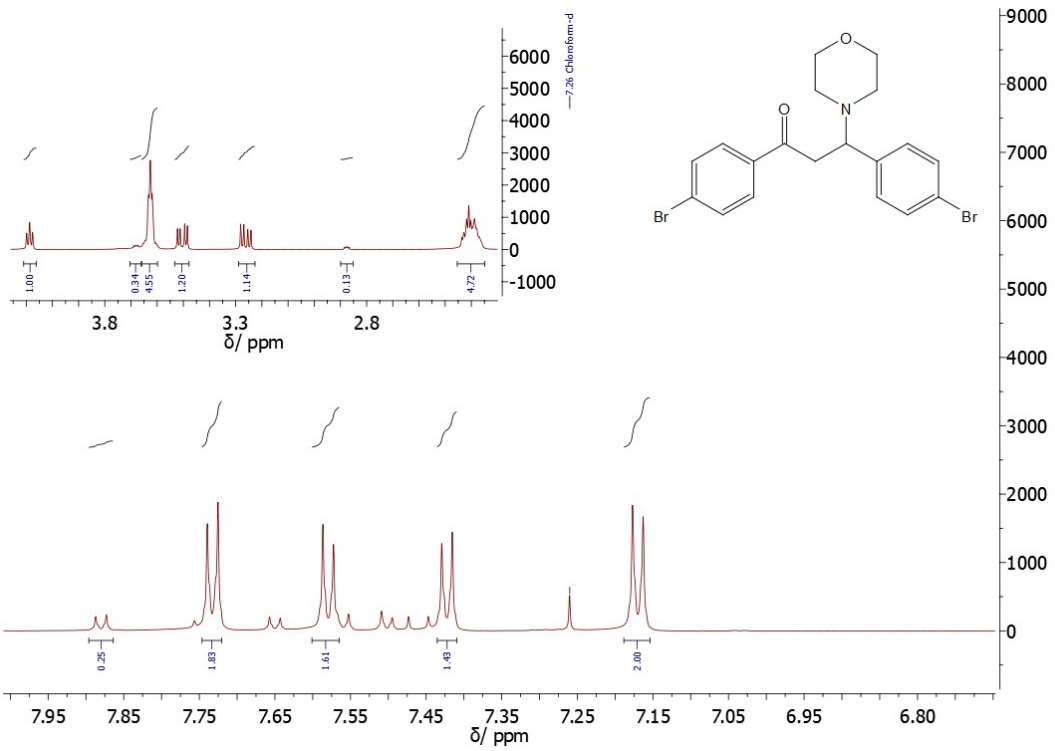

Figure S81. ^{1}H NMR spectrum ($CDCl_3$, 600 MHz) of a **3c** formed after milling **1** and **2c** for 120 min.

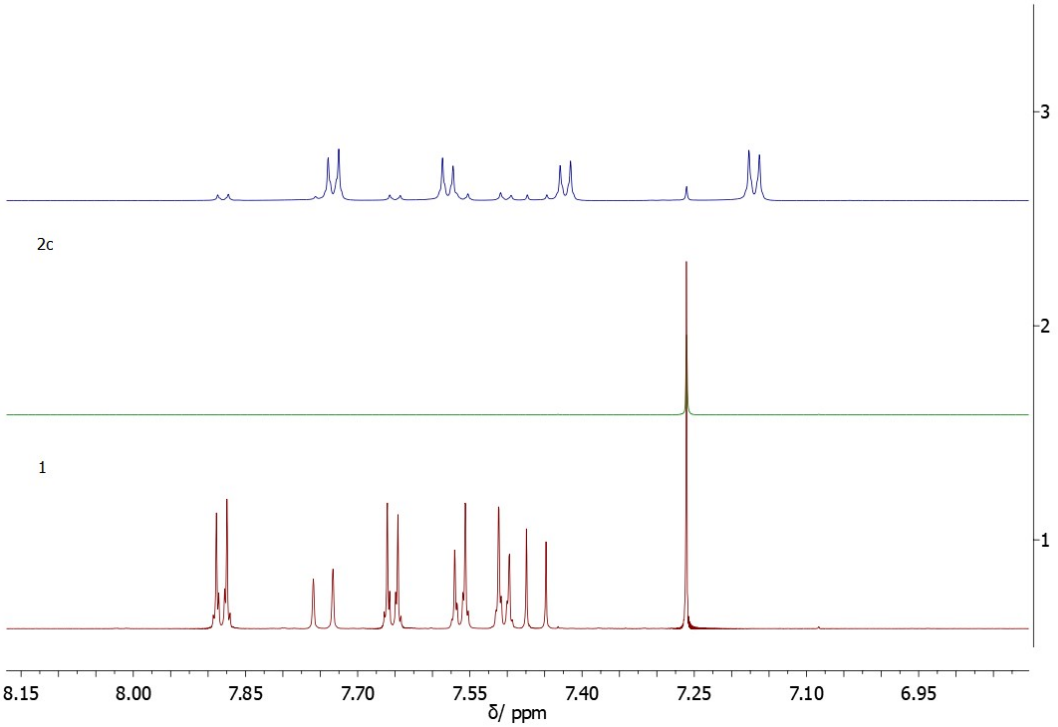

Figure S82. Comparison of ^{1}H NMR spectra ($CDCl_3$, 600 MHz) of a mixture of (from top to bottom): mixture collected after milling **1** and **2c** (1 equiv.) for 120 min corresponding to the **3c**, starting material **2c** and **1**.

4. Raman data

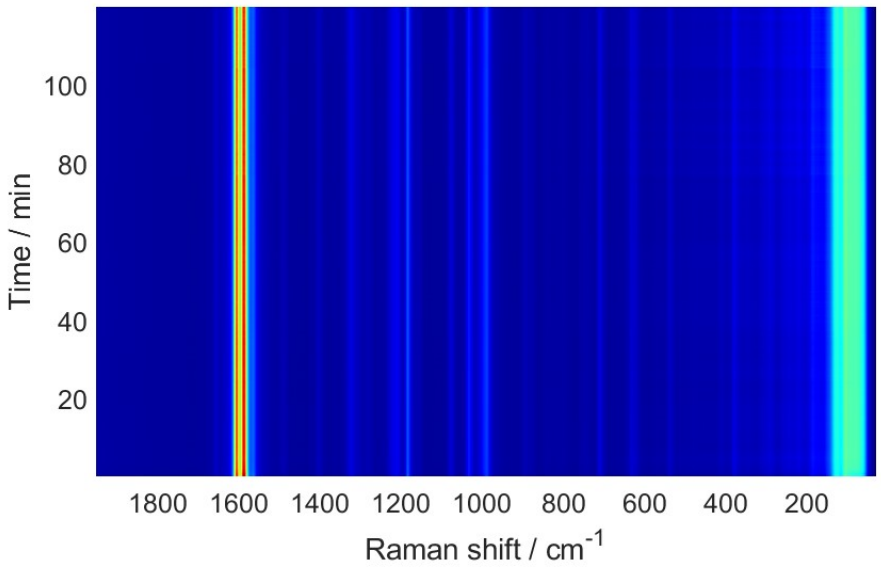

Figure S83. 2d time-resolved Raman spectra of monitoring the milling between **1** and diphenylamine (1 equiv.) for 120 min in a vibratory ball mill at 30 Hz milling frequency. No changes in the Raman bands were observed, indicating no formation of a new phase.

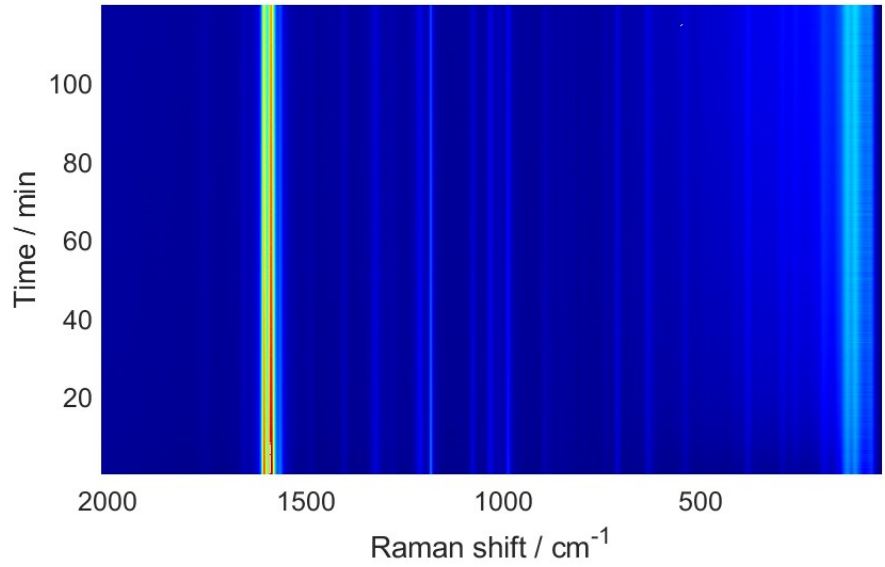

Figure S84. 2d time-resolved Raman spectra of monitoring the milling between **1** and succinimide

(1 equiv.) for 120 min in a vibratory ball mill at 30 Hz milling frequency. No changes in the Raman bands were observed, indicating no formation of a new phase.

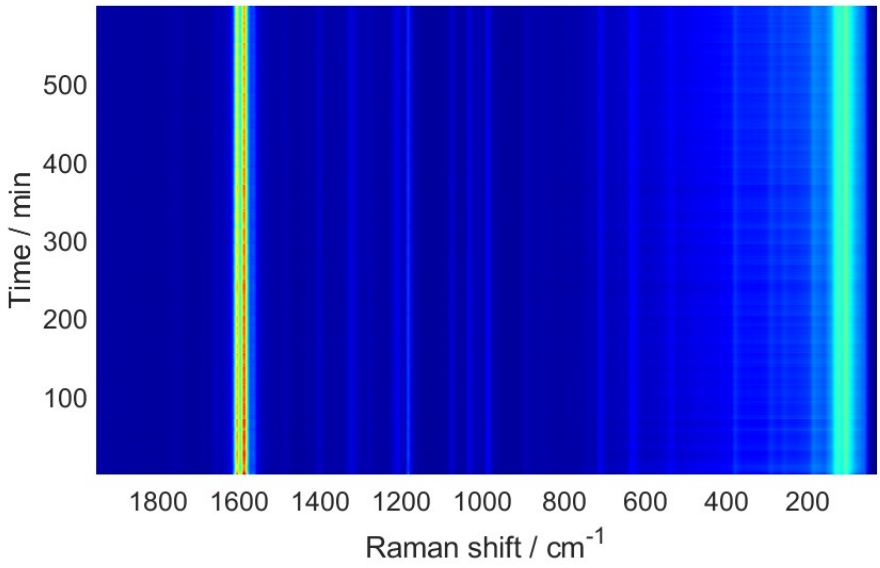

Figure S85. 2d time-resolved Raman spectra of monitoring the overnight milling between **1** and succinimide (1 equiv.) in a vibratory ball mill at 30 Hz milling frequency. No changes in the Raman bands were observed, indicating no formation of a new phase.

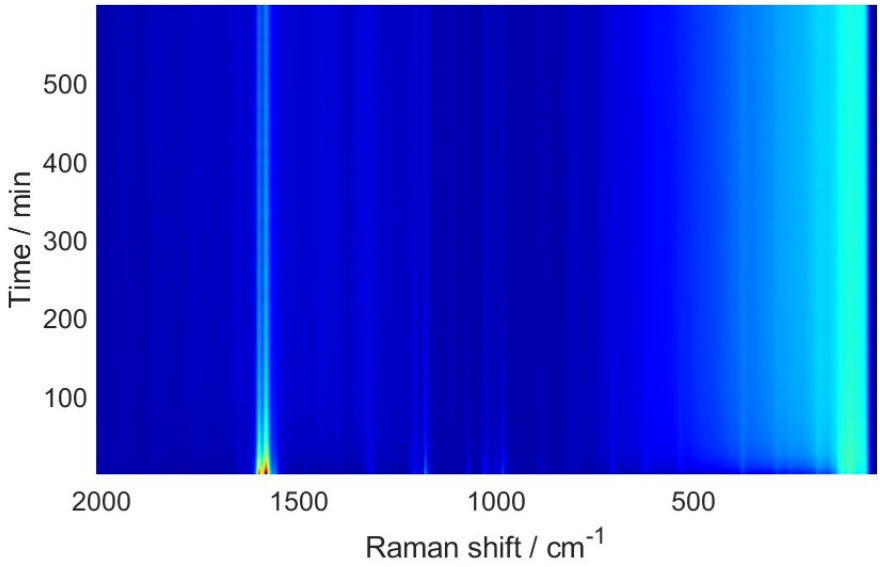

Figure S86. 2d time-resolved Raman spectra of monitoring the overnight milling between **1** and benzylamine (1 equiv.) in a vibratory ball mill at 30 Hz milling frequency. No changes in the Raman bands were observed, indicating no formation of a new phase. The decrease in Raman bands around 1600 cm^{-1} corresponds to the sticking of the reaction mixture to the walls of the reaction jar due to the presence of the liquid starting material.

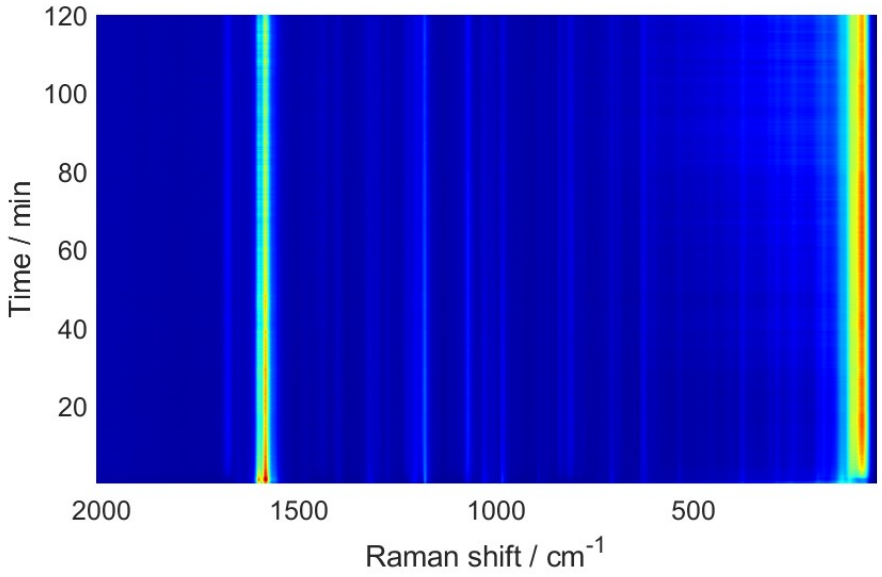

Figure S87. 2d time-resolved Raman spectra of monitoring the milling between **1** and **2a** (1 equiv.) in a vibratory ball mill for 120 min at 30 Hz milling frequency. The changes in the phononic region (below 200 cm^{-1}) as well between 1500 cm^{-1} and 1700 cm^{-1} indicate the formation of a new phase, identified as a new product **3a**.

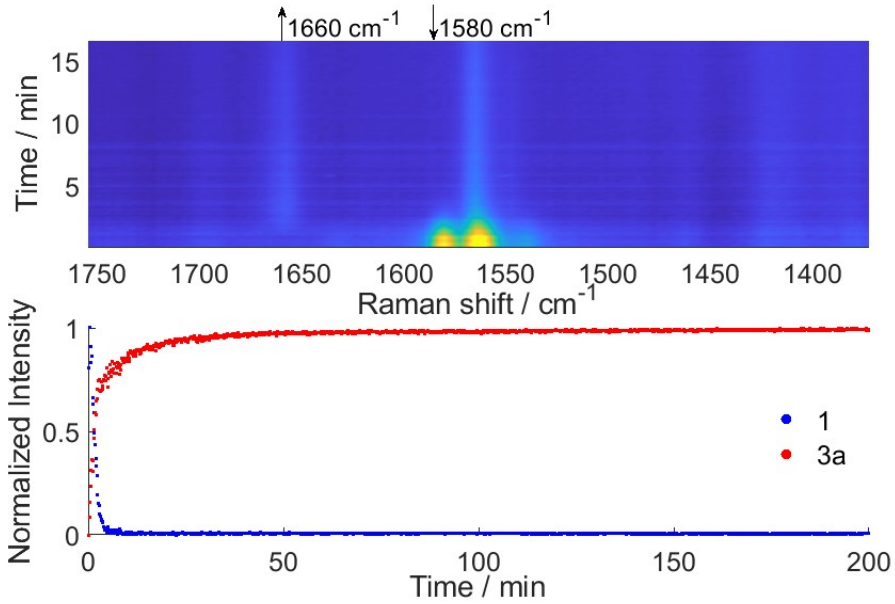

Figure S88. (top) 2d time-resolved Raman plot of monitoring milling between **1** and **2a** (1 equiv.) in a vibratory ball mill at 30 Hz milling frequency. (bottom) Intensity change during time for characteristic Raman band for C=C bond vibration of **1** (at 1580 cm^{-1}) and for C-N bond vibration of **3a** (at 1658 cm^{-1}).

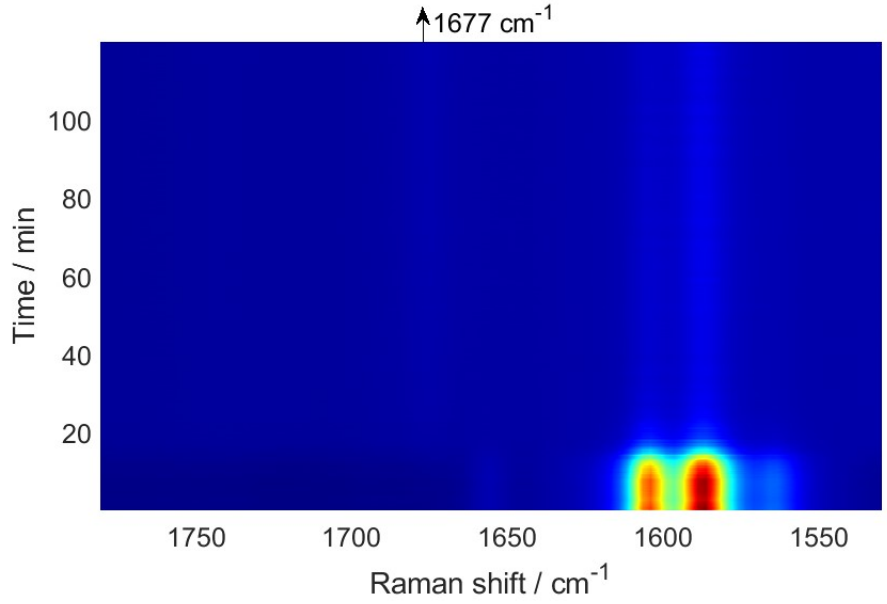

Figure S89. 2d time-resolved Raman spectra of monitoring the liquid-assisted milling (V($CHCl_3$=20 µL) between **1** and **2b** (1 equiv.) in a vibratory ball mill for 120 min at 30 Hz milling frequency. The increase in Raman bands at 1677 cm^{-1} indicate the formation of a new C-N bond.

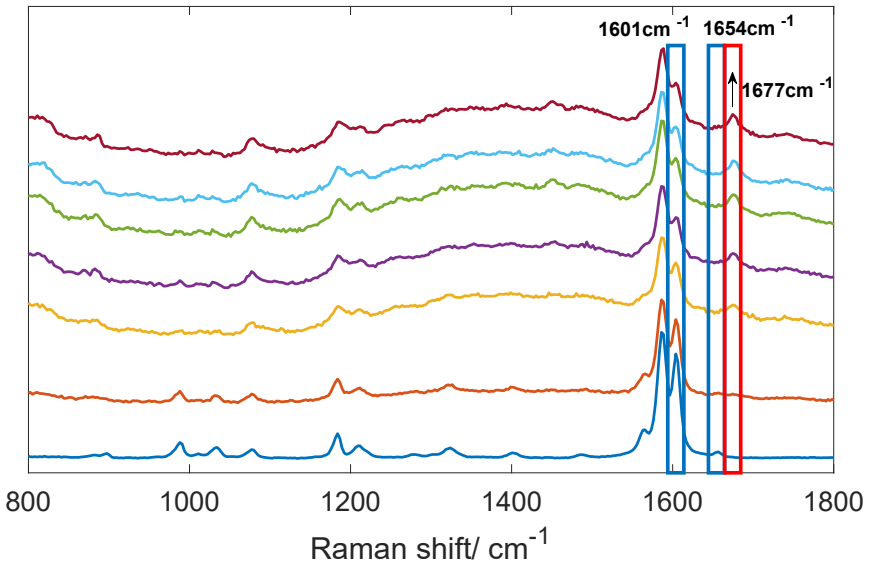

Figure S90. Stacked Raman spectra of monitoring the liquid-assisted milling (V($CHCl_3$=20 µL) between **1** and **2b** (1 equiv.) in a vibratory ball mill for 120 min at 30 Hz milling frequency. The increase in Raman bands at 1677 cm^{-1} indicate the formation of a new C-N bond, while the decrease of bands at 1601 cm^{-1} and 1654 cm^{-1} corresponds to the consumption of starting material (disruption of C=C bond).

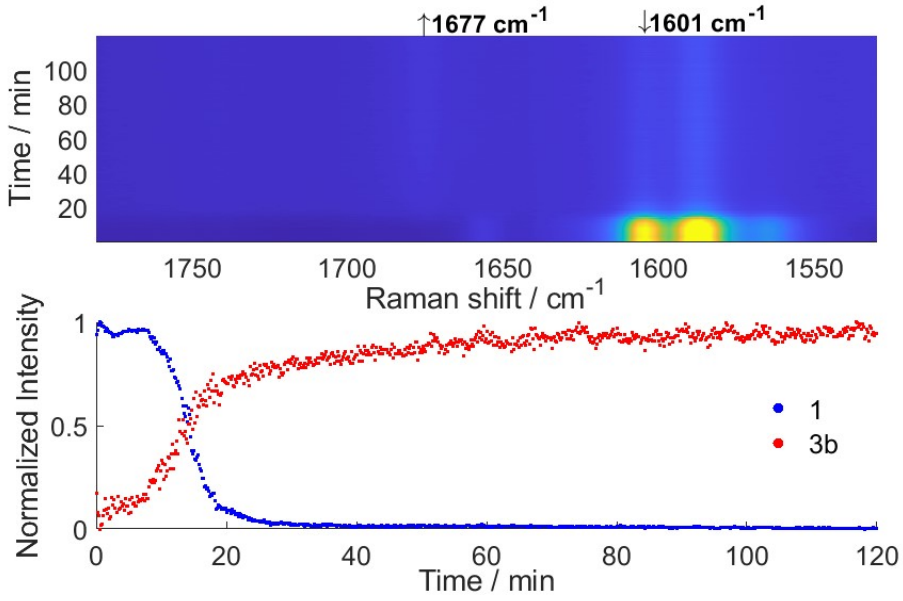

Figure S91. (top) 2d time-resolved Raman plot of monitoring liquid-assisted milling (V($CHCl_3$=20 µL) between **1** and **2b** (1 equiv.) in a vibratory ball mill for 120 min at 30 Hz milling frequency. (bottom) Intensity change during time for characteristic Raman band for C=C bond vibration of **1** (at 1601 cm^{-1}) and for C-N bond vibration of **3b** (at 1677 cm^{-1}).

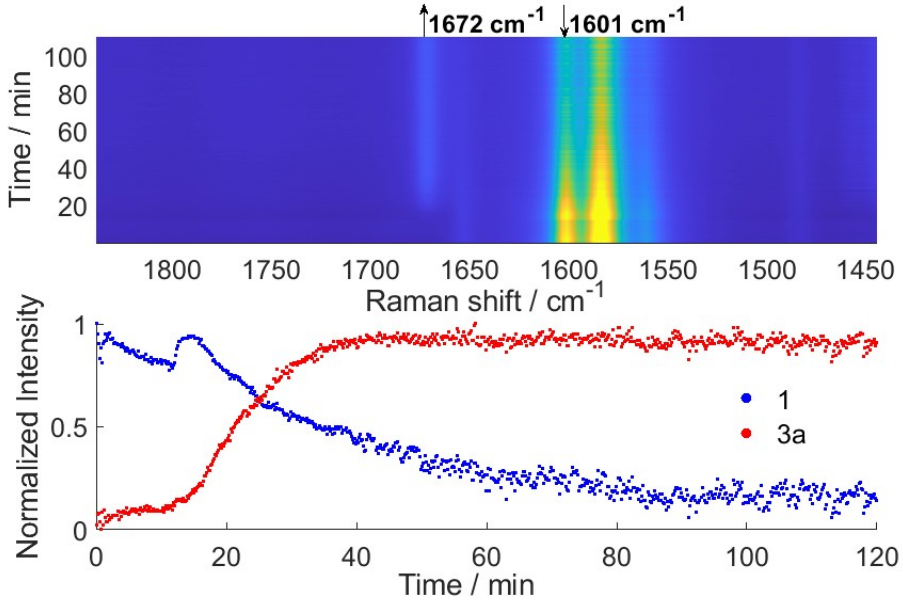

Figure S92. (top) 2d time-resolved Raman spectra of monitoring the milling between **1** and **2c** (1 equiv.) in a vibratory ball mill for 120 min at 30 Hz milling frequency. (bottom) Intensity change during time for characteristic Raman band for C=C bond vibration of **1** (at 1601 cm^{-1}) and for C-N bond vibration of **3c** (at 1672 cm^{-1}).

5. References

(1) S. Lukin, K. Užarević, I. Halasz, *Nat. Protoc.* 2021, **16 (7)**, 3492–3521.
(2) S. Bhattacharjee, A. Shaikh, W. Ahn, *Catal. Lett.* 2021, **151**, 1–8.
(3) D. R. Palleros, *J. Chem. Educ.* 2004, **81 (9)**, 1345.
(4) E. Saraci, M. Andreoli, E. Casali, M. Verzini, M. Argese, R. Fanelli, G. Zanoni, *RSC Sustain.* 2023, **1 (3)**, 504–510.
(5) S.-L. Ng, V. Shettigar, I. A. Razak, H.-K. Fun, P. S. Patil, S. M. Dharmaprakash, *Acta Crystal. E Struct. Rep. Online* 2006, **62 (4)**, o1421–o1423.